Mathematisches Forschungsinstitut Oberwolfach

Report No. 15/2013

DOI: 10.4171/OWR/2013/15

Interfaces and Free Boundaries: Analysis, Control and Simulation

Organised by
Charles M. Elliott, Warwick
Yoshikazu Giga, Tokyo
Michael Hinze, Hamburg
Vanessa Styles, Brighton

24 March – 30 March 2013

Abstract. The field of mathematical and numerical analysis of systems of nonlinear partial differential equations involving interfaces and free boundaries is a flourishing area of research. Many such systems arise from mathematical models in material science, fluid dynamics and biology, for example phase separation in alloys, epitaxial growth, dynamics of multiphase fluids, evolution of cell membranes and in industrial processes such as crystal growth. The governing equations for the dynamics of the interfaces in many of these applications involve surface tension expressed in terms of the mean curvature and a driving force. Here the forcing terms depend on variables that are solutions of additional partial differential equations which hold either on the interface itself or in the surrounding bulk regions. Often in applications of these mathematical models, suitable performance indices and appropriate control actions have to be specified. Mathematically this leads to optimization problems with partial differential equation constraints including free boundaries. Because of the maturity of the field of computational free boundary problems it is now timely to consider such control problems.

In order to carry out design, control and simulation of such problems interaction is required between distinct mathematical fields such as analysis, modeling, computation and optimization. By bringing together leading experts and young researchers from these separate fields we intended to develop novel research directions in applied and computational mathematics. The aim of the workshop here was to focus on emerging new themes and developments in these fields and to establish and extend links between them.

Mathematics Subject Classification (2010): MSC: 35-XX, 49-XX, 65-XX; IMU: 11, 16, 17.

Introduction by the Organisers

The meeting was attended by 51 participants from Austria, France, Germany, Great Britain, Japan, and the United States, with expertise from three main areas: optimal control of partial differential equations, modeling involving free boundary problems and mathematical and numerical analysis of free boundary problems. Apart from discussing current problems, techniques and issues across the differing communities the focus of the workshop was set on

(1) Computational and analytical approaches to interfaces and free boundaries,
(2) Control and optimization of interfaces and free boundaries,
(3) Numerical treatment and control of surface partial differential equations.

The presentations of Abels, Bellettini, Chambolle, Fischer, Giga, Hamamuki, Monneau, Nakayasu, Ohtsuka, Rocca, and Röger concerned analytical approaches to interfaces and free boundaries. While Bartels, Forcadel, Gräser, Ranner, Reusken, Sethian, Stinner, and Venkataraman gave talks on numerical approaches to interfaces and free boundaries. Control and optimization with focus on interfaces and free boundaries was the subject of the talks of Brett, Kahle, Leugering, Meyer, Pinnau, and Yamamoto. Kenmochi and King considered mathematical modeling of problems from biology. Finally, Garcke and Leugering in their talks reported on the state of the art in material and topology optimization.

To offer young researchers a stage for presenting their research, a young researcher session was organized on Wednesday evening where Brett, Gräser, Venkataraman together with the Heizaemon Honda Scholar Nakayasu and the Oberwolfach Leibniz Graduate Students Fischer, Hamamuki, Kahle, and Ranner took this opportunity and gave talks on their current research results.

Surveys and articles concerning mathematical and numerical approaches to interfaces and free boundary problems may be found in the conference proceedings [5, 6, 2, 8]. The level set approach to related problems of optimal design are surveyed in [3]. The book [1] contains theoretical results for optimal control of variational inequalities. Modern mathematical concepts of control and optimization with partial differential equation constraints are developed in the book [7]. Also we mention a survey of numerical methods for interface evolution involving curvature, [4]. Finally we remark that many recent references concerning the issues of the workshop are provided at the end of the each extended abstract.

References

[1] V. Barbu *Optimal control of Variational Inequalities* Pitman Research Notes in Mathematics **100** Pitman Boston London Melbourne (1984).
[2] A. Bossavit, A. Damlamian and M. Fremond (editors) *Free Boundary Problems: applications and theory* Pitman Research Notes in Mathematics **121** Pitman Boston London Melbourne (1985).
[3] M. Burger and S. Osher *A survey on level set methods for inverse problems and optimal design* Euro. J. Appl. Math. **16** (2005) 263–301.
[4] K.P. Deckelnick, G. Dziuk and C.M. Elliott *Computation of Geometric PDEs and Mean Curvature Flow* Acta Numerica (2005) 139–232.

[5] C.M. Elliott and J.R. Ockendon *Weak and variational methods for moving boundary problems.* Pitman Research Notes in Mathematics **59** Pitman Boston London Melbourne (1982).
[6] A. Fasano and M. Primicerio (editors) *Free Boundary Problems, Theory Applications* Pitman Research Notes in Mathematics **79** Pitman Boston London Melbourne (1983).
[7] M. Hinze, R. Pinnau, M. Ulbrich, S. Ulbrich *Optimization with PDE constraints* MMTA 23, Springer (2009).
[8] K.H. Hoffman and J. Sprekels (editors) *Free Boundary Problems, Theory and Applications* Pitman Research Notes in Mathematics **186** Pitman Boston London Melbourne (1990).

Workshop: Interfaces and Free Boundaries: Analysis, Control and Simulation

Table of Contents

Abstracts

On Sharp Interface Limits for Diffuse Interface Models

Helmut Abels
(joint work with Daniel Lengeler, Stefan Schaubeck)

We consider the sharp interface limit "$\varepsilon \to 0$" for the following diffuse interface model

$$\rho\partial_t \mathbf{v} + \rho\mathbf{v}\cdot\nabla\mathbf{v} - \operatorname{div}(2\nu(c)D\mathbf{v}) + \nabla p = -\varepsilon \operatorname{div}(\nabla c \otimes \nabla c), \tag{1}$$

$$\operatorname{div}\mathbf{v} = 0, \tag{2}$$

$$\partial_t c + \mathbf{v}\cdot\nabla c = m_\varepsilon \Delta\mu, \tag{3}$$

$$\mu = \varepsilon^{-1} f'(c) - \varepsilon\Delta c, \tag{4}$$

together with no-slip boundary condition for $\mathbf{v}$ and Neumann boundary conditions for c and μ in a sufficiently smooth bounded domain $\Omega \subseteq \mathbb{R}^d$, $d = 2, 3$. Here $\mathbf{v}$ is the mean velocity, $D\mathbf{v} = \frac{1}{2}(\nabla\mathbf{v} + \nabla\mathbf{v}^T)$, p is the pressure, c is an order parameter related to the concentration of the fluids (e.g. the concentration difference or the concentration of one component), and μ is a chemical potential. Moreover, $\nu(c) > 0$ is the viscosity of the mixture, $\varepsilon > 0$ is a (small) parameter, which will be related to the "thickness" of the interfacial region, $m_\varepsilon > 0$ is a mobility coefficient, and f the homogeneous free energy density. Furthermore ρ is the density of the fluids, which is chosen constant for simplicity. The model is known as "Model H" in the literature and goes back to Hohenberg and Halperin [6], cf. also [5]. It describes the flow of a binary mixture of two partly miscible viscous incompressible Newtonian fluids. For analytic results for the system and further reference we refer to [1]. The following results are also true for the generalization of this model to the case of different densities that was derived in [2].

In applications the parameter $\varepsilon > 0$ is often very small. Therefore a rigorous understanding of the limit $\varepsilon \to 0$ and the relation to classical sharp interface models is of interest. But convergence and the limit system as $\varepsilon \to 0$ depends on the choice of the scaling of m_ε. Using the method of matched asymptotic expansions it was shown in [2] formally that solutions of (1)-(4) converge to solutions of

$$\partial_t \mathbf{v} + \mathbf{v}\cdot\nabla\mathbf{v} - \operatorname{div}(\nu^\pm D\mathbf{v}) + \nabla p = 0 \quad \text{in } \Omega^\pm(t), \tag{5}$$

$$\operatorname{div}\mathbf{v} = \Delta\mu = 0 \quad \text{in } \Omega^\pm(t), \tag{6}$$

$$-\left[\mathbf{n}\cdot(\nu^\pm D\mathbf{v} - pI)\right] = \sigma H\mathbf{n} \quad \text{on } \Gamma(t), \tag{7}$$

$$V = \mathbf{n}\cdot\mathbf{v}|_{\Gamma(t)} - m_0[\mathbf{n}\cdot\nabla\mu] \quad \text{on } \Gamma(t), \tag{8}$$

$$[\mathbf{v}] = 0, \quad \mu|_{\Gamma(t)} = \sigma H \quad \text{on } \Gamma(t) \tag{9}$$

provided that $m_\varepsilon = \tilde{m}\varepsilon$ for some $\tilde{m} > 0$ and $m_0 = 0$ or $m_\varepsilon = m_0$. Here $\Omega^\pm(t)$ are two disjoint domains such that $\overline{\Omega^+(t)} \cap \overline{\Omega^-(t)} = \Gamma(t)$ is a smooth $(d-1)$-dimensional manifold (the interface), $\mathbf{n}$ denotes a normal field on $\Gamma(t)$, V is the normal velocity and H denotes the mean curvature of $\Gamma(t)$. Furthermore, $[.]$ denotes the jump of

a function across the interface $\Gamma(t)$ and $\sigma > 0$ depends explicitly on f. In the first case $m_0 = 0$ the system is a classical sharp interface model for a two-phase flow of two immiscible, viscous, incompressible Newtonian fluids with surface tension. While the case $m_0 > 0$ is a non-classical variant, where the Navier-Stokes system is coupled to a convective Mullins-Sekerka system. In this case diffusion of mass particle through the bulk phases and the Ostwald ripening effect can occur.

In the joint-work with D. Lengeler [3] it is shown that weak solutions of (1)-(4) converge (for a suitable subsequence) to so-called varifold solutions of (5)-(9) provided the initial energy is bounded uniformly in $\varepsilon > 0$ and $m_\varepsilon \to_{\varepsilon\to 0} m_0$ as well as $\lim_{\varepsilon\to 0} \varepsilon m_\varepsilon^{-1} = 0$. We note that the latter condition means that m_ε converges sublinearly to 0 as $\varepsilon \to 0$ in the case $m_0 = 0$. In the notion of varifold solutions all equations are satisfied in a usual weak sense accept for the equations involving the mean curvature H of the interface, which are satisfied as first variation of a general varifold in the same manner as in [4]. Furthermore it is shown that in general solutions of (1)-(4) do not converge to solutions of (5)-(9) if $m_\varepsilon = m_0\varepsilon^\alpha$ with $\alpha > 3$. To this end radially symmetric solutions of (5)-(9) in an annulus

$$\Omega = \{x \in \mathbb{R}^d : 1 < |x| < R\}$$

are considered together with inflow and outflow boundary conditions for $\mathbf{v}$ and Dirichlet boundary conditions for c. In this case it is shown that the solutions do not satisfy the Young-Laplace law (7) in the limit.

Finally, we considered the following simplified question: For which $\alpha > 0$ do solutions $(c_\varepsilon)_{\varepsilon>0}$ of the convective Cahn-Hilliard equation (3)-(4) for a given smooth, solenoidal velocity field $\mathbf{v}$ converge to the transport equation

$$\partial_t \chi_{\Omega^+(t)} + \mathbf{v} \cdot \nabla \chi_{\Omega^+(t)} = 0$$

and

$$\varepsilon \int_\Omega \nabla c \otimes \nabla c : \nabla \boldsymbol{\varphi}\, dx \to_{\varepsilon\to 0} \sigma \int_{\partial\Omega^+(t)} \mathbf{n} \otimes \mathbf{n} : \nabla \boldsymbol{\varphi}\, dx \tag{10}$$

holds for all divergence free smooth test vector fields $\boldsymbol{\varphi}$? We note that the right-hand side is a weak formulation of $\sigma H \mathbf{n}$. This convergence is essential to prove convergence for the full system. In [7] it is shown that, if $k = 1$, then solutions converge and (10) holds. Moreover, it is proved that (10) does not hold in general if $\alpha > 3$.

References

[1] H. Abels. On a diffuse interface model for two-phase flows of viscous, incompressible fluids with matched densities. *Arch. Rat. Mech. Anal.*, 194(2):463–506, 2009.

[2] H. Abels, H. Garcke, and G. Grün. Thermodynamically consistent, frame indifferent diffuse interface models for incompressible two-phase flows with different densities. *Math. Models Methods Appl. Sci.*, 22(3):1150013 (40 pages), 2012.

[3] H. Abels and D. Lengeler. On Sharp Interface Limits for Diffuse Interface Models for Two-Phase Flows. *Preprint*, arXiv:/1212.5582.

[4] X. Chen. Global asymptotic limit of solutions of the Cahn-Hilliard equation. *J. Differential Geom.*, 44(2):262–311, 1996.

[5] M. E. Gurtin, D. Polignone, and J. Viñals. Two-phase binary fluids and immiscible fluids described by an order parameter. *Math. Models Methods Appl. Sci.*, 6(6):815–831, 1996.
[6] P.C. Hohenberg and B.I. Halperin. Theory of dynamic critical phenomena. *Rev. Mod. Phys.*, 49:435–479, 1977.
[7] S. Schaubeck. Forthcoming PhD thesis

Total variation minimization with finite elements

Sören Bartels
(joint work with Ricardo H. Nochetto, Abner J. Salgado)

Functions of bounded variation provide a useful framework to describe processes in which quantities may be discontinuous or to model functions that jump across lower dimensional subsets. A function $u \in L^1(\Omega)$ is of bounded variation denoted $u \in BV(\Omega)$ if it has bounded total variation, i.e., if

$$|Du|(\Omega) = \sup\Big\{ -\int_\Omega u \operatorname{div} \phi \,\mathrm{d}x : \phi \in C_c^1(\Omega;\mathbb{R}^d),\ |\phi| \le 1\Big\} < \infty.$$

A simple model problem proposed in [ROF92] to denoise a given gray-level image $g \in L^\infty(\Omega)$ seeks a function $u \in BV(\Omega) \cap L^2(\Omega)$ that minimizes the functional

$$I(u) = |Du|(\Omega) + \frac{\alpha}{2}\|u-g\|_{L^2(\Omega)}^2.$$

The weak lower semicontinuity of the total variation and a compactness property of $BV(\Omega)$ imply the existence of a minimizer. The strong convexity of the lower order term implies that the minimizer $u \in BV(\Omega) \cap L^2(\Omega)$ is uniquely defined. It satisfies $u \in L^\infty(\Omega)$.

Numerical approximations are typically obtained by replacing $BV(\Omega) \cap L^2(\Omega)$ by a finite dimensional subspace V_h, e.g., continuous or discontinuous finite element functions that are piecewise polynomial on a given triangulation. If $u_h \in V_h$ denotes the uniquely defined minimizer in the subspace then the convexity of the total variation and the strong convexity of the lower order term imply

$$\frac{\alpha}{2}\|u-u_h\|_{L^2(\Omega)}^2 \le I(u_h) - I(u) = \min_{v_h \in V_h} I(v_h) - I(u).$$

Provided that one can construct a sequence $(v_h)_{h>0} \subset BV(\Omega) \cap L^2(\Omega)$ such that $v_h \in V_h$ for all $h > 0$ and $v_h \to u \in L^1(\Omega)$ and $|Dv_h|(\Omega) \to |Du|(\Omega)$ as $h \to 0$ it follows that the numerical approximations converge to the exact solution. These requirements are equivalent to the condition that the finite element spaces are intermediately dense in $BV(\Omega)$. This property is satisfied whenever the spaces V_h, $h > 0$, contain continuous, piecewise affine finite element functions. One can show that the intermediate density is not satisfied if V_h contains only piecewise constant functions.

Letting $\mathcal{S}^1(\mathcal{T}_h)$ denote the space of piecewise linear, globally continuous finite element functions a construction in [BNS12] implies that there exists for every

$u \in BV(\Omega)$ and $\varepsilon > 0$ a function $\widetilde{u}_h \in \mathcal{S}^1(\mathcal{T}_h)$ such that $\|\widetilde{u}_h\|_{L^\infty(\Omega)} \le c\|u\|_{L^\infty(\Omega)}$ and

$$|D\widetilde{u}_h|(\Omega) \le (1 + c\varepsilon + c\varepsilon^{-1}h)|Du|(\Omega),$$
$$\|\widetilde{u}_h - u\|_{L^1(\Omega)} \le c(h^2\varepsilon^{-1} + \varepsilon)|Du|(\Omega).$$

Using the particular structure of the functional I we then deduce that

$$\begin{aligned}\frac{\alpha}{2}\|u - u_h\|^2_{L^2(\Omega)} &\le |D\widetilde{u}_h|(\Omega) - |Du|(\Omega) + \frac{\alpha}{2}\int_\Omega (u - \widetilde{u}_h)(u + \widetilde{u}_h + 2g)\,\mathrm{d}x \\ &\le c(\varepsilon + h\varepsilon^{-1}) \le ch^{1/2}\end{aligned}$$

for the optimal choice $\varepsilon = h^{1/2}$. This estimate is suboptimal in the sense that $\inf_{v_h \in \mathcal{S}^1(\mathcal{T}_h)} \|u - v_h\|_{L^2(\Omega)} \le ch^{1/2}$. For generic discontinuous functions the convergence rate $1/2$ is sharp. The optimal convergence rate can be obtained for the minimization problem if one can construct an approximation $\widetilde{u}_h \in \mathcal{S}^1(\mathcal{T}_h)$ such that $|D\widetilde{u}_h|(\Omega) \le |Du|(\Omega)$ and $\|u - \widetilde{u}_h\|_{L^1(\Omega)} \le ch$. Such a construction is given in [NS12] for partitions consisting of rectangles. For less symmetric partitions or triangulations consisting of triangles this cannot be expected to hold in general.

The numerical solution of the finite-dimensional minimization problem is often based on a regularization of the total variation norm, e.g., by considering for $\delta > 0$ the modified functional

$$I_\delta(u_h) = \int_\Omega (|\nabla u_h|^2 + \delta^2)^{1/2}\,\mathrm{d}x + \frac{\alpha}{2}\|u_h - g\|^2_{L^2(\Omega)}.$$

A large class of iterative methods can be used to compute minimizers for this differentiable modification of the functional I. A drawback is that minimizers lose the desired properties such as sharp practical discontinuities or sparsity properties of the gradient. It is therefore desirable to compute minimizers without modifications of the functional. A successful approach is based on a discrete duality argument. The total variation of $u_h \in \mathcal{S}^1(\mathcal{T}_h)$ is given by

$$|Du_h|(\Omega) = \|\nabla u_h\|_{L^1(\Omega)} = \sup\Big\{ \int_\Omega \nabla u_h \cdot p_h\,\mathrm{d}x : p_h \in \mathcal{L}^0(\Omega)^d,\ |p_h| \le 1\Big\}.$$

Here, $\mathcal{L}^0(\mathcal{T}_h)^d$ denotes piecewise constant vector fields on $\mathcal{T}_h$. The minimization problem can thus be formulated as a saddle-point problem, i.e., we have

$$\inf_{u_h} I(u_h) = \inf_{u_h}\sup_{p_h} \int_\Omega \nabla u_h \cdot p_h\,\mathrm{d}x + \frac{\alpha}{2}\|u_h - g\|^2_{L^2(\Omega)} - I_{K_1(0)}(p_h),$$

where $I_{K_1(0)}$ denotes the indicator funcional of the set $K_1(0) = \{q \in H_N(\mathrm{div}\,;\Omega) : |q| \le 1 \text{ a.e. in } \Omega\}$. We let the expression in the min-max problem be denoted by $L(u_h, p_h)$. Classical arguments imply the existence of a saddle-point (u_h, p_h). These can be found with primal-dual methods but it is not obvious to define such an iteration that converges under moderate conditions on step sizes and which only leads to equations that are linear or can be solved explicitly. An appropriate semi-implicit discretization of the time-dependent problems

$$\partial_t u_h = -\delta_u L(u_h, p_h), \quad \partial_t p_h \in \partial_p L(u_h, p_h),$$

where $\delta_u L$ and $\partial_p L$ denote the Fréchet derivative and the subdifferential of L with respect to u and p, respectively, has been proposed and analyzed in [CP11]. Letting d_t denote the backward difference quotient defined through a step size $\tau > 0$ it leads to the equations

$$\begin{aligned}
&(1) \quad \widehat{u}_h^n = u_h^{n-1} + \tau d_t u_h^n,\\
&(2) \quad (-d_t p_h^n + \nabla \widehat{u}_h^n, q_h - p_h^n) + I_{K_1(0)}(p_h^n) \le I_{K_1(0)}(q_h),\\
&(2) \quad (d_t u_h^n, v_h) + (p_h^n, \nabla v_h) = -\alpha(u_h^n - g, v_h).
\end{aligned}$$

The equations can be solved successively and the solution of the variational inequality in step (2) is given by

$$p_h^n = \frac{p_h^{n-1} + \tau \nabla \widehat{u}_h^n}{\max\{1, |p_h^{n-1} + \tau \nabla \widehat{u}_h^n|\}}$$

which can be evaluated elementwise. Convergence of the iteration follows if $\tau \le ch_{min}$ in the sense that

$$\sum_{n \ge 0} \|u_h^n - u_h\|_{L^2(\Omega)}^2 \le c,$$

cf. [CP11, Bar12]. In general, a large number of iterations is required to guarantee a small residual in the discrete equations. An algorithm that approximates solutions of the dual problem on cartesian grids has been devised and analyzed in [Cha04].

A continuous duality argument shows that the dual formulation of the minimization of I consists in the maximization of the functional

$$D(p) = \frac{-1}{2\alpha} \|\operatorname{div} p + \alpha g\|_{L^2(\Omega)}^2 + \frac{\alpha}{2} \|g\|_{L^2(\Omega)}^2 - I_{K_1(0)}(p)$$

among vector fields $p \in H_N(\operatorname{div}; \Omega)$. The duality relation $D(q) \le I(u)$ for all $q \in H_N(\operatorname{div}; \Omega)$ leads to the fully computable a posteriori error estimate

$$(\alpha/2) \|u - u_h\|_{L^2(\Omega)}^2 \le I(u_h) - D(q_h)$$

with an arbitray vector field $q_h \in H_N(\operatorname{div}; \Omega)$. The above described primal-dual method computes a non-conforming approximation p_h of solutions of the dual problem and is therefore not admissible in the error estimate. The construction of a conforming approximation $\widetilde{p}_h \in \mathcal{S}^1(\mathcal{T}_h)^d$ is discussed in [Bar13]. Related adaptive mesh-refinement strategies refine the triangulation in regions where discontinuities occur and lead to optimally convergent approximations, i.e., experimental convergence rates $\overline{h}^{1/2} \sim N^{-1/4}$ with respect to the number of unknowns N.

The described techniques are also useful for evolution problems that are defined through the subdifferential of functionals similar to I possibly not involving a strongly convex lower order term. An implicit discretization in time leads to a recursive sequence of minimization problems of the form

$$u_h^n = \operatorname{argmin}_{v_h \in \mathcal{S}^1(\mathcal{T}_h)} \frac{1}{2\tau} \|v_h - u_h^{n-1}\|_{L^2(\Omega)}^2 + I(v_h).$$

A combination of the estimates outlined above with error estimates available from [NSV00] lead to the error estimate

$$\max_{n=0,1,\dots,N} \|u(t_n) - u_h^n\|_{L^2(\Omega)} \leq c(\tau^{1/2} + h^{1/6})$$

with $t_n = n\tau$ and provided that $u_0 \in BV(\Omega) \cap L^\infty(\Omega)$. In certain situations the estimate can be improved to the optimal bound $\tau + h^{1/2}$. We refer the reader to [BNS12] for details.

References

[Bar12] S. Bartels, *Total variation minimization with finite elements: Convergence and iterative solution*, SIAM J. Numer. Anal. **50** (2012), no. 3, 1162–1180.

[Bar13] S. Bartels, *Error control and adaptivity for a variational model defined on functions of bounded variation*, Preprint (2012).

[BNS12] S. Bartels, R. H. Nochetto, and A. J. Salgado, *Discrete total variation flows without regularization*, Preprint (2012).

[Cha04] A. Chambolle, *An algorithm for total variation minimization and applications*, J. Math. Imaging Vision **20** (2004), no. 1-2, 89–97.

[CP11] A. Chambolle and T. Pock, *A first-order primal-dual algorithm for convex problems with applications to imaging*, J. Math. Imaging Vision **40** (2011), no. 1, 120–145.

[NS12] R. H. Nochetto and A. J. Salgado, *A total variation diminishing interpolation operator and applications*, Preprint (2012).

[NSV00] R. H. Nochetto, G. Savaré, and C. Verdi, *A posteriori error estimates for variable time-step discretizations of nonlinear evolution equations*, Comm. Pure Appl. Math. **53** (2000), no. 5, 525–589.

[ROF92] L. I. Rudin, S. Osher, and E. Fatemi, *Nonlinear total variation based noise removal algorithms*, Physica D: Nonlinear Phenomena **60** (1992), no. 1-4, 259 – 268.

On the area of the graph of a map from the plane to the plane with a line discontinuity

Giovanni Bellettini

(joint work with Maurizio Paolini and Lucia Tealdi)

In [4] De Giorgi drawn attention on the possible nonlocality of the relaxed area of the graph of a discontinuous map from the plane to the plane. More precisely, given a bounded open set $\Omega \subset \mathbb{R}^2$ recall that the area functional $A(\cdot, \Omega)$ is given by

$$A(v, \Omega) := \int_\Omega \sqrt{1 + |\nabla v_1|^2 + |\nabla v_2|^2 + \left(\frac{\partial v_1}{\partial x} \frac{\partial v_2}{\partial y} - \frac{\partial v_1}{\partial y} \frac{\partial v_2}{\partial x} \right)^2} \, dxdy$$

if $v = (v_1, v_2) \in \mathcal{C}^1(\Omega; \mathbb{R}^2)$; let us extend for convenience $A(\cdot, \Omega)$ to $+\infty$ in $L^1(\Omega; \mathbb{R}^2) \setminus \mathcal{C}^1(\Omega; \mathbb{R}^2)$. Consider next the L^1-lower semicontinuous envelope of A (or relaxed area), defined for any $v \in L^1(\Omega; \mathbb{R}^2)$ as

$$\overline{A}(v, \Omega) := \inf \left\{ \liminf_{\epsilon \to 0} A(v^\epsilon, \Omega) : (v^\epsilon) \subset \mathcal{C}^1(\Omega; \mathbb{R}^2), v^\epsilon \to v \text{ in } L^1(\Omega; \mathbb{R}^2) \right\}. \tag{1}$$

The conjecture of [4], proven in [1], states that $\overline{A}(u,\cdot)$ is not a measure, more precisely is not subadditive, for the function u (called triple junction map) taking as values the three vertices of an equilateral triangle, each vector taken in a sector of the source plane of 120^o angles. In particular, $\overline{A}(u,\Omega)$ cannot be written as an integral over Ω (differently to what happens in the scalar case for any real-valued function with bounded variation in Ω). In [2] the authors refine the upper bound for $\overline{A}(u,\Omega)$, showing a connection with Plateau-type problems; if the construction of [2] were optimal (namely, if the upper bound would coincide with $\overline{A}(u,\Omega)$, which is not known at present), this would shed some light on the nonlocality phenomenon.

The question arises as to whether the nonlocality is due to the special form of the triple junction map u, or whether it can be obtained for other qualitatively different maps v. Even if we still are not able to answer this question, we start analyzing the case when $v \in BV(\Omega;\mathbb{R}^2)$ is a map which is smooth out of a simple $\mathcal{C}^2$ curve J_v with two endpoints, with $\overline{J}_v \subset \Omega$. Assume, for simplicity, that the space curve Γ, obtained by joining the graphs of the two traces of v on J_v, is closed and simple, and that it has a one-to-one convex parallel projection on the two-plane generated by the t-direction parametrizing J_v and one of the two coordinate directions in the target space $\mathbb{R}^2$. In order to keep boundedness of the gradient of at least one approximating sequence (v_ϵ) as in (1), we suppose in addition that Γ has two corners, in correspondence of the first and last value of the parameter t (namely, at the two crack tips). The main result, proven in [3], is that over the set J_v, the contribute $\mathcal{H}^2(\Sigma_{\min})$ appears as an upper bound for the singular part of $\overline{A}(v,\Omega)$, where $\Sigma_{\min}$ is an area-minimizing nonparametric surface bounding Γ. Other situations can be analyzed, in particular removing the assumption that Γ has a one-to-one convex parallel projection. Then, again an upper bound involving $\mathcal{H}^2(\Sigma_{\min})$ can be obtained, under suitable assumptions on Γ. These assumptions are needed, in particular, to exclude boundary branch points for $\Sigma_{\min}$, which is now an area-minimizing surface of disk-type bounding Γ.

References

[1] E. Acerbi, G. Dal Maso, *New lower semicontinuity results for polyconvex integrals*, Calc. Var. Partial Differential Equations **2** (1994), 329–371.

[2] G. Bellettini, M. Paolini, *On the area of the graph of a singular map from the plane to the plane taking three values*, Adv. Calc. Var. **3** (2010), 371-386

[3] G. Bellettini, M. Paolini, L. Tealdi *On the area of the graph of a BV map from the plane to the plane with a line discontinuity*, in preparation.

[4] E. De Giorgi, *On the relaxation of functionals defined on cartesian manifolds*, in Developments in Partial Differential Equations and Applications in Mathematical Physics (Ferrara 1992), Plenum Press, New York 1992.

Binary image recovery using phase field methods

Charles Brett
(joint work with Andreas Dedner, Charlie Elliott)

A common problem in the field of image processing is the following. We have a function $\bar{u}$ defined on a bounded and piecewise smooth subset $\Omega \subset \mathbb{R}^N$ for $N \leq 3$. Suppose $\bar{u}$ has been transformed by a linear operator S, and then corrupted by additive noise ζ, such that we have observed data

$$y_d := S\bar{u} + \zeta.$$

The problem is to recover $\bar{u}$ given y_d. Two immediate issues are that (a) ζ is unknown, so we will not be able to find $\bar{u}$ even with a good model for the space in which it lies (b) inverting S may be ill-posed, so it will be difficult to find an approximation to $\bar{u}$ even if $\zeta = 0$.

We assume that $\bar{u}$ is binary, S is a known continuous linear operator, and ζ is Gaussian noise. We follow the approach used in [1] and [2] and base our formulation on the Mumford-Shah model [3], but minimised over $BV(\Omega, \{a_0, a_1\})$, and generalised to include the blurring operator S. So we have the following nonconvex model consisting of an L^2 fidelity term plus a perimeter regularisation term:

$$\min_{u \in BV(\Omega, \{a_0, a_1\})} \frac{1}{2}||Su - y_d||^2_{L^2(\Omega)} + \sigma \mathrm{Per}(\{u = a_1\}).$$

This problem is difficult to solve numerically so we take a phase field approximation. This involves replacing the perimeter term by the Ginzburg-Landau functional and instead minimising over $H^1(\Omega)$. So we consider the approximate problem

$$\min_{u \in H^1(\Omega)} \frac{1}{2}||Su - y_d||^2_{L^2(\Omega)} + \frac{\sigma}{c(\Psi)} \left(\int_\Omega \frac{\varepsilon}{2} |\nabla u|^2 + \frac{1}{\varepsilon} \Psi(u) \right).$$

We focus on two different forms of the potential Ψ; the smooth double well potential and the double obstacle potential. Rather than developing separate theory for each, it is advantageous to introduce an abstract framework that both fit into.

We show existence of solutions to the abstract minimisation problem, derive necessary optimality conditions, and introduce an iterative method for finding functions satisfying the necessary optimality conditions. We then prove a result showing that the energy of the iterates decreases, and that subsequences of iterates converge to a function satisfying the necessary optimality conditions. We also introduce an abstract discrete framework which satisfies the above result, and for which subsequences of functions satisfying the discrete necessary optimality conditions converge to functions satisfying the continuous necessary optimality conditions.

A finite element discretisation of the binary image recovery problem fits into this framework, which we implement in the Distributed and Unified Numerics Environment (DUNE) using DUNE-FEM [4]. We test our method on a variety of

test problems in both 1 and 2 dimensions (see for example Figure 1). We then compare the performance of the method with the smooth double well and double obstacle potentials for the 1D barcode problem.

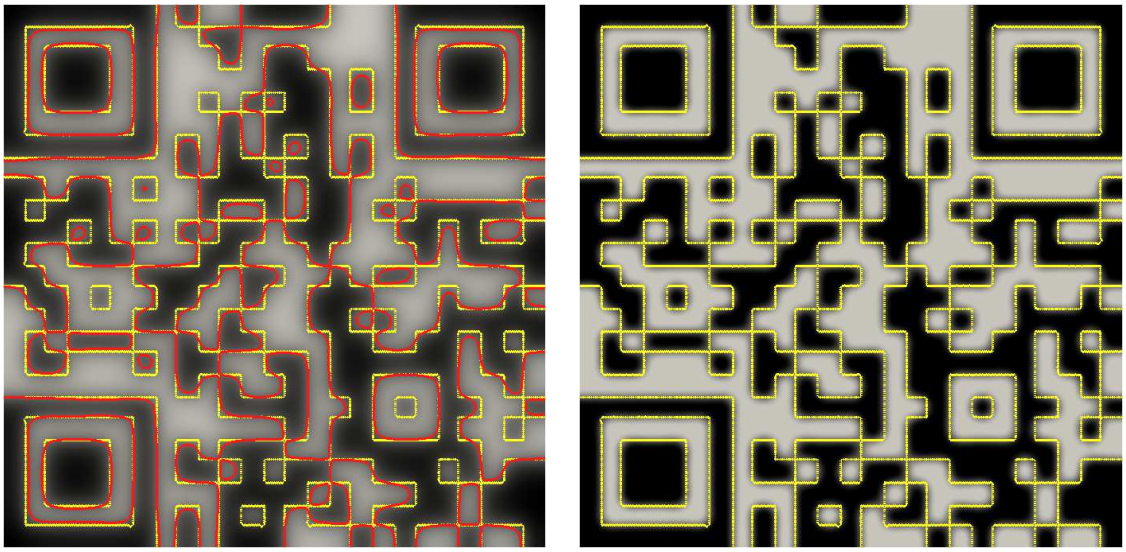

(a) (b)

FIGURE 1. The red line is the zero level set of the blurred barcode, and the yellow lines are those of the true barcode. We see that the true barcode is accurately recovered in (b), even though some features are missing in the blurred barcode (a).

REFERENCES

[1] S. Esedoglu, *Blind deconvolution of bar code signals*, Inverse Problems **20** (2004), 121–135.
[2] R. Choksi and Y. Gennip, *Deblurring of one dimensional bar codes via total variation energy minimisation*, SIAM Journal on Imaging Sciences **3** (2010), 735–764.
[3] D. B. Mumford and J. Shah, *Optimal approximations by piecewise smooth functions and associated variational problems*, Communications on Pure and Applied Mathematics **42** (1989), 577–685.
[4] http://www.dune-project.org/ and http://dune.mathematik.uni-freiburg.de/

On a class of nonlocal mean curvature flows

ANTONIN CHAMBOLLE
(joint work with Massimiliano Morini, Marcello Ponsiglione)

The idea in this talk was to describe a general approach for building geometric evolution to a class of "perimeters", described in [2, 3]. This class is defined as follows: we say that $E \mapsto P(E)$, $E \subset \mathbb{R}^d$, is a perimeter if it satisfies

- $P(E) \geq 0$ for all E, $P(\emptyset) = P(\mathbb{R}^d) = 0$;

- $E \mapsto P(E)$ is l.s.c. with respect to the L^1 convergence of characteristic functions of sets;
- for any sets E, F, $P(E \cup F) + P(E \cap F) \leq P(E) + P(F)$.

This last property is known in discrete combinatorial optimization as "submodularity" and is a form of "convexity". Indeed, one can show that under these assumptions, the functional defined for $u \in L^1_{loc}(\mathbb{R}^d)$ by

$$J(u) \ := \ \int_{-\infty}^{+\infty} P(\{u > s\})\, ds$$

is not only one-homogeneous (which is trivial), but also *convex*. It follows easily that for any $g \in L^1_{loc}(\mathbb{R}^d)$ with $\int_{\mathbb{R}^d} g^-\, dx < +\infty$, the problem

$$\min_E P(E) \ + \ \int_E g\, dx$$

has a minimizer, and, also, that if $g' > g$ a.e., the minimizer E' with potential g' is a subset (up to a negligible set) of the minimizer E with potential g.

We wish to define the motion of sets by the "geometric gradient descent" of P. In case P is the classical perimeter, it is well known that the first variation of P, defined for sets E sufficiently regular by

$$\lim_{t \to 0} \frac{P(E_t) - P(E)}{t} \ = \ \int_{\partial E} \kappa(x, E) \phi(x) \cdot \nu(x)\, d\mathcal{H}^{d-1}$$

where $\phi \in C^\infty_c(\mathbb{R}^d; \mathbb{R}^d)$ and $E_t = \{x + t\phi(x) \ : \ x \in E\}$, is the mean curvature $\kappa(x, E)$ of the boundary ∂E at x. One then can define the gradient descent, formally, as the mean curvature flow where the normal speed of a boundary ∂E at x is given by $\kappa(x, E)$. A way to extend this definition to arbitrary (not necessarily smooth) sets, or beyond singularities, is through the so-called level set approach and the degenerate parabolic equation

$$\frac{\partial u}{\partial t} \ = \ |Du| \kappa(x, \{u > u(x)\}) \ = \ |Du| \mathrm{div} \frac{Du}{|Du|}$$

which moves each level set of u by the mean curvature flow. It is well known that this equation has bounded, uniformly continuous (starting from a bounded, uniformly continuous initial data u^0) solutions in the viscosity sense, that is, such that

(i) for any $\phi \in C^2(\mathbb{R}^d \times [0, +\infty))$ and (x, t) a global maximum of $u - \phi$,

$$\frac{\partial \phi}{\partial t}(x, t) \ \leq \ |D\phi(x, t)| \kappa(x, \{\phi(\cdot, t) \geq \phi(x, t)\})$$

(ii) for any $\phi \in C^2(\mathbb{R}^d \times [0, +\infty))$ and (x, t) a global minimum of $u - \phi$,

$$\frac{\partial \phi}{\partial t}(x, t) \ \geq \ |D\phi(x, t)| \kappa(x, \{\phi(\cdot, t) \geq \phi(x, t)\})\,.$$

A function which satisfies (i) is a subsolution, while (ii) defines a supersolution. In the case of the classical curvature, these solutions are also unique.

What we can show is that such solutions exist for quite general perimeters $P(E)$, with some regularity conditions. To simplify we assume always that P is translational invariant, that is, $P(x+E) = P(E)$ for any set E and any $x \in \mathbb{R}^d$. We assume then that P is finite on sets with bounded C^2 boundary, and that such sets have a "curvature" $\kappa(x, E)$ satisfying the following conditions

a. if $E_n \to E$ in C^2 and $x_n \in \partial E_n$, $x_n \to x$ then $\kappa(x_n, E_n) \to \kappa(x, E)$;
b. if E is a C^2 set, $x \in \partial E$, then for any $\varepsilon > 0$ there exists δ such that for any $W \subset B(x, \delta)$,

$$P(E \cup W) \;\geq\; P(E) \;+\; (\kappa(x, E) - \varepsilon)|W \setminus E|$$

and symmetrically

$$P(E) \;\leq\; P(E \setminus W) \;+\; (\kappa(x, E) + \varepsilon)|W \cap E|\,;$$

c. there exists $K < +\infty$ such that for any $\rho > 0$, $\min_{x \in \partial B_\rho} \kappa(x, B_\rho) \geq -K$.

In this case, we show the following:

Theorem. *Assume that u^0 is a compactly supported, bounded, uniformly continuous function defined on $\mathbb{R}^d$. Then, there exists at least one viscosity solution, that is, a bounded, uniformly continuous function $u(x,t)$ with $u(x,0) = u^0(x)$ and which satisfies (i) and (ii).*

The solution can be obtained by the variational approach introduced in [1, 4]. It consists in fixing a time step $h > 0$ and defining an evolution starting from a set E_0 (which to simplify is assumed to be bounded, otherwise we might need to consider its complement) by letting, for each $n \geq 0$, E_{n+1} be a solution (for instance the maximal solution) of

$$\min_E P(E) \;+\; \frac{1}{h} \int_E d_{E_n}(x)\, dx$$

where $d_{E_n}(x) = \mathrm{dist}(x, E) - \mathrm{dist}(x, \mathbb{R}^d \setminus E)$ is the signed distance function to the set E_n.

We then let $E_h(t) = E_{\lfloor t/h \rfloor}$ for any $t \geq 0$. Since this scheme has a comparison principle ($E_0 \subset E_0' \Rightarrow E_h(t) \subset E_h'(t)$ for any $t \geq 0$), we can apply it to all the level sets of a bounded, compactly supported and uniformly continuous function $u^0(x)$ and define in this way for each t a function $u_h(x,t)$, which is easily shown to be also bounded, compactly supported and uniformly continuous. (Some uniform "regularity" in time can also be shown.) Up to a subsequence, it converges locally uniformly to a function $u(x,t)$ which is shown to be a viscosity solution to our problem.

In [2], the particular case of

$$P(E) \;=\; \frac{1}{2\delta} |\{\mathrm{dist}(x, \partial E) \leq \delta\}|$$

had been studied in detail. Up to a small regularization (in fact, we consider rather the set function

$$P(E) \;=\; \int_{\mathbb{R}^d} \mathcal{X}(d_E(x))\, dx$$

where $\mathcal{X}$ is a slightly smoothed variant of $t \mapsto 1/(2\delta)\chi_{[-\delta,\delta]}$), we show that this P enters the framework described here. Hence, the associated "mean curvature flow" is well-defined and can be approximated by the variational scheme. The corresponding curvature is quite singular and non-local.

We can also numerically compute the corresponding evolutions. As predicted, it behaves roughly like the standard curvature flow at large scales, but smoothes in a much slower way oscillating boundaries, see Figure 1.

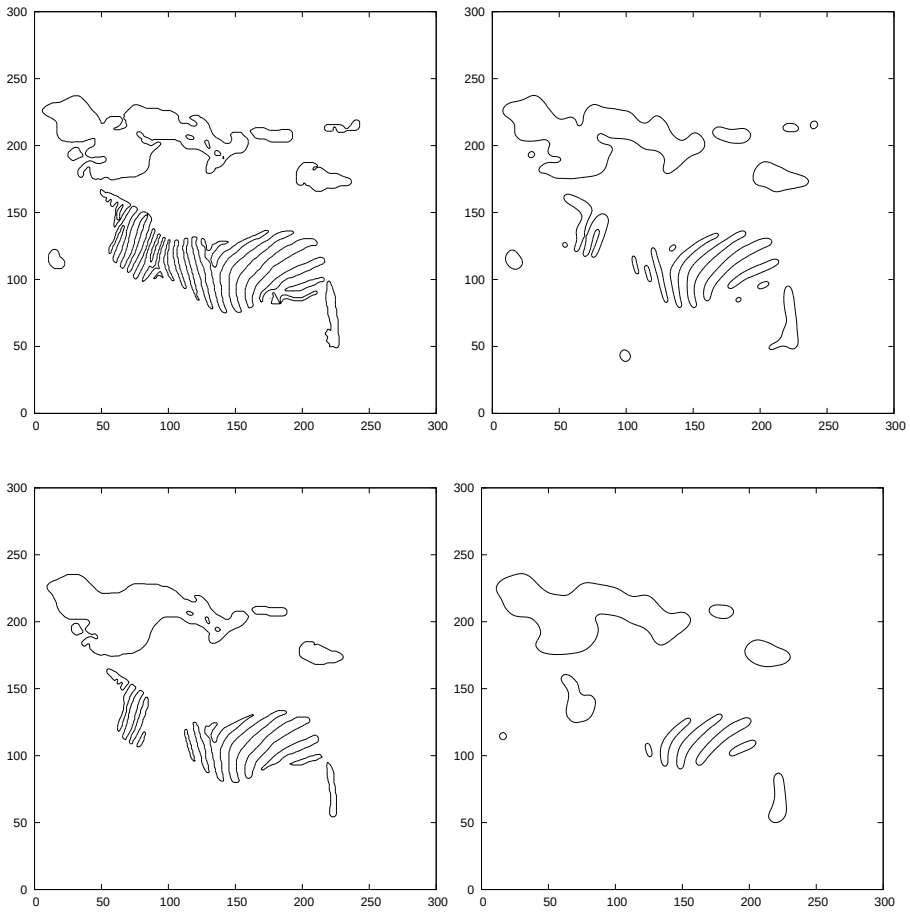

FIGURE 1. Comparison of the flows of two different perimeters (left: the non-local motion, right: the standard curvature flow).

REFERENCES

[1] F. Almgren, J. E. Taylor, and L.-H. Wang. *Curvature-driven flows: a variational approach.* SIAM J. Control Optim., **31**(2) (1993), 387–438.

[2] A. Chambolle, M. Morini, M. Ponsiglione. *A nonlocal mean curvature flow and its semi-implicit time-discrete approximation.* SIAM J. Math. Analysis, **44**(6) (2012), 4048-4077.

[3] A. Chambolle, M. Morini, M. Ponsiglione. *Nonlocal variational curvature flows.* (In preparation.)

[4] S. Luckhaus and T. Sturzenhecker. *Implicit time discretization for the mean curvature flow equation.* Calc. Var. Partial Differential Equations, **3**(2) (1995), 253–271.

Optimal estimates on interface propagation in thin-film flow

Julian Fischer

Lower bounds on the propagation of the free boundary are well-established in the theory of second-order degenerate parabolic equations like the porous medium equation

$$u_t = \Delta u^m \ .$$

For example, it is known that for large times the support of a nonnegative solution to the porous medium equation on $\mathbb{R}^d$ almost coincides with the support of the corresponding self-similar solution. Such results are typically derived using the comparison principle or Harnack inequalities.

However, for higher-order degenerate parabolic equations like the thin-film equation

$$u_t = -\nabla \cdot (u^n \nabla \Delta u)$$

no estimates from below on front propagation have been available at all: Given some point on the initial free boundary, it has not even been known whether the free boundary ever moves near this point.

In the recent papers [3, 4], we devise a technique for the derivation of lower bounds on front propagation for higher-order parabolic equations, allowing for the first time for the derivation of lower bounds on contact line propagation for the thin-film equation. The key ingredient of our approach are new monotonicity formulas for the thin-film equation of the form

$$\frac{d}{dt} \int u^{1+\alpha} |x - x_0|^\gamma \, dx \geq c \int u^{1+\alpha+n} |x - x_0|^{\gamma-4} \, dx$$

(for certain $\alpha \in (-1, 0)$ and $\gamma < 0$); these formulas are valid as as long as the support of u does not touch the singularity of the weight at x_0. Combining these formulas with a differential inequality argument due to Chipot and Sideris [2], we obtain estimates from below on support propagation. More precisely, we derive upper bounds on waiting times, sufficient criteria for immediate forward motion of the free boundary, as well as lower bounds on asymptotic support propagation rates.

In the case of one spatial dimension and $n \in (2, 3)$, our upper bounds on waiting times read as follows: given initial data u_0 with $\operatorname{supp} u_0 \subset [0, \infty)$ and $u_0(x) \geq S x_+^{\frac{4}{n}}$ in some neighbourhood of 0, the left free boundary will start moving forward at time $c(n) S^{-n}$ the latest. If the initial data even satisfy $\lim_{x \downarrow 0} x^{-\frac{4}{n}} u_0(x) = \infty$, the left interface starts moving forward instantaneously. These upper bounds on waiting times coincide up to a constant factor with the known lower bounds on waiting times [7] and are therefore optimal. The sufficient condition for immediate forward motion of the interface is also sharp.

In the borderline case $n = 2$, we obtain upper bounds on waiting times and sufficient conditions for immediate forward motion of the interface which are optimal up to a logarithmic correction term.

In the multidimensional case (at least for $d \leq 3$), similar assertions can be derived for $n \in [2,3)$ if the initial free boundary locally is regular enough. The proof proceeds by using a singular weight which is adapted to the shape of the initial support and a cutoff argument, resulting in an almost monotonicity formula.

The expected waiting-time behaviour for $n < 2$ is more complex; see [1] for conjectures obtained by formal asymptotic analysis. Our approach yields some limited rigorous results for $n \in (1,2)$ [3, 5].

Regarding lower bounds on asymptotic support propagation rates, we prove the following assertion: Given $n \in (1.5,3)$ and $x_s \in \operatorname{supp} u_0$, a solution to the thin-film equation on $\mathbb{R}^d$ satisfies for all $t \geq 0$

$$B_{R(t)}(x_s) \subset \operatorname{supp} u(.,t) \ ,$$

where

$$R(t) := c(d,n)||u_0||_{L^1}^{\frac{n}{4+n\cdot d}} t^{\frac{1}{4+n\cdot d}} - \operatorname{diam}(\operatorname{supp} u_0) \ .$$

This in particular implies that for large t, the support of a solution to the thin-film equation contains a ball whose diameter is of the same order as the diameter of the corresponding self-similar solution.

Finally, we would like to point out that our method is not limited to the thin-film equation, but is flexible enough to be applied to other higher-order nonnegativity-preserving parabolic equations: For example, in the case of the Derrida-Lebowitz-Speer-Spohn equation

$$u_t = -\nabla \cdot \left(u \nabla \frac{\Delta \sqrt{u}}{\sqrt{u}} \right)$$

an adaption of our ansatz can be used to prove infinite speed of propagation [6].

References

[1] J. Blowey, J. King, and S. Langdon, *Small- and waiting-time behaviour of the thin-film equation*, SIAM J. Appl. Math. **67** (2007), 1776–1807.

[2] M. Chipot and T. Sideris, *An upper bound for the waiting time for nonlinear degenerate parabolic equations*, Trans. Amer. Math. Soc. **288** (1985), 423–427.

[3] J. Fischer, *Upper bounds on waiting times for the thin-film equation: the case of weak slippage*, Preprint (2012).

[4] J. Fischer, *Optimal lower bounds on asymptotic support propagation rates for the thin-film equation*, Preprint (2012).

[5] J. Fischer, *Optimality of sufficient conditions for the occurrence of waiting time phenomena in thin-film flow*, in preparation.

[6] J. Fischer, *Infinite speed of propagation for the Derrida-Lebowitz-Speer-Spohn equation and quantum drift-diffusion models*, Preprint (2012).

[7] L. Giacomelli and G. Grün, *Lower bounds on waiting times for degenerate parabolic equations and systems*, Interfaces Free Bound. **8** (2006), 111–129.

Numerical schemes for dislocation dynamics

Nicolas Forcadel

Dislocations are linear defects which move in crystal. Their studies is very important since it is the main explanation at the microscopic scale of the plastic deformation of material. From a mathematical point of view, a dislocation is represented by the boundary of an open set $\Omega(t)$ which moves with a normal non-local velocity V_n defined by

$$V_n = c_0 \star 1_{\Omega(t)}$$

where c_0 is a given kernel.

The goal of this talk is to present two numerical schemes to solve this problem. The first one is based on the Fast Marching Method introduced by Sethian while the second is of level set type.

Fast marching method for dislocation dynamics

The Fast Marching Method, which has been introduced by Sethian [7], is a very efficient numerical method to solve front propagation problem where the front moves in its normal direction with a velocity $V_n = V_n(x) > 0$. The main idea of this method is to use the fact that the normal velocity and hence it is possible to defined the time $T(x)$ at which the front will reach the point x. It is also easy to see that this arrival time solve the following eikonal equation

$$||\nabla T(x)|| = \frac{1}{V_n(x)}.$$

The goal is then to solve numerically this eikonal equation and this is done in a very efficient way by solving the scheme in a special order (see [7]). In the first part of the talk, we present a generalization of this scheme to the case where the velocity V_n depends on space and time and can change sign in space and time. The stationary approach is no longer useful. Nevertheless, we will see how it is possible to use almost the same algorithm and to have a convergence result (see [1, 5].

We will also show some applications to this algorithm, in particular for the dislocation dynamics (see [2]) and in image segmentation (see [6]).

Level set method for dislocation dynamics

We consider a monotone model for the dislocations dynamics :

$$u_t(x,t) = \left(c[u](x,t) - \frac{1}{2}\int_{\mathbb{R}2} J \right) |Du|, \quad \text{with} \quad c[u](x,t) = \left(J \star 1_{\{u(\cdot,t) \geq u(x,t)\}} \right)(x)$$

where J is a positive kernel and the dislocation line is represented by the zero level set of the function u. The scheme we propose is then the following

$$\frac{v_I^{n+1} - v_I^n}{\Delta t} = \left(c_I^{n+1}[v] - \frac{1}{2}\int_{\mathbb{R}2} J \right) \text{"}|Dv|_I^{n+1}\text{"}$$

with

$$c_I^{n+1}[v] = \sum_{K\in\mathbb{Z}2} \bar{J}_{I-K} 1_{\{v_K^{n+1}\geq v_I^{n+1}\}}(\Delta x)2$$

and where "$|Dv|_I^{n+1}$" is a monotone approximation of the gradient (for example, the one one proposed by Rouy and Tourin or by Osher and Sethian). The main properties of this scheme is that it is implicit and not monotone (but "almost" monotone). In particular, due to the discontinuity of the velocity, the discrete solution of the scheme are not unique. Nevertheless, for every solution, we have the following error estimate:

Theorem 1 (see [4]). *Under certain regularity assumptions, we have the following error estimate between the continuous solution u of the dislocations dynamics equation (with J) and its numerical approximation v:*

$$\sup_{\mathbb{R}2\times(0,T)} |u-v| \leq K\sqrt{T}\,(\Delta x+\Delta t)^{1/2}$$

provided $\Delta x+\Delta t \leq \dfrac{1}{K2}$.

Using the convergence result for the dislocation dynamics to mean curvature motion, we can then get a numerical scheme for mean curvature motion. More precisely, we have the following convergence result.

Theorem 2 (see [3, 4]). *We define $u^\varepsilon(x,t) = \varepsilon u\left(\frac{x}{\varepsilon}, \frac{t}{\varepsilon 2|\ln\varepsilon|}\right)$. Under regularity assumptions, when $\varepsilon\to 0$, u^ε converges uniformly on compact sets to $u0$, which is the unique solution of the limit problem :*

$$\begin{cases} u0_t - g\left(\frac{(Du0)^\perp}{|Du0|}\right)\operatorname{trace}\left(D^2u0\cdot\left(Id-\frac{Du0}{|Du0|}\otimes\frac{Du0}{|Du0|}\right)\right)=0 \\ \\ u0(\cdot,0)=u_0 \end{cases}$$

Moreover, the difference between u^ε and $u0$ is given, for $T\leq 1$, by

$$\sup_{\mathbb{R}2\times(0,T)} |u^\varepsilon - u0| \leq K\left(\frac{T}{|\ln\varepsilon|}\right)^{\frac{1}{6}}.$$

This implies the following error estimate for the numerical scheme for the mean curvature motion.

Theorem 3 (see [4]). *Let $T\leq 1$. Under certain regularity assumptions, we have the following error estimate between the continuous solution $u0$ of the mean curvature motion and its numerical approximation v^ε:*

$$\sup_{\mathbb{R}2\times(0,T)} |u0 - v^\varepsilon| \leq C\left(\frac{T}{|\ln\varepsilon|}\right)^{\frac{1}{6}} \quad \textit{where } \varepsilon \geq \Delta x + \sqrt{\Delta t}$$

References

[1] E. Carlini, M. Falcone, N. Forcadel and R. Monneau, *Convergence of a Generalized Fast Marching Method for an Eikonal equation with a Velocity Changing Sign*, SIAM journal on numerical analysis, 46(6), 2008, pp. 2920-2952.

[2] E. Carlini, N. Forcadel and R. Monneau, *Generalized Fast Marching Method for dislocation dynamics*, SIAM Journal on Numerical Analysis 49(6), 2011, pp.2470-2500.

[3] F. Da Lio, N. Forcadel and R. Monneau, *Convergence of a non-local eikonal equation to anisotropic mean curvature motion. Application to dislocations dynamics*, Journal of the European Mathematical Society, 10(4), 2008, pp 1105-1119.

[4] N. Forcadel, *An error estimate for a new scheme for mean curvature motion*, SIAM journal on numerical analysis, 46(5), 2008, pp. 2715-2741.

[5] N. Forcadel, *Comparison principle for a Generalized Fast Marching Method*, SIAM Journal on numerical analysis, 47(3), 2009, pp. 1923-1951.

[6] N. Forcadel, C. Gout and C. Le Guyader, *Generalized Fast Marching Method: Applications to Image Segmentation*, Numerical Algorithms, 48(1-3), 2008, pp 189-212.

[7] J. A. Sethian, *fast marching level set method for monotonically advancing fronts*, Proc. Natl. Acad. Sci. USA, 93 (1996), pp. 1591–1595.

Multi-material structural topology optimization using phase field methods

Harald Garcke

(joint work with Luise Blank, Hassan Farshbaf-Shaker, Vanessa Styles)

In structural topology optimization one aims to minimize functionals such as the mean compliance

$$\int_{\Omega^M} \boldsymbol{f} \cdot \boldsymbol{u}\, dx + \int_{\Gamma_{\boldsymbol{g}} \cap \partial\Omega^M} \boldsymbol{g} \cdot \boldsymbol{u}\, ds$$

or the error compared to a target displacement $\boldsymbol{u}_\Omega$, i.e.

$$\int_{\Omega^M} c|\boldsymbol{u} - \boldsymbol{u}_\Omega|^2 dx$$

where Ω^M is a domain to be specified, $\boldsymbol{f}, \boldsymbol{g}$ are volume and surface forces and c is a weighting function. We will always search Ω^M as a subset of a design domain $\Omega \subset \mathbb{R}^d$. The displacement $\boldsymbol{u}$ is the solution of the system of linearized elasticity

$$-\nabla \cdot (\mathbb{C}^M \mathcal{E}(\boldsymbol{u})) = \boldsymbol{f} \quad \text{in } \Omega^M$$

subject to the boundary conditions

$$\begin{aligned} \boldsymbol{u} &= \boldsymbol{0} && \text{on } \Gamma_D \\ \left[\mathbb{C}^M \mathcal{E}(\boldsymbol{u})\right] \boldsymbol{n} &= \boldsymbol{g} && \text{on } \Gamma_{\boldsymbol{g}} \\ \left[\mathbb{C}^M \mathcal{E}(\boldsymbol{u})\right] \boldsymbol{n} &= \boldsymbol{0} && \text{on } \Gamma_0 \end{aligned}$$

where $\mathbb{C}^M$ is the elasticity tensor, $\boldsymbol{n}$ is the outer unit normal to $\partial\Omega^M$, $\Gamma_D \subset \partial\Omega$ is the Dirichlet boundary, on $\Gamma_{\boldsymbol{g}} \subset \partial\Omega^M$ outer fources act and $\Gamma_0 \subset \partial\Omega^M$ is the part of the domain boundary on which a homogeneous Neumann condition has to hold. We refer to [2, 4, 5] for further details.

As it stands the problem is not well posed and in some situations a perimeter regularization is used to ensure existence of solutions, see [1] and [2]. In this work we regularize with the help of the Ginzburg-Landau energy

$$E^\varepsilon(\boldsymbol{\varphi}) = \int_\Omega (\tfrac{\varepsilon}{2}|\nabla\boldsymbol{\varphi}|^2 + \tfrac{1}{\varepsilon}\Psi(\boldsymbol{\varphi}))dx$$

which typically arises in phase field approaches. Here $\varepsilon > 0$ is a small interfacial parameter which is related to the thickness of a diffuse interfacial layer between void and material and $\Psi : \mathbb{R}^N \to \mathbb{R}_0^+ \cup \{\infty\}$ is a multi-well potential, see [5]. We want to consider multi-material topology optimization and hence $\boldsymbol{\varphi}$ takes values in $\mathbb{R}^N$. The potential Ψ is assumed to have minima of height 0 at the standard unit vectors $\boldsymbol{e}_i \in \mathbb{R}^N$, $i = 1, \dots, N$. We always take φ_N as the fraction of void and $\varphi_1, \dots, \varphi_{N-1}$ as the fraction of $N-1$ materials. As the $\varphi_1, \dots, \varphi_N$ are fractions we always consider the constraint $\boldsymbol{\varphi} \in G = \{\boldsymbol{v} \in \mathbb{R}^N | \sum_{i=1}^N v_i = 1, v_i \geq 0\}$.

In the phase field context the mean compliance is given as

$$F(\boldsymbol{u}, \boldsymbol{\varphi}) = \int_\Omega (1-\varphi^N)\, \boldsymbol{f}\cdot\boldsymbol{u} + \int_{\Gamma_{\boldsymbol{g}}} \boldsymbol{g}\cdot\boldsymbol{u}$$

and the functional realising the error to a given target displacement is

$$J_0(\boldsymbol{u}, \boldsymbol{\varphi}) = \int_\Omega c(1-\varphi^N)|\boldsymbol{u} - \boldsymbol{u}_\Omega|^2 dx\,.$$

The overall minimization problem is now as follows.

Given $(\boldsymbol{f}, \boldsymbol{g}, \boldsymbol{u}_\Omega, c) \in L^2(\Omega, \mathbb{R}^d) \times L^2(\Gamma_{\boldsymbol{g}}, \mathbb{R}^d) \times L^2(\Omega, \mathbb{R}^d) \times L^\infty(\Omega)$ and measurable sets $S_i \subseteq \Omega$, $i \in \{0, 1\}$, with $S_0 \cap S_1 = \emptyset$ we consider

$$(\mathcal{P}^\varepsilon) \qquad \begin{cases} \min & J^\varepsilon(\boldsymbol{u}, \boldsymbol{\varphi}) := \alpha F(\boldsymbol{u}, \boldsymbol{\varphi}) + \beta J_0(\boldsymbol{u}, \boldsymbol{\varphi}) + \gamma E^\varepsilon(\boldsymbol{\varphi}), \\ \text{over} & (\boldsymbol{u}, \boldsymbol{\varphi}) \in H^1_D(\Omega, \mathbb{R}^d) \times H^1(\Omega, \mathbb{R}^N), \\ \text{s.t.} & (SE) \text{ is fulfilled and } \boldsymbol{\varphi} \in \boldsymbol{\mathcal{G}^m} \cap \boldsymbol{U}_c, \end{cases}$$

where $\alpha, \beta \geq 0$, $\gamma, \varepsilon > 0$, $\boldsymbol{m} \in (0,1)^N \cap \Sigma^N$, $\boldsymbol{\mathcal{G}^m} = \{\boldsymbol{v} \in H^1(\Omega, \mathbb{R}^N) \mid \boldsymbol{v} \in G \text{ a.e. and } \fint_\Omega \boldsymbol{v} = \boldsymbol{m}\}$ and

$$\boldsymbol{U}_c := \{\boldsymbol{\varphi} \in H^1(\Omega, \mathbb{R}^N) \mid \varphi^N = 0 \text{ a.e. on } S_0 \text{ and } \varphi^N = 1 \text{ a.e. on } S_1\}.$$

It can be shown that this problem has a solution. An optimum fulfills first order optimality conditions which are stated in the following theorem.

Theorem. *Let $\boldsymbol{\varphi} \in \boldsymbol{\mathcal{G}^m} \cap \boldsymbol{U}_c$ denote a minimizer of the problem $(\mathcal{P}^\varepsilon)$ and $S(\boldsymbol{\varphi}) = \boldsymbol{u} \in H^1_D(\Omega, \mathbb{R}^d)$, $\boldsymbol{p} \in H^1_D(\Omega, \mathbb{R}^d)$ are the corresponding state and adjoint variables, respectively. Then the functions $(\boldsymbol{u}, \boldsymbol{\varphi}, \boldsymbol{p}) \in H^1_D(\Omega, \mathbb{R}^d) \times (\boldsymbol{\mathcal{G}^m} \cap \boldsymbol{U}_c) \times H^1_D(\Omega, \mathbb{R}^d)$ fulfill the following optimality system in a weak sense. The displacement $\boldsymbol{u}$ fulfills the state equations*

$$(SE) \begin{cases} -\nabla\cdot[\mathbb{C}(\boldsymbol{\varphi})\mathcal{E}(\boldsymbol{u})] &=& \left(1-\varphi^N\right)\boldsymbol{f} & \text{in } \Omega, \\ \boldsymbol{u} &=& \boldsymbol{0} & \text{on } \Gamma_D, \\ [\mathbb{C}(\boldsymbol{\varphi})\mathcal{E}(\boldsymbol{u})]\,\boldsymbol{n} &=& \boldsymbol{g} & \text{on } \Gamma_{\boldsymbol{g}}, \\ [\mathbb{C}(\boldsymbol{\varphi})\mathcal{E}(\boldsymbol{u})]\,\boldsymbol{n} &=& \boldsymbol{0} & \text{on } \Gamma_0, \end{cases}$$

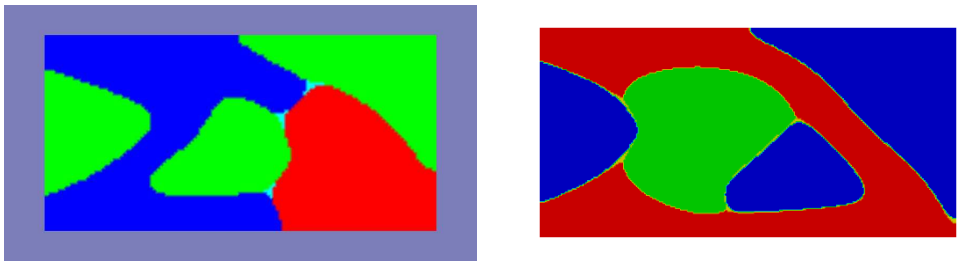

FIGURE 1

$\boldsymbol{p}$ *fulfills the adjoint equations*

$$(AE)\quad \begin{cases} -\nabla\cdot[\mathbb{C}(\boldsymbol{\varphi})\mathcal{E}(\boldsymbol{p})] &=& \alpha\left(1-\varphi^N\right)\boldsymbol{f}+2\beta c(1-\varphi^N)(\boldsymbol{u}-\boldsymbol{u}_\Omega) & \text{in } \Omega,\\ \boldsymbol{p} &=& \boldsymbol{0} & \text{on } \Gamma_D,\\ [\mathbb{C}(\boldsymbol{\varphi})\mathcal{E}(\boldsymbol{p})]\,\boldsymbol{n} &=& \alpha\boldsymbol{g} & \text{on } \Gamma_{\boldsymbol{g}},\\ [\mathbb{C}(\boldsymbol{\varphi})\mathcal{E}(\boldsymbol{p})]\,\boldsymbol{n} &=& \boldsymbol{0} & \text{on } \Gamma_0 \end{cases}$$

and $\boldsymbol{\varphi}$ *fulfills the gradient inequality*

$$(GI)\quad \begin{cases} \gamma\varepsilon\int_\Omega \nabla\boldsymbol{\varphi}:\nabla(\tilde{\boldsymbol{\varphi}}-\boldsymbol{\varphi})+\frac{\gamma}{\varepsilon}\int_\Omega \Psi_0'(\boldsymbol{\varphi})\cdot(\tilde{\boldsymbol{\varphi}}-\boldsymbol{\varphi})-\beta\int_\Omega c(\tilde{\varphi}^N-\varphi^N)|\boldsymbol{u}-\boldsymbol{u}_\Omega|^2\\ -\int_\Omega(\tilde{\varphi}^N-\varphi^N)\boldsymbol{f}\cdot(\alpha\boldsymbol{u}+\boldsymbol{p})-\langle\mathcal{E}(\boldsymbol{p}),\mathcal{E}(\boldsymbol{u})\rangle_{\mathbb{C}'(\boldsymbol{\varphi})(\tilde{\boldsymbol{\varphi}}-\boldsymbol{\varphi})}\geq 0,\\ \forall\tilde{\boldsymbol{\varphi}}\in\boldsymbol{\mathcal{G}}^{\boldsymbol{m}}\cap\boldsymbol{U}_c. \end{cases}$$

With the help of formally matched asymptotic expansions it can be shown that in the limit as $\varepsilon\to 0$ classical shape derivatives can be obtained, see [5]. In the case where one has only one material and void one obtains for example the classical first order condition

$$(1)\qquad -(\gamma\sigma\varkappa+\mathbb{C}^M\mathcal{E}(\boldsymbol{u}):\mathcal{E}(\boldsymbol{p}))+\beta C|\boldsymbol{u}-\boldsymbol{u}_\Omega|^2+\boldsymbol{f}\cdot(\alpha\boldsymbol{u}+\boldsymbol{p})=0$$

on the homogeneous Neumann boundary. Here σ is a constant related to Ψ , $\varkappa$ is the mean curvature of the material-void boundary and $\boldsymbol{p}$ is an adjoint defined as the solution of

$$(\mathrm{AE})^{MV}\quad \begin{cases} -\nabla\cdot\left[\mathbb{C}^M\mathcal{E}(\boldsymbol{p})\right] &=& \alpha\boldsymbol{f}+2\beta c(\boldsymbol{u}-\boldsymbol{u}_\Omega) & \text{in } \Omega^M,\\ \left[\mathbb{C}^M\mathcal{E}(\boldsymbol{p})\right]\boldsymbol{\nu} &=& \boldsymbol{0} & \text{on } \Gamma_{MV},\\ \boldsymbol{p} &=& \boldsymbol{0} & \text{on } \Gamma_D^M,\\ \left[\mathbb{C}^M\mathcal{E}(\boldsymbol{p})\right]\boldsymbol{n} &=& \alpha\boldsymbol{g} & \text{on } \Gamma_{\boldsymbol{g}}^M,\\ \left[\mathbb{C}^M\mathcal{E}(\boldsymbol{p})\right]\boldsymbol{n} &=& \boldsymbol{0} & \text{on } \Gamma_0^M, \end{cases}$$

where $\boldsymbol{\nu}$ is a unit normal at the void-material boundary. The expression on the left hand side in (1) is the Hadamard form of the shape differential which has to vanish in an optimum.

In multi-material topology optimization it is not desired that a large corner appears at an interface between void and two materials. Using the asymptotic expansions we found a way of choosing Ψ such that inappropriate angles can be avoided, see Figure 1 and consult [5] for details. We solve the first order optimality system formulated in the theorem above with the help of a gradient descent method which is discretized with the help of a finite element approximation and the resulting discrete variational inequalities are solved with the help of a

primal dual active set method, see [3]. In Figure 1 we show two solutions of a multi-material topology optimization problem. We refer to [5] for further details and for other references related to phase field structural topology optimization.

References

[1] L. Ambrosio, G. Buttazzo, *An optimal design problem with perimeter penalization*, Cal. Var. **1** (1993), 55–69.

[2] G. Allaire, F. Jouve, A.-M. Toader, *Strucutral optimization using sensitivity analysis and a level set method*, J. Comput. Phys. **194** (2004), 363–393.

[3] L. Blank, H. Garcke, L. Sarbu, V. Styles, *Non-local Allen-Cahn systems: Analysis and a primal dual active set method*, IMA Journal of Numerical Analysis (2013) DOI: 10.1093/imanum/drs039

[4] L. Blank, H. Garcke, L. Sarbu, T. Srisupattarawanit, V. Styles, A. Voigt, *Phase-field approaches to structural topology optimization*, Leugering, G.; Engell, S.; Griewank, A.; Hinze, M.; Rannacher, R.; Schulz, V.; Ulbrich, M.; Ulbrich, S.(Eds.): International Series of Numerical Mathematics **160** (2012), 245–255.

[5] L. Blank, H. Farshbaf-Shaker, H. Garcke, V. Styles, *Relating phase field and sharp interface approaches to structural topology optimization*, Preprint No. 03/2013, Fakultät für Mathematik, Universität Regensburg (2013).

Motion of an interface by crystalline energy: Full faceting phenomena in planar crystalline curvature flow with driving force

Mi-Ho Giga

(joint work with Yoshikazu Giga)

A planar anisotropic curvature flow equation with constant driving force term is considered when the interfacial energy is crystalline. The driving force term is given so that a closed convex set grows if it is sufficiently large. If initial shape is convex, it is shown that a flat part called a facet (with admissible orientation) is instantaneously formed. Moreover, if the initial shape is convex and slightly bigger than the critical size, the shape becomes fully faceted in a finite time provided that the Frank diagram of interfacial energy density is a regular polygon centered at the origin. The proofs of these statements are based on approximation by crystalline algorithm whose foundation was established a decade ago. Our results indicate that the anisotropy of interfacial energy plays a key role when crystal is small in the theory of crystal growth. In particular, our theorems explain a reason why snow crystal forms a hexagonal prism when it is very small. This is a joint work with Yoshikazu Giga of the University of Tokyo. The detail is in [7].

Description of the problem. We consider an anisotropic curvature flow equations for an evolving (hyper)surface $\{\Gamma_t\}_{t\geq 0}$ (physically a crystal surface) in $\mathbf{R}^n$ $(n \geq 2)$ of the form

$$V = M(\vec{n})(\kappa_\gamma + \sigma) \quad \text{on} \quad \Gamma_t, \tag{1}$$

where V denotes the normal velocity of Γ_t in the direction of unit normal $\vec{n}$ of Γ_t. The function M is called a *mobility*. It is a positive function defined on a unit sphere. In many models it is considered as a given function. The quantity κ_γ is

a *weighted mean curvature* or *anisotropic mean curvature*. It is the first variation of the interfacial energy I of the hypersurface Γ:

$$I(\Gamma) = \int_\Gamma \gamma_0(\vec{n}) \mathrm{d}\mathbf{H}^{n-1},$$

where γ_0 is a given positive function depending on the normal (orientation) called the *interfacial energy density* and $\mathrm{d}\mathbf{H}^{n-1}$ denotes the area element. We may write

$$\kappa_\gamma = -\delta I/\delta\Gamma$$

in a symbolic way. Its explicit form is formally as

$$\kappa_\gamma = -\operatorname{div}_\Gamma \left[(\nabla_p \gamma)(\vec{n})\right] \quad \text{on} \quad \Gamma,$$

where $\gamma(p) = |p|\gamma_0\left(p/|p|\right)$ is the 1-homogeneous extension of γ_0 to $\mathbf{R}^n$ and $\operatorname{div}_\Gamma$ is the surface divergence and $\nabla_p\gamma$ is the gradient of γ. If γ_0 is identically equal to 1 so that γ_0 is isotropic, the interfacial energy I is nothing but the surface area of Γ. In this case $\gamma(p) = |p|$ and $\kappa_\gamma = -\operatorname{div}_\Gamma \vec{n}$ which is $(n-1)$-times mean curvature.

To see the structure of (1) it is convenient to recall notion of the Frank diagram

$$\operatorname{Frank}\gamma = \{\, p \mid \gamma(p) \le 1\}\,.$$

If $\operatorname{Frank}\gamma$ is convex, then (1) is at least degenerate parabolic under suitable regularity of γ, say C^2. If $\operatorname{Frank}\gamma$ is convex but loses C^1 regularity, then (1) becomes a very singular diffusion equation and is nontrivial to handle. A typical example is the case when $\operatorname{Frank}\gamma$ is a convex polytope. In this case γ_0 is called a crystalline energy density and (1) is called a crystalline flow. Formally, the polar set of $\operatorname{Frank}\gamma$ called a Wulff shape of γ of the form

$$W_\gamma = \bigcap_{|\vec{m}|=1} \{\, x \mid x\cdot\vec{m} \le \gamma(\vec{m})\}$$

plays a role of a sphere in the sense that

$$\kappa_\gamma = -(n-1) \quad \text{on} \quad \partial W_\gamma \tag{2}$$

where $\vec{n}$ is taken outward. If $\operatorname{Frank}\gamma$ has a corner, then W_γ has a flat portion (a facet) with normal corresponding to the corner direction. To understand (2) in a reasonable way, one should interpret that the curvature κ_γ on the facet of ∂W_γ is not zero but some positive quantity despite the fact that the surface is flat. This suggests that κ_γ is not an infinitesimal quantity. It should be defined in a nonlocal way. This nonlocal character causes several difficulties. For an evolving curve (i.e. $n = 2$) various well-posedness results are established for the initial value problem for (1) when σ is a spatially constant [5], [6].

Results. In this work we consider (1) in a very simple setting. We consider a planar motion (i.e. $n = 2$) and postulate that γ_0 is crystalline and σ is a given positive constant. We start with a convex crystal surrounded by Γ_0 and show that facets are instantaneously formed. Such a kind of result is already proved for a different setting in [5] and recently studied for a case when $\operatorname{Frank}\gamma$ has a curved part by P. Mucha [9] and P. Mucha and P. Rybka [10], [11] but for graphs. We call this phenomenon the instant formation of a facet. We next study whether

or not a crystal becomes fully faceted after some short time. We only discuss a simple situation when Frank γ is a regular polygon centered at the origin. We show that if M has some "monotonicity property", a growing convex crystal starting from nearly the "critical size" (i.e. the curve satisfying $\kappa_\gamma + \sigma = 0$) becomes fully faceted in a finite time. Moreover, if M has the same symmetry as γ_0, the fully faceted shape is a similar (homothetic) to W_γ provided that the initial shape has the same symmetry. We prove these statements by approximating by a crystalline flow which is a system of ordinary differential equations [1], [12]. The approximation is justified by [6]. Note that even solvability is nontrivial for (1) for general (convex) initial data Γ_0 and it is established in [6]. The merit of crystalline approximation is that one can prove these statements as we intuitively observed. A fully faceted crystal grows further and its large time asymptotic is once influenced by the mobility. In fact, it is known that $\Gamma_t/t \to \sigma W_M$ (Hausdorff distance sense) as $t \to \infty$ [8]. So a fully faceted crystal may be rounded again. Our results support a recent numerical simulation by J.Barret, H. Garcke and R. Nürnberg [2], [3], [4] for the quasi-static approximation of one-phase Stefan problem with Gibbs-Thomson effect and kinetic supercooling with singular interfacial energy. In their simulation a fully faceted shape is observed.

References

[1] S. Angenent & M. E. Gurtin, *Multiphase thermomechanics with interfacial structure. II. Evolution of an isothermal interface,* Arch. Rational Mech. Anal. **108** (1989), 323–391.

[2] J. W. Barrett, H. Garcke & R. Nürnberg, *On stable parametric finite element methods for the Stefan problem and the Mullins-Sekerka problem with applications to dendritic growth,* J. Comput. Phys. **229** (2010), 6270–6299.

[3] J. W. Barrett, H. Garcke, & R. Nürnberg, *Finite element approximations of one-sided Stefan problems with anisotropic approximately crystalline, Gibbs-Thomson law,* Adv. Differential Equations **18** (2013), 383–432.

[4] J. W. Barrett, H. Garcke, & R. Nürnberg, *Numerical computations of facetted pattern formation in snow crystal growth,* Physical Review E **86** (2012), 011604, arXiv:1202.1272v1.

[5] M.-H. Giga & Y. Giga, *Evolving graphs by singular weighted curvature,* Arch. Rational Mech. Anal. **141** (1998), 117–198.

[6] M.-H. Giga & Y. Giga, *Generalized motion by nonlocal curvature in the plane,* Arch. Ration. Mech. Anal. **159** (2001), 295–333.

[7] M.-H. Giga & Y. Giga, *On the role of kinetic and interfacial anisotropy in the crystal growth theory,* (2012), preprint.

[8] H. Ishii, G. Pires, & P. Souganidis, *Threshold dynamics type approximation schemes for propagating fronts,* J. Math. Soc. Japan **51** (1999), 267–308.

[9] P. B. Mucha, *Regular solutions to a monodimensional model with discontinuous elliptic operator,* Interfaces Free Bound. **14** (2012), 145–152.

[10] P. B. Mucha, & P. Rybka, *A note on a model system with sudden directional diffusion,* J. Stat. Phys. **146** (2012), 975–988.

[11] P. B. Mucha, & P. Rybka, *Well-posedness of sudden directional diffusion equations,* http://arxiv.org/abs/1207.4929

[12] J. E. Taylor, *Constructions and conjectures in crystalline nondifferential geometry,* In: Differential Geometry (eds. B. Lawson and K. Tanenblat), Proceedings of the Conference on Differential Geometry (Rio de Janeiro, 1991), Pitman Monographs Surveys Pure Appl. Math. **52** Pitman London (1991), 321–336.

Nonsmooth Schur–Newton methods for multicomponent Cahn–Hilliard equations

Carsten Gräser
(joint work with Ralf Kornhuber, Uli Sack)

We consider vector-valued Cahn–Hilliard systems with logarithmic and obstacle free energy describing the decomposition of multicomponent alloys [3, 4, 11]. Such equations are governed by an H^{-1}-type gradient flow for the Ginzburg–Landau free energy

$$\mathcal{E}(u) = \int_\Omega \frac{\varepsilon}{2} \sum_{i=1}^N |\nabla u_i|^2 + \frac{1}{\varepsilon} \Psi_\theta(u)\, dx$$

subject to the local constraint $u(x) \in G = \{y \in \mathbb{R}^N \,|\, y \geq 0, \mathbf{1} \cdot y = 1\}$ where $\mathbf{1}$ denotes the 1-vector $\mathbf{1} = (1, \ldots, 1) \in \mathbb{R}^N$. The local free energy $\Psi_\theta : \mathbb{R}^N \to \mathbb{R} \cup \{\infty\}$ is given by

$$\Psi_\theta(u) = \Phi_\theta(u) + \tfrac{1}{2} K u \cdot u$$

with a negative semi-definite interaction matrix $K \in \mathbb{R}^{N \times N}$ and the temperature dependent convex part

$$\Phi_\theta(u) = \theta \sum_{i=1}^N u_i \ln(u_i) \quad \text{for } \theta > 0, \qquad \Phi_\theta(u) = \sum_{i=1}^N \chi_{[0,\infty)}(u_i) \quad \text{for } \theta = 0.$$

After semi-implicit discretization in time [1, 2] and finite element discretization in space we arrive at the discrete problems: Find $u \in \mathcal{S}_1^N, w_0 \in \mathcal{S}_0^N$ such that

$$\begin{aligned} \varepsilon^2(\nabla u, \nabla(v-u)) + \phi_\theta^{\mathcal{T}}(v) - \phi_\theta^{\mathcal{T}}(u) - (w_0, v-u) &\geq -(Ku^{\text{old}}, v-u) \quad \forall v \in \mathcal{S}_1^N, \\ -(u, v) - \tau(L\nabla w_0, \nabla v) &= -(u^{\text{old}}, v) \qquad\quad \forall v \in \mathcal{S}_0^N. \end{aligned}$$

Here, $\mathcal{T}$ is a conforming triangulation of Ω, $\mathcal{S}$ is the space of first order finite elements on $\mathcal{T}$, $\mathcal{S}_m^N$ is the constrained subset

$$\mathcal{S}_m^N = \{v \in \mathcal{S}^N \,|\, \mathbf{1} \cdot v = m\},$$

L is a symmetric positive semi-definite mobility matrix with $L\mathbf{1} = 0$, $\tau > 0$ is a time step size, u^{old} is the solution from the last time step, and $\phi_\theta^{\mathcal{T}}(v)$ is a lumped approximation of $\int_\Omega \Phi_\theta(v)$.

This variational inequality formulation has the advantage, that it can be used for the logarithmic case $\theta > 0$ as well as for the obstacle case $\theta = 0$. However, it effectively imposes the full simplex constraints $u(x) \in G$ explicitly by the indicator functional in Φ_θ and the linear constraint in $\mathcal{S}_1^N$.

To simplify the algebraic solution of this problem we introduce a Lagrange multiplier $w_1 \in \mathcal{S}^1$ for the local linear constraint $u(x) \cdot \mathbf{1} = 1$. Setting $w = w_0 + w_1\mathbf{1} \in \mathcal{S}^N$ it turns out [9] that the above problem is equivalent to: Find

$u \in \mathcal{S}^N, w \in \mathcal{S}^N$ such that

$$\begin{aligned} \varepsilon^2(\nabla u, \nabla(v-u)) + \phi_\theta^{\mathcal{T}}(v) - \phi_\theta^{\mathcal{T}}(u) - (w, v-u) &\geq -(Ku^{\mathrm{old}}, v-u) \quad \forall v \in \mathcal{S}^N, \\ -(u, v) - \tau(L\nabla w, \nabla v) &= -(u^{\mathrm{old}}, v) \qquad \forall v \in \mathcal{S}^N. \end{aligned}$$

Existence of solutions and uniqueness of u and ∇w_0 can be shown under the condition $\int_\Omega u^{\mathrm{old}} > 0$ while uniqueness of w requires that the mesh resolves the interface reasonably [9].

This formulation has the advantage that no explicit simplex constraints but only obstacles have to be considered for the algebraic solver, allowing to use the nonsmooth Schur–Newton method. While originally introduced for saddle point problems [8] with obstacles the method has recently been generalized to other nonsmooth free energies like the logarithmic potential [5, 6].

The method applies nonsmooth Newton techniques to the nonlinear Schur-complement of the saddle point problem. The fact that the Schur–Newton method is a descent methods for a dual energy functional can be used to prove global convergence even in the case of inexact solution of subproblem. Each iteration step requires the solution of a nonsmooth unconstrained primal minimization problem and a reduced linear saddle point problem. While we use the *truncated nonsmooth Newton multigrid* method [7, 10, 5] for the former standard techniques can be used for the latter.

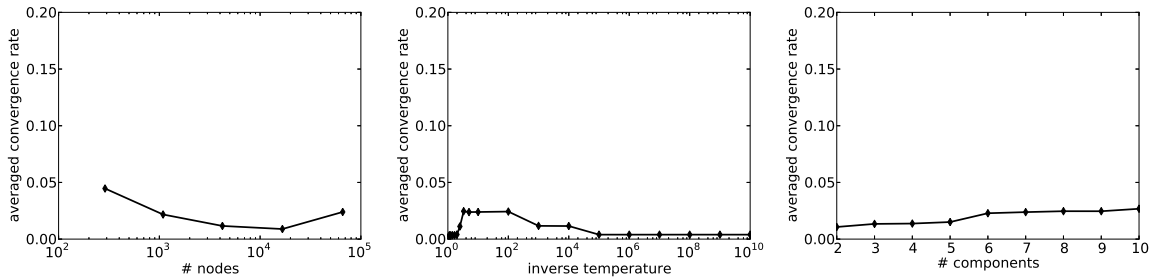

FIGURE 1. Averaged convergence rate of the Schur–Newton method over the number of vertices (left), the temperature θ (middle), and the number of components N (right).

Figure 1 (taken from [9]) shows the averaged convergence rate if the initial value is the solution from a coarser grid. The left, middle, and right plot depict the rates for varying mesh size, temperature θ, and number of components N. In our numerical examples none of these quantities seems to influence the rate, indicating that the method is mesh independent and robust with respect to θ and N.

REFERENCES

[1] J.F. Blowey, M.I.M. Copetti, and C.M. Elliott. Numerical analysis of a model for phase separation of a multi-component alloy. *IMA J. Numer. Anal.*, 16(1):111–139, 1996.

[2] J.F. Blowey and C.M. Elliott. The Cahn-Hilliard gradient theory for phase separation with non-smooth free energy part II: Numerical analysis. *European J. Appl. Math.*, 3:147–179, 1992.
[3] C.M. Elliott and S. Luckhaus. A generalised diffusion equation for phase separation of a multicomponent mixture with interfacial free energy. Preprint 195, University of Bonn, 1991.
[4] D. De Fontaine. An analysis of clustering and ordering in multicomponent solid solutions I. Stability criteria. *J. Phys. Chem. Solids*, 33:287–310, 1972.
[5] C. Gräser. *Convex Minimization and Phase Field Models*. PhD thesis, Freie Universität Berlin, 2011.
[6] C. Gräser. Nonsmooth Schur–Newton methods for nonsmooth saddle point problems. Preprint, Matheon Berlin, 2013.
[7] C. Gräser and R. Kornhuber. Multigrid methods for obstacle problems. *J. Comp. Math.*, 27(1):1–44, 2009.
[8] C. Gräser and R. Kornhuber. Nonsmooth Newton methods for set-valued saddle point problems. *SIAM J. Numer. Anal.*, 47(2):1251–1273, 2009.
[9] C. Gräser, R. Kornhuber, and U. Sack. Nonsmooth Schur–Newton methods for vector-valued Cahn–Hilliard equations. Preprint, Serie A 01/2013, Freie Universität Berlin, 2013. submitted.
[10] C. Gräser, U. Sack, and O. Sander. Truncated nonsmooth Newton multigrid methods for convex minimization problems. In M. Bercovier, M. Gander, R. Kornhuber, and O. Widlund, editors, *Domain Decomposition Methods in Science and Engineering XVIII*, LNCSE, pages 129–136. Springer, 2009.
[11] J. E. Morral and J. E. Cahn. Spinodal decomposition in ternary systems. *Acta Met.*, 19:1037, 1971.

Asymptotically self-similar solutions to curvature flow equations with prescribed contact angle

Nao Hamamuki

We study the asymptotic behavior of solutions to fully nonlinear second order parabolic equations of the form

$$u_t = F(\nabla_x u, \nabla_x^2 u).$$

A typical equation we consider is a generalized curvature flow equation given by

$$\frac{u_t}{\sqrt{1+u_x^2}} = 1 - e^{-k}$$

in the spatially one-dimensional case. Here $k = u_{xx}/\sqrt{1+u_x^2}^3$ denotes a curvature. This equation was introduced by a materials scientist Mullins in 1957 as a model of evaporation-condensation ([2]). We prove that, in the multi-dimensional half space $\{x_1 > 0\}$, viscosity solutions of the initial-value problem with a prescribed contact angle condition

$$u_{x_1} = \beta > 0 \quad \text{on } \{x_1 = 0\}$$

converge to a self-similar solution v of the associated problem under a suitable rescaling. This result especially implies the asymptotic convergence

$$\frac{1}{\sqrt{t}} u(\sqrt{t}x, t) \to V(x) \quad \text{as } t \to \infty,$$

where V is the profile function of v. For example, if u is a solution of the generalized curvature flow equation in Mullins' problem, then the associated problem for the self-similar solution v is

$$v_t = \frac{v_{xx}}{1+v_x^2}.$$

This is the usual curvature flow equation for graph.

We also study the depth of the groove, which is represented by the value of the profile function at the boundary. It turns out that, as the contact angle β tends to zero, the depth of the groove is well approximated by the linearized problem, which is, in Mullins' problem, the heat equation with a diffusion coefficient one.

This talk is based on the paper [1].

References

[1] N. Hamamuki, *Asymptotically self-similar solutions to curvature flow equations with prescribed contact angle and their applications to groove profiles due to evaporation-condensation*, preprint, UTMS Preprint Series 2012-17 (http://faculty.ms.u-tokyo.ac.jp/users/preprint/preprint2012.html).

[2] W. W. Mullins, *Theory of thermal grooving*, J. Appl. Phys. **28** (1957), 333–339.

Instantaneous Control of two-phase flow with different densities

Christian Kahle

(joint work with Michael Hinze)

In this talk we present a model predictive control (mpc) framework (see e.g. [5]) for two-phase flows with variable densities governed by a diffuse interface model proposed in [1]. Special emphasis is taken on quick control responses which are achieved through the inexact solution of the optimal control problems appearing in the mpc strategy. The resulting control concept is known as instantaneous control and is applied to feedback control of the Navier-Stokes system in e.g. [3, 8, 10]. We provide numerical investigations which indicate that instantaneous wall parallel boundary control of the flow part is well suited to achieve a prescribed concentration distribution in the variable density Cahn-Hilliard Navier-Stokes system.

1. The diffuse interface model

We use the diffuse interface model of [1] with a double-obstacle free energy according to [2]. Denoting the velocity field by y, the pressure field by p, the phase-field variable by c and the chemical potential by w this model is given by

$$\rho\partial_t y + ((\rho y + j)\cdot\nabla)\, y - \operatorname{div}(2\eta Dy) + \nabla p = -\sigma\epsilon \operatorname{div}(\nabla c \otimes \nabla c) + \rho g \tag{1}$$

$$\operatorname{div} y = 0 \tag{2}$$

$$\partial_t c - \operatorname{div}(m\nabla w) + y\cdot\nabla c = 0 \tag{3}$$

$$\sigma\epsilon(\nabla c, \nabla(c-v)) - \sigma\epsilon^{-1}(c, c-v) \geq (w, c-v) \quad \forall v \in H^1(\Omega),\ |v| \leq 1, \tag{4}$$

where $2Dy = \nabla y + (\nabla y)^t$, and $j = -\rho'(c)m(c)\nabla w$. The density of the fluid is denoted by $\rho(c)$, its viscosity is denoted by $\eta(c)$, and its mobility is given by $m(c)$. The constant ϵ is related to the width of the diffuse interface while σ denotes a scaled surface tension due to [1, sec.4.3.4] and in case of the double-obstacle free energy relates to the physical surface tension σ^{phys} as $\sigma = 2\pi^{-1}\sigma^{phys}$.

Numerical Treatment. We use a time discretization motivated by the research of [12], which sequentially couples (3) – (4) and (1) – (2). The variational inequality is relaxed with a Moreau–Yosida approach according to [7, 6], which substitutes (4) by the nonsmooth equations

$$\lambda(c) = \max(0, c-1) + \min(0, c+1),$$
$$-\sigma\epsilon\Delta c + \sigma\epsilon^{-1}(s\lambda(c) - c_{old}) = w,$$

where the subscript $_{old}$ labels the previous time instance and here is taken according to [4].

The resulting nonlinear system is solved by a semi-smooth Newton method. The spatial discretization uses piecewise linear and continuous finite elements for both c and w, and the Taylor-Hood finite element for the variable pair (y, p). The spatial resolution of the finite element meshes is controlled by the reliable and effective residual based a posteriori error control concept developed in [6].

With this numerical approach we for the first rising bubble benchmark from [11] obtain the results in Table 1. In this table $c_{\min}$ denotes the minimal circularity of the bubble which is achieved at time $t_{c=c_{\min}}$, $V_{c,\max}$ denotes the maximal rising velocity achieved at time $t|_{V_c=V_{c,\max}}$, and $y_c(t=3)$ denotes the y-component of the center of mass at final time $t = 3$.

ϵ	$c_{\min}$	$t\|_{c=c_{\min}}$	$V_{c,\max}$	$t\|_{V_c=V_{c,\max}}$	$y_c(t=3)$
0.0200	0.9035	1.9486	0.2370	1.0000	1.0759
0.0100	0.9019	1.9076	0.2402	0.9375	1.0782
0.0050	0.9015	1.9012	0.2412	0.9286	1.0788
0.0025	0.9013	1.9063	0.2419	0.9103	1.0791

TABLE 1. Numerical results for first rising bubble benchmark in [11].

2. MPC OF THE CAHN-HILLIARD NAVIER-STOKES SYSTEM

The aim of mpc consists in steering or keeping the state of a dynamical system to or at a given desired trajectory, see e.g. [5]. To fix the concept, let us rewrite our Cahn-Hilliard Navier-Stokes system as an abstract dynamical system with initial condition x^0, state $x(t)$, observation $y(t)$ and control $u(t)$;

$$\begin{aligned} \dot{x}(t) + Ax(t) &= b(x,t) + \mathcal{B}u(t), \\ y(t) &= \mathcal{C}x(t), \\ x(0) &= x^0. \end{aligned} \tag{5}$$

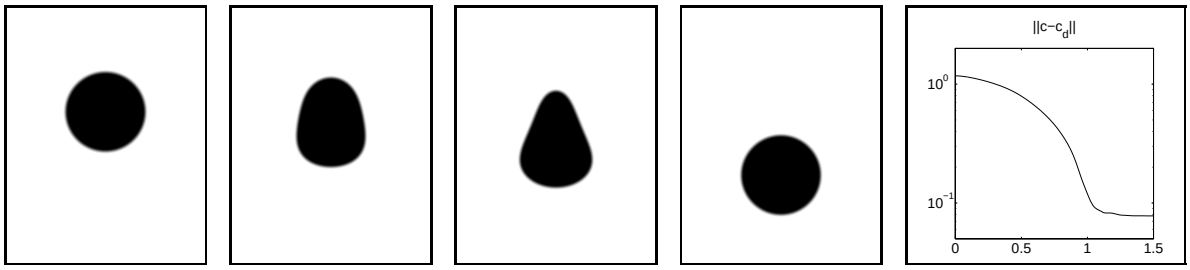

FIGURE 1. Control light bubble against gravitational force.

The aim of mpc consists in constructing a nonlinear feedback control law K with $\mathcal{B}u(t) = K(y(t))$, which steers the observable part of the dynamical system to the desired trajectory $\bar{y}(t)$ in the observation space, i.e.

$$y(t) \overset{!}{\to} \bar{y}(t),\ (t \to \infty).$$

To prepare for model predictive control, system (5) is discretized in time using the semi-implicit Euler method on a time grid $0 = t_0 \leq t_1 \leq \dots$ with $t_{k+1} - t_k = \tau_k$ for $k = 0, 1, 2, \dots$. Here x^k denotes the state at time t_k and b^k denotes the nonlinearity $b(x^k, t_k)$. For given initial state x^0 we obtain the time discrete model

$$(I + \tau_k A)x^{k+1} = x^k + \tau_k b^k + u^{k+1}, \quad k = 0, 1, \dots \tag{6}$$

and consider for given time horizon $L > 0$ and $\alpha > 0$ the optimal control problem

$$(\mathcal{P}_k) \qquad \begin{aligned} &\min J(x^{j+1}, \dots, x^{j+L}, u^{j+1}, \dots, u^{j+L}) \\ &\qquad \text{s.t. (6) for } j = k, \dots, k + L - 1, \end{aligned}$$

where

$$J(x^{j+1}, \dots, x^{j+L}, u^{j+1}, \dots, u^{j+L}) := \sum_{i=1}^{L} \left(\frac{1}{2} \|x^{k+i} - \bar{x}^{k+i}\|^2 + \frac{\alpha}{2} \|u^{k+i}\|^2 \right).$$

Let us note that problem $(\mathcal{P}_k)$ for $L = 1$ admits a unique solution. However, for $L > 1$ solutions in general need not be unique since (6) then represents a nonlinear constraint. In that case we assume that $(\mathcal{P}_k)$ admits a solution. Details can be found in [9].

In Figure 1 we from left to right show time snapshots of the rising bubble benchmark controlled with an instantaneous control strategy using one steepest descent step for the approximate solution of the mpc control problem in the case $L = 1$, together with the evolution of $\|c - c_d\|_{L^2(\Omega)}$. As control action we take wall parallel Dirichlet boundary control. The control goal consists in steering the bubble back to the bottom of the column.

REFERENCES

[1] H. Abels, H. Garcke, and G. Grün, *Thermodynamically consistent, frame indifferent diffuse interface models for incompressible two-phase flows with different densities*, Mathematical Models and Methods in Applied Sciences **22**(3) 2012.

[2] J. Blowey, and C. Elliott, *The Cahn-Hilliard gradient theory for phase separation with non-smooth free energy. Part I: Mathematical analysis*, European Journal of Applied Mathematics **2** 1991, 233-280.
[3] H. Choi, M. Hinze, and K. Kunisch, *Instantaneous control of backward-facing step flows*, Applied numerical mathematics **31**(2), 133–158.
[4] D. Eyre, *Unconditionally Gradient Stable Time Marching the Cahn-Hilliard Equation*, Computational and Mathematical Models of Microstructural Evolution, MRS Proceedings 529, 1998, 140–171.
[5] L. Grüne, and J. Pannek, *Nonlinear Model Predictive Control*, Communications and Control Engineering 370, Springer 2011.
[6] M. Hintermüller, M. Hinze, and C. Kahle, *An adaptive finite element Moreau–Yosida-based solver for a coupled Cahn–Hilliard/Navier–Stokes system*, Journal of Computational Physics **235** 2013, 810–827.
[7] M. Hintermüller, M. Hinze, and M.H. Tber, *An adaptive finite element Moreau–Yosida-based solver for a non-smooth Cahn–Hilliard problem*, Optimization Methods and Software **25** 2011, 777–811.
[8] M. Hinze, *Instantaneous closed loop control of the Navier-Stokes system*, SIAM J. Contr.Optim., **44**(2), 564–583.
[9] M. Hinze, and C. Kahle, *A nonlinear Model Predictive Concept for the Control of Two-Phase Flows governed by the Cahn–Hilliard Navier–Stokes System*, Proceedings of the 25th IFIP TC7 Conference 2012.
[10] M. Hinze, and S. Volkwein, *Instantaneous control for the Burgers equation: Convergence analysis and numerical implementation*, Nonlinear Analysis **50**(1), 1–26.
[11] S. Hysing, S. Turek, D. Kuzmin, N. Parolini, E. Burman, S. Ganesan, and L. Tobiska, *Quantitative benchmark computations of two-dimensional bubble dynamics*, International Journal for Numerical Methods in Fluids **60** 2009, 1259–1288.
[12] D. Kay, V. Styles, and R. Welford, *Finite element approximation of a Cahn-Hilliard-Navier-Stokes system*, Interfaces and Free Boundaries **10** 2008, 15–43.

A model of bacteria's activities under environmental constraints

Nobuyuki Kenmochi

This work was motivated by "the brewing process of Japanese sake (rice wine)". The process proceeds with several bacreria's activities and one of important questions is how to control them in appropriate artificial ways; for instance heat source control and stirring materials. The objective of this research is to establish some mathematical tools for modeling a class of nonlinear phenomena with quasi-variational structure, arising in such a brewing process of Japanese sake.

Let Ω be a bounded domain in $\mathbf{R}^3$, $\Gamma = \partial\Omega$, $Q = \Omega \times (0,T)$, $\Sigma = \Gamma \times (0,T)$. In our problem the unknowns are $\mathbf{w} = (w_1, w_2)$, densities of two species of bacteria, θ, temperature and $\mathbf{v} = (v_1, v_2, v_3)$, velocity of a fluid flow. They are respectively governed by reaction-diffusion inclusion, heat-convection equation and Navier-Stokes inclusion in Q with appropriate initial-boundary boundary conditions.

(Bacteria's activities in environment constraint $\mathbf{E}(\theta)$ in a fluid)

$$(BA)\quad \begin{cases} \mathbf{w}_t - \tau\Delta\mathbf{w} + (\mathbf{v}\cdot\nabla)\mathbf{w} + \partial I_{\mathbf{E}(\theta)}(\mathbf{w}) \ni \mathbf{g}(\theta,\mathbf{w}) \text{ in } Q, \\ \dfrac{\partial \mathbf{w}}{\partial n} = 0 \text{ on } \Sigma,\ \mathbf{w}(\cdot,0) = \mathbf{w}_0 \text{ in } \Omega, \end{cases}$$

where $\mathbf{g}(\theta, \mathbf{w}) : \mathbf{R}^3 \to \mathbf{R}^2$ is Lipschitz continuous;

$\mathbf{E}(\theta) \subset \mathbf{R}^2$ is an environmental constraint which is a compact convex set in $\mathbf{R}^2$ such that int.$\mathbf{E}(\theta) \neq \emptyset$ in $\mathbf{R}^2$, $\theta \to \mathbf{E}(\theta)$ is continuous in the Hausdorff distance in $\mathbf{R}^2$ and

$$\cup_{\theta \in \mathbf{R}} \mathbf{E}(\theta) \subset \mathbf{E}_0, \ \mathbf{E}_0 \text{ is bounded in } \mathbf{R}^2, \ \cap_{\theta \in \mathbf{R}} \text{int.} \mathbf{E}(\theta) \neq \emptyset;$$

$I_{\mathbf{E}(\theta)}$ is the indicator function of $\mathbf{E}(\theta)$ and $\partial I_{\mathbf{E}(\theta)}(\cdot)$ is its subdifferential in $\mathbf{R}^2$; $\mathbf{w}_0 \in \mathbf{E}(\theta_0)$ is an initial datum.

(Heat equation with convection v)

$$(H) \ \begin{cases} \theta_t - \kappa \Delta \theta + \mathbf{v} \cdot \nabla \theta = h(x, \theta, \mathbf{w}) \text{ in } Q, \\ \theta = \theta_\Gamma \text{ on } \Sigma, \ \theta(\cdot, 0) = \theta_0 \text{ in } \Omega, \end{cases}$$

where $h(x, \theta, \mathbf{w}) : \overline{\Omega} \times \mathbf{R}^3 \to \mathbf{R}$ is Lipschitz continuous; θ_Γ is smooth on $\overline{\Sigma}$; $\theta_0$is smooth in $\overline{\Omega}$,; κ is a positive constant.

(Navier-Stokes equation with velocity constraint $\mathbf{V}(\theta)$)

$$(NS) \ \begin{cases} \mathbf{v}_t - \nu \Delta \mathbf{v} + (\mathbf{v} \cdot \nabla)\mathbf{v} + \partial I_{\mathbf{V}(\theta)}(\mathbf{v}) \ni \nabla P + \mathbf{f}(x, \theta, \mathbf{w}) \textbf{ in } Q, \\ \text{div} \mathbf{v} = 0 \text{ in } Q, \\ \mathbf{v} = 0 \text{ on } \Sigma, \ \mathbf{v}(\cdot, 0) = \mathbf{v}_0 \text{ in } \Omega, \end{cases}$$

where $\mathbf{V}(\theta) := \{\mathbf{z} = (z_1, z_2, z_3) \in \mathbf{H}^1_{0,\sigma}(\Omega) \mid |\nabla \mathbf{z}| \leq \rho(\theta) \text{ a.e. in } \Omega\}$ and $|\nabla \mathbf{z}| := (\sum_{i=1}^3 |\nabla z_i|^2)^{1/2}$; $\rho(\theta) : \mathbf{R} \to \mathbf{R}$ is a smooth function such that $0 < C_0 \leq \rho(\theta) \leq C_1, \ \forall \theta \in \mathbf{R}$ for positive constants C_0 and C_1; $\mathbf{v}_0 \in \mathbf{H}^1_{0,\sigma}(\Omega) \cap \mathbf{V}(\theta_0)$;
$\mathbf{f}(x, \theta, \mathbf{w}) : \overline{\Omega} \times \mathbf{R}^3 \to \mathbf{R}^3$ is Lipschitz continuous.

Expressions (NS) and (BA) are quite formal. They are rigorously reformulated as variational inequalities (VNS) and (VBA) as formulated below. We denote by (*) the following regularlity property of θ:

$$(*) \ \theta \in W^{1,2}(0, T; H^1(\Omega)) \cap L^\infty(0, T; H^2(\Omega)) \subset C(\overline{Q}).$$

(VNS) $\forall \theta$ with (*), $\forall \mathbf{w} \in \mathbf{E}_0$ a.e. in Q, $\mathbf{w} \in L^2(0, T; H^1)$,
$\exists_1 \mathbf{v} \in C([0, T]; \mathbf{L}^2_\sigma(\Omega)), \ \mathbf{v}(0) = \mathbf{v}_0, \ \mathbf{v} \in \mathbf{V}(\theta)$ a.e. in Q such that

$$\int_0^T (\eta', \mathbf{v} - \eta) dt + \nu \int_0^T (\nabla \mathbf{v}, \nabla(\mathbf{v} - \eta)) dt + \int_0^T ((\mathbf{v} \cdot \nabla)\mathbf{v}, \mathbf{v} - \eta) dt$$

$$+ \frac{1}{2} |\mathbf{v}(T) - \eta(T)|^2 \leq \int_0^T (\mathbf{f}(\cdot, \theta, \mathbf{w}), \mathbf{v} - \eta) dt + \frac{1}{2} |\mathbf{v}_0 - \eta(0)|^2$$

$$\forall \eta \in \mathbf{V}(\theta) \text{ a.e. in } Q, \ \eta' \in L^2(0, T; \mathbf{L}^2_\sigma(\Omega)).$$

(VBA) $\forall \mathbf{v}, \ |\nabla \mathbf{v}| \leq C_1$ a.e. in Q, $\forall \theta$ with (*),

$\exists_1 \mathbf{w} \in C([0,T];L^2(\Omega)^2),\ \mathbf{w}(0)=\mathbf{w}_0,\ \mathbf{w}\in\mathbf{E}(\theta)$ a.e. in Q such that

$$\int_0^T(\xi',\mathbf{w}-\xi)dt+\tau\int_0^T(\nabla\mathbf{w},\nabla(\mathbf{w}-\xi))dt+\int_0^T((\mathbf{v}\cdot\nabla)\mathbf{w},\mathbf{w}-\xi)dt$$
$$+\frac{1}{2}|\mathbf{w}(T)-\xi(T)|^2\le\int_0^T(\mathbf{g}(\theta,\mathbf{w}),\mathbf{w}-\xi)dt+\frac{1}{2}|\mathbf{v}_0-\xi(0)|^2$$
$$\forall\xi\in\mathbf{E}(\theta)\text{ a.e. in }Q,\ \xi\in W^{1,2}(0,T;L^2(\Omega)^2)\cap L^2(0,T;H^1(\Omega)^2).$$

Now, our system $\{(H),(NS),(BA)\}$ are understood as a quasi-variational inequality $\{(H),(VNS),(VBA)\}$ and we have the following existence result.

Theorem Assume that $\theta_0\in H^2(\Omega),\mathbf{w}_0\in H^1(\Omega)^2,\mathbf{v}_0\in\mathbf{H}^1_{0,\sigma}(\Omega)$ and
$$\theta_0=\theta_\Gamma\text{ on }\Gamma,\ \mathbf{w}_0\in\mathbf{E}(\theta_0),\mathbf{v_0}\in\mathbf{V}(\theta_0)\text{ a.e. in }\Omega.$$

Then, $\exists\{\theta,\mathbf{v},\mathbf{w}\}$ solving (H),(VNS),(VBA) in the space

$$\theta\in W^{1,2}(0,T;H^1(\Omega))\cap L^\infty(0,T;H^2(\Omega))\subset C(\overline{Q}),$$
$$\mathbf{v}\in C([0,T];\mathbf{L}^2_\sigma(\Omega)),\mathbf{v}\in\mathbf{V}(\theta)\text{ a.e. in }Q,$$
$$\mathbf{w}\in C([0,T];L^2(\Omega)^2)\cap L^2(0,T;H^1(\Omega)^2),\mathbf{w}\in\mathbf{E}(\theta)\text{ a.e. in }Q.$$

Proof. (cf. [3,5]) Put

$$\Phi:=\{\theta\in C(\overline{Q})\mid|\theta|_{W^{1,2}(0,T;H^1(\Omega))}+|\theta|_{L^\infty(0,T;H^2(\Omega))}\le Const.\}$$

which is compact in $C(\overline{Q})$. Consider the mapping $S:\Phi\to\Phi$ as follows: For each $\theta\in\Phi$, solve the system of (VNS)-(VBA) and denote by $\{\mathbf{v},\ \mathbf{w}\}$ the solution. Next, to this pair $\{\mathbf{v},\ \mathbf{w}\}$, solve (H) and denote by $\tilde{\theta}$ the solution of (H). Now we define a mapping S by $S\theta=\tilde{\theta}$. Then we can show that S maps Φ into itself and is continuous in Φ in the topology of $C(\overline{Q})$, whence S possesses at least one fixed point θ in Φ. This fixed point θ gives a solution $\{\theta,\mathbf{v},\mathbf{w}\}$ of our problem, where $\{\mathbf{v},\mathbf{w}\}$ is the solution of $(VNS)-(VBA)$.

References

[1] A. Kadoya, N. Kenmochi and Y. Murase, *A class of nonlinear parabolic systems with environmental constraints*, Adv. Math. Sci. Appl., **20** (2010), 281-313.

[2] R. Kano, N. Kenmochi and Y. Murase, *Nonlinear evolution equations generated by subdifferentials with nonlocal constraints*, Banach Center Publications, Polish Acad. Sci., Inst. Math., **86** (2009), 175-194.

[3] N. Kenmochi, *Prabolic quasi-variational diffusion problems with gradient constraints*, Disc. Cont. Dyn. Systems, Ser. S, **6-2** (2013), 423-438.

[4] T. Fukao and N. Kenmochi, *Variational inequality for the Navier-Stokes equations with time dependent constraint*, Gakuto Intern. Math. Sci. Appl., **34**, 2011, 87-102.

[5] T. Fukao and N. Kenmochi, *Weak solvability for parabolic quiasi-variational inequalities*, in preparation.

Interface development in biological tissue growth

John R. King

Interfaces can arise in mathematical models of tissue growth for a variety of reasons and our goal here is to illustrate some of the considerations that arise in analysing some of the simplest of these. The most obvious is that the (growing) tissue itself will be of finite extent, but others (which may be interpreted in terms of sharp-interface-limit processes) include internal boundaries of viable and necrotic regions, interfaces generated by cell sorting into distinct cell types and boundaries between domains comprising close-packed and more disperse cells.

The last of these can conveniently be exemplified by the simplest level of modelling of such processes, namely via a single PDE

$$\frac{\partial n}{\partial t} = \nabla \cdot (D(n)\nabla n) + kn, \tag{1}$$

wherein $n(\boldsymbol{x}, t) \in [0, 1]$ is the volume fraction of cells (normalised such that $n = 1$ represents the close-packed state), the nonlinearity $D(n)$ reflects cell-cell ineractions (we revisit such issues below), with $D(n) \to +\infty$ as $n \to 1^-$ to reflect repulsion as close packing is approached; the propensity of cells to aggregate can result in $D(n) < 0$ applying for some n, in which case regularisation is required (we restrict ourselves here to the case $D(n) > 0$ for all n). Finally, the positive constant k is the birth rate of cells (which are assumed nutrient rich): this explicitly biological feature of the model leads to a tendency for n to seek to exceed the physical limit $n = 1$ and a question of much broader mathematical interest in the context of tissue-growth models is whether the model forbids this *a priori* or whether an interface must be introduced, with $n \equiv 1$ holding on one side of it. Equation (1) provides perhaps the simplest such example. We set

$$D(n) \sim 1/(1-n)^\gamma \quad \text{as} \quad n \to 1^-$$

for positive constant γ and introduce $w = 1 - n$ (this would typically represent the volume fraction of water). For $0 \le w \ll 1$, in the one-dimensional case we then have dominant balance

$$\frac{\partial w}{\partial t} \sim \frac{\partial}{\partial x}(w^{-\gamma}\frac{\partial w}{\partial x}) - k. \tag{2}$$

For $\gamma > 1$, the model then suffices as it stands: as $t \to +\infty$ we have

$$w \sim e^{-2kt/(\gamma-1)}\Phi(\eta),\ \eta = x/e^{kt},$$

$$\Phi(\eta) = (\frac{k(\gamma-1)}{2}(M^2 - \eta^2))^{-\frac{1}{\gamma-1}} \quad \text{for} \quad |\eta| < M, \tag{3}$$

where the form of η is dictated by overall conservation of mass and the exponent in w then follows on balancing terms on the right-hand side of (2), the time derivative being negligible, and where the constant M reflects the initial mass of tissue. It is clear that (3) is singular at $\eta = \pm M$, so these do act as moving boundaries in the

sharp-interface limit associated with the large-time behaviour, and inner regions with scalings

$$x = s(t) + \zeta/e^{kt},\ w = O(1)\ s(t) \sim \pm M e^{kt} \quad \text{as} \quad t \to +\infty$$

alleviate the singularities. More interesting in some respects, however, is the less singular case $\gamma < 1$: here n_{max} reaches 1 in finite time and a moving boundary must of necessity be introduced, with one possibility being to replace the source term in (1) by 0 if $w = 0$ (i.e. kn becomes $knH(w)$ for a Heaviside function H) to reflect that cell birth is not possible when the constituents required to produce new cells are absent. The resulting moving-boundary problem (assuming symmetry in x for simplicity) has $n = 1, w = 0$ for $|x| < s(t)$, while (1) holds in $x > s(t)$ with

$$\text{at } x = s(t) \quad n = 1, \quad D(n)\frac{\partial n}{\partial x} = 0, \quad \text{as } x \to +\infty \quad n \to 0.$$

This formulation is closely related to the Stefan problem for the freezing of a supercooled liquid, so there are issues of stability and well-posedness, but all being well the large-time behaviour is likely to be or travelling-wave form, the wavespeed selection mechanism being akin to that of Fisher's equation. Analysis of the local behaviour at the interface reveals the two scenarios above indeed to be mutually exclusive, and $\gamma = 1$ is an interesting (and significant) borderline case.

More realistic continuum-level models need to be of multiphase form to account for distinct cell types and so forth. It is instructive to consider a three-phase case, with $n(\boldsymbol{x}, t)$, $m(\boldsymbol{x}, t)$ and $w(\boldsymbol{x}, t)$ being respectively the volume fractions of cells, dead cell matter and water. Typical conservation of mass equations would involved cell birth and death rates k_b and k_d in the form

$$\frac{\partial n}{\partial t} + \nabla \cdot (\boldsymbol{v}_n n) = k_b n - k_d n, \ \frac{\partial m}{\partial t} + \nabla \cdot (\boldsymbol{v}_m m) = \theta k_d n,$$
$$\frac{\partial w}{\partial t} + \nabla \cdot (\boldsymbol{w}\boldsymbol{v}_w) = -k_b n + (1-\theta) k_d n,$$

where distinct velocity fields are introduced in the three (incompressible) phases, with the no-voids condition then taking the two equivalent forms

$$n + m + w = 1, \quad \nabla \cdot (\boldsymbol{v}_n n + \boldsymbol{v}_m m + \boldsymbol{v}_w w) = 0. \tag{4}$$

The momentum equations, as derived by for example a Rayleighian-based variational argument involving a free-energy density $f(n, m, w)$, take the form

$$\begin{aligned}
\mathbf{0} &= -n\nabla\left(p + \frac{\partial f}{\partial n}\right) - \kappa_{nm}(\boldsymbol{v}_n - \boldsymbol{v}_m) - \kappa_{nw}(\boldsymbol{v}_n - \boldsymbol{v}_w), \\
\mathbf{0} &= -m\nabla\left(p + \frac{\partial f}{\partial m}\right) - \kappa_{nm}(\boldsymbol{v}_m - \boldsymbol{v}_n) - \kappa_{mw}(\boldsymbol{v}_m - \boldsymbol{v}_w), \\
\mathbf{0} &= -w\nabla\left(p + \frac{\partial f}{\partial w}\right) - \kappa_{nw}(\boldsymbol{v}_w - \boldsymbol{v}_n) - \kappa_{mw}(\boldsymbol{v}_w - \boldsymbol{v}_m).
\end{aligned} \tag{5}$$

An overall momentum balance (i.e. summing equations (5)) leads to Legendre-transform expression for the hydrostatic pressure p:

$$p = f - n\frac{\partial f}{\partial n} - m\frac{\partial f}{\partial m} - w\frac{\partial f}{\partial w}. \tag{6}$$

That a scalar relationship (6) results from a vector system leaves the model underspecified – this is associated with Noether's second theorem, given that the continuum-mechanical equations (i.e. (5) and the second of (4)) are invariant under $\boldsymbol{v}_i \to \boldsymbol{v}_i + \boldsymbol{V}$ for $i = n, m, w$ provided only that $\nabla \cdot \boldsymbol{V} = 0$. A closed system can be recovered either by introducing viscous terms, say, into the intraphase constitutive relations or, as we do here, by the (usually simply mathematical) expedient of imposing $n\boldsymbol{v}_n + m\boldsymbol{v}_m + w\boldsymbol{w}_w = \boldsymbol{0}$, rather than just (4). The balance between the drag and other terms in (5) can (in the light of (6)) induce backward-diffusive effects for suitable f, again typically reflecting cell aggregation: these can be regularised by, for example, introducing viscous effects as above (leading to regularisations of pseudoparabolic type) or by requiring f to depend also on spatial derivatives (cf. the Cahn-Hilliard equation).

We conclude here by further simplifying the formulation via some biologically motivated limits, namely $\kappa_{nm} \to \infty,\ \kappa_{nw},\ \kappa_{mw} \to 0$ with $w = O(\kappa_w^{1/2}),\ |\boldsymbol{v}_{\boldsymbol{w}}| = O(\kappa_w^{-1/2})$, where $\kappa_w = \kappa_{nw} + \kappa_{mw}$. Taking, for the sake of illustration, f to be purely entropic in form then under suitable scalings we obtain at leading order

$$n + m = 1,\ \boldsymbol{v}_n = \boldsymbol{v}_m = w\nabla w/\kappa_w,\ \boldsymbol{v}_w = -\nabla w/\kappa_w,$$

and, for suitable $\kappa_w(n, m, w)$, the novel free boundary problem

$$\frac{\partial n}{\partial t} + \nabla \cdot (\frac{nw}{\kappa_w}\nabla w) = (k_b - k_d)n,\ \nabla \cdot (\frac{w}{\kappa_w}\nabla w) = (k_b - (1-\theta)k_d)n \text{ in } \Omega(t),$$
$$\frac{\partial n}{\partial \nu} = 0,\ V_\nu = \frac{w}{\kappa_w}\frac{\partial w}{\partial \nu} \text{ on } \partial\Omega(t),$$

where V_ν is the outward normal velocity, and $\partial/\partial\nu$ the outward normal derivative, of the free boundary. Note that

$$\frac{\partial n}{\partial t} + \boldsymbol{v}_n \cdot \nabla n = k_b n(1-n) - k_d n(1-(1-\theta)n),$$

so here n is prevented from reaching 1 without any need to impose such a constraint. While the system can be reduced to a free-boundary problem for a pair of reaction-degenerate-diffusion equations without exploiting these limits, the above is instructive as representative of the simplest formulations of the current class.

Numerous effects are omitted in the above discussion: more realistic intraphase constitutive relations should be considered, nutrient transport and consumption should be included, other phases are needed in typical regenerative-medicine contexts in order to capture cellular differentiation and many other such phenomena warrant consideration. It is hoped that the above remarks nevertheless serve to illustrate the novel free-boundary formulations that are applicable in such systems-biology applications.

Material optimization: control in the coefficients of nonlinear elliptic problems

Günter Leugering
(joint work with Peter I. Kogut)

In recent years functionalization of materials has become a major field of reseach in materials sciences and applied mathematics, where in particular inverse problems and optimization problems have been investigated in order to find optimal material distributions, inclusions, layers, holes and more generally microstructures embedded into bulk material such that a given merit function which, in turn, describes macroscopic material properties is optimized. There are several different approaches to cope with this problem: one is to use phase field models that model bulk material and, say, inclusions or holes (even cracks) via phase variables and evolve the phases whereas a second one uses transmission conditions and shape or topological sensitivities in order to optimally move the interfaces of the inclusions or the holes. The phase field models, as discussed thoroughly during the conference, contain a relaxation parameter ϵ governing the 'sharpness' of the 'interfaces' between the phases. In principle, letting ϵ tend to zero, sharp interfaces occur. This provides the chance, which however still has to be explored mathematically, to perform optimization with respect to material and geometrical properties of the phases on a given positive ϵ level and then converge towards sharp interfaces. The other approach insists on sharp interfaces to begin with and relies on shape and/or topological sensitivities which may be difficult to obtain due to potential non-smoothness. In a third approach one is less specific about a particular material distributions or distributions of inclusions, rather one looks at the stiffness tensors (matrices) as a whole object of optimization. In that approach the material may change 'pixel by pixel' in an L^∞ manner while keeping symmetry as the only underlined structural property. This approach, which has come to be known as Free material Optimization (FMO), is the most radical one, as it provides in a sense 'utopia material'. One needs to add certain manufacturability constraints in order to make the procedure practical and comparable to the other more classical procedures. The limited space prohibits a fair account of references for the three approaches mentioned. We instead just refer to [7] and the references therein. Clearly, FMO relates to optimization in the coefficients of typically elliptic problems and, in fact, this is also true for the other approaches, at least in principle. It turns out in a variety of applications that the corresponding matrices may exhibit degeneration (e.g. damage, fissures, cracks, cloaking). Thus, a general theory for control in the coefficients should reflect this necessity. Moreover, almost all of the results available for material optimization appear to rely on linear constitutive equations for elasticity, piezoelectricity or in Maxwell systems. However, the models should reflect nonlinear behavior as well. Therefore, we concentrated in this lecture on the problem of control in the coefficients for the heterogeneous p-Laplacian. Problems of control in the coefficients have been the subject of a number of publications. We refer to [1] and [2] and the references therein. Clearly,

in an 'all-at-once' approach, a minimizing sequence involves the matrices (say A_k) and the states (say y_k), typically in a product of A_k and (a function of) the gradient of y_k. This situation is closely related to the framework of homogenization and it is no surprise that H-convergence of matrices plays a dominant role also in the context of coefficient-control. However, unfortunately, a lower strictly positive bound (a.e.) has to be employed in order to prove the necessary H-compactness results needed in the proofs. This is the point of departure for the recent work of the authors. See [3, 4, 5]. When dealing with degenerate matrices, even in the linear elliptic case, one has to treat the problem in the setting of weighted Sobolev spaces, the weights being in terms of the matrices. Consequently, once dealing again with minimizing sequences, one then has to work in sequences of such weighted spaces. This makes the analysis interesting on the one side but also quite tedious. In addition to the inherent difficulties, degeneration may give rise to the so-called Laverentiev gap-phenomenon. Below, we formulate the problem and present our recent result on optimality conditions[6] which in the linear case coincide with those in the literature, e.g.[1]. We define $M_p^{\alpha,\beta}(\Omega)$ as a set of $\mathcal{U}(x) = [a_{i\,j}(x)]_{1\le i,j\le N}$ in $L^\infty(\Omega;\mathbb{R}^{N\times N})$ with:

$$|a_{ij}(x)| \le \beta \quad \text{a.e. in } \Omega\ \forall\, i,j \in \{1,\dots,N\},$$

$$\big(\mathcal{U}(x)([\zeta^{p-2}]\zeta - [\eta^{p-2}]\eta), \zeta-\eta\big)_{\mathbb{R}^N} \ge 0 \quad \text{a.e. in } \Omega\ \forall\, \zeta,\eta \in \mathbb{R}^N,$$

$$\big(\mathcal{U}(x)[\zeta^{p-2}]\zeta,\zeta\big)_{\mathbb{R}^N} = \sum_{i,j=1}^{N} a_{i\,j}(x)|\zeta_j|^{p-2}\,\zeta_j\,\zeta_i \ge \alpha\,|\zeta|_p^p \quad \text{a.e in } \Omega,$$

$$[\eta^{p-2}] = \operatorname{diag}\{|\eta_1|^{p-2}, |\eta_2|^{p-2}, \dots, |\eta_N|^{p-2}\} \quad \forall \eta \in \mathbb{R}^N.$$

Let ξ_1, ξ_2 be given functions of $L^\infty(\Omega)$ such that $0 \le \xi_1(x) \le \xi_2(x)$ a.e. in Ω. Let Q_i be nonempty compact convex in $W^{-1,\,q}(\Omega)$. Let

$$U_b := \big\{\mathcal{U} = [a_{i\,j}] \in M_p^{\alpha,\beta}(\Omega)\big|\ \xi_1(x) \le a_{i\,j}(x) \le \xi_2(x) \text{ a.e. in } \Omega,\ \forall\, i,j = 1,\dots,N\big\},$$

$$U_{sol} := \big\{\mathcal{U} = [u_1,..,u_N] \in M_p^{\alpha,\beta}(\Omega)\big|\ \operatorname{div} u_i \in Q_i,\ \forall\, i = 1,..,N\big\},\ U_{ad} := U_b \cap U_{sol}.$$

$$\text{Minimize} \quad \left\{ I_\Omega(\mathcal{U},y) = \int_\Omega |y(x) - y_d(x)|^p\,dx \right\}$$

subject to the constraints

$$\mathcal{U} \in U_{ad} \subset L^\infty(\Omega;\mathbb{R}^{N\times N}), \quad y \in W_0^{1,p}(\Omega),$$

$$-\operatorname{div}\,\big(\mathcal{U}[(\nabla y)^{p-2}]\nabla y\big) + |y|^{p-2}y = f \quad \text{in } \Omega,$$

$$y = 0 \quad \text{on } \partial\Omega,$$

For the sake of simplicity, we restrict our consideration here to diagonal matrices. We define $\mathfrak{M}(\Omega) \subset W_0^{1,p}(\Omega)$: $y \in \mathfrak{M}(\Omega)$ if and only if

$$\exists\, \zeta \in L^1(\Omega) \ \text{ such that } \ \zeta > 0 \text{ a. e. in } \Omega,\ \zeta^{-1} \in L^1(\Omega),$$

$$\big(\xi,\mathcal{U}[(\nabla y)^{p-2}]\xi\big)_{\mathbb{R}^N} \ge \zeta(x)\,\|\xi\|_{\mathbb{R}^N}^2 \quad \text{a.e. in } \Omega,\ \forall\, \xi \in \mathbb{R}^N, \ \text{ and } \ |y|^{2-p} \in L^1(\Omega).$$

(H1) For $f \in W^{-1,q}(\Omega)$ with $q = \frac{p}{p-1}$ and $p \geq 2$, $y(\mathcal{U}) \in \mathfrak{M}(\Omega)$ $\forall \mathcal{U} \in U_{ad} := U_b \cap U_{sol}$. (H2) Let $\zeta_{ad} : \Omega \to \mathbb{R}^1_+$ satisfy

$$\zeta_{ad} \in L^1(\Omega), \quad \zeta_{ad}^{-1} \in L^1(\Omega), \quad \zeta_{ad}^{-1} \notin L^\infty(\Omega),$$

There exist elements f_* and ζ_* in $L^1(\Omega)$ such that $f_* > \zeta_* \geq \zeta_{ad}$ and, for each $\left(\widehat{\mathcal{U}}, \widehat{y}\right) \in U_{ad} \times \mathfrak{M}(\Omega)$, $\eta \in \mathbb{R}^1$, and $\xi \in \mathbb{R}^N$, the following conditions hold true almost everywhere in Ω:

$$(\eta^2 + \|\xi\|^2_{\mathbb{R}^N})\zeta_* \leq |\widehat{y}|^{p-2}\eta^2 + \left(\xi, \widehat{\mathcal{U}}[(\nabla\widehat{y})^{p-2}]\xi\right)_{\mathbb{R}^N} \leq (\eta^2 + \|\xi\|^2_{\mathbb{R}^N})f_*.$$

Theorem:[6] Assume (H1), (H2), $p \geq 2$, $f \in W^{-1,q}(\Omega)$, $U_{ad} \neq \emptyset$.
Let $(\mathcal{U}_0, y_0) \in L^\infty(\Omega; \mathbb{R}^{N\times N}) \times W_0^{1,p}(\Omega)$ be an optimal pair. There exists an element $\psi \in H^p_{\mathcal{U}_0,y_0}(\Omega)$ such that

$$\int_\Omega \left((\mathcal{U} - \mathcal{U}_0)[(\nabla y_0)^{p-2}]\,\nabla y_0, \nabla\psi\right)_{\mathbb{R}^N} dx \geq 0, \quad \forall \mathcal{U} \in U_{ad},$$

$$\int_\Omega \left(\mathcal{U}_0[(\nabla y_0)^{p-2}]\nabla y_0, \nabla\varphi\right)_{\mathbb{R}^N} dx + \int_\Omega |y_0|^{p-2}y_0\varphi\, dx = \\ = \langle f, \varphi\rangle_{W_0^{1,p}(\Omega)}, \ \forall\varphi \in W_0^{1,p}(\Omega),$$

$$(p-1)\int_\Omega \left([(\nabla y_0)^{p-2}]\,\mathcal{U}_0\nabla\psi, \nabla\varphi\right)_{\mathbb{R}^N} dx + (p-1)\int_\Omega |y_0|^{p-2}\,\psi\,\varphi\, dx = \\ = p\int_\Omega |y_0 - y_d|^{p-1}\varphi\, dx, \ \forall\varphi \in C_0^\infty(\Omega).$$

References

[1] K. Deckelnick and M. Hinze, Convergence and error analysis of a numerical method for the identification of matrix parameters in elliptic PDEs Iinverse Problerms, **28(11)** (2012), doi:10.1088/0266-5611/28/11/115015, 15p.

[2] J. Haslinger, M. Kocvara, G. Leugering and M. Stingl, Multidisciplinary free material optimization. SIAM J. Appl. Math. 70 no. 7, 2709-2728 (2010).

[3] P. Kogut and G. Leugering, *Optimal control of partial differential eqautions on reticulated domains: Approximation and Asymptotic analysis* , Birkhäuser Verlag (2011).

[4] P.I. Kogut and G. Leugering, Optimal L1-control in coefficients for Dirichlet elliptic problems: W-optimal solutions. J. Optim. Theory Appl. 150, no. 2, 205-232 (2011).

[5] P.I. Kogut and G. Leugering, Optimal L1-control in coefficients for Dirichlet elliptic problems: H-optimal solutions. Z. Anal. Anwend. 31, no. 1, 31-53 (2012).

[6] P.I. Kogut and G. Leugering, Optimal Control Problems in Coefficients for Nonlinear Dirichlet Problems of Monotone Type: Optimality Conditions, submitted 2013.

[7] G. Leugering and M.Stingl, PDE-constrained optimization for advanced materials. GAMM-Mitt. 33 no. 2, 209-229 (2010).

Boundary Control of the Obstacle Problem

Christian Meyer
(joint work with Daniel Wachsmuth)

We consider an optimal control problem governed by the obstacle problem. The control enters the system via the Neumann boundary data. To be more precise the optimization problem reads

$$\text{(1)} \qquad \begin{cases} \min & g(y) + j(u) \\ \text{s.t.} & a(y, v-y) \geq \displaystyle\int_\Gamma u(v-y)\,dx \quad \forall\, v \in K \\ & y \in K, \end{cases}$$

where $\Omega \subset \mathbb{R}^d$, $d = 2, 3$, is a given bounded Lipschitz domain with boundary Γ. Moreover, $a : H^1(\Omega) \times H^1(\Omega) \to \mathbb{R}$ is a coercive and bounded bilinear form corresponding to a second-order differential operator with $C^{(0,1)}$-coefficients. The feasible set K is given by $K = \{v \in H^1(\Omega) : v \leq \psi \text{ a.e. in } \Omega\}$ with a given function $\psi \in W^{1,\infty}(\Omega)$. The two parts $g : H^1(\Omega) \to \mathbb{R}$ and $j : L^2(\Gamma) \to \mathbb{R}$ in the objective are assumed to be twice continuously Fréchet-differentiable. In order to guarantee existence of an optimal solution, we moreover assume that g is bounded from below and j is radially unbounded. It is well known that the solution mapping associated with a variational inequality (VI) is in general not Gâteaux differentiable, see for instance [5]. Therefore the standard implicit programming approach for the derivation of first-order necessary optimality, which is usually applied in optimal control of PDEs, does not work for problems of type (1). Thus several alternative stationarity concepts are known such as for instance weak, C(larke)-, B(ouligand)-, and strong stationarity. For an overview we refer to [2]. The most rigorous concept is strong stationarity which is also essential for second-order sufficient conditions and a priori finite element error estimates, see [3] and [4]. C-stationarity conditions for (1) can be proven by a meanwhile fairly standard penalization technique following e.g. the lines of [7], where the same result is proven in case of distributed controls. The question arise if also strong stationarity can be proven to be necessary for local optimality. These conditions differ from C-stationarity conditions in the sign conditions for the multipliers. For the case of distributed controls strong stationarity was proven in a classical work of Mignot and Puel [6]. Their technique can be adapted to the boundary control problem if the feasible set is replaced by $K = \{v \in H^1(\Omega) : v \leq \psi \text{ a.e. on } \Gamma\}$, i.e. in case of the simplified Signorini problem. However, for a problem of type (1), a one-dimensional counterexample shows that strong stationarity is *not* necessary for local optimality. The counterexample is constructed as follows: By means of a slack variable $\xi \in H^1(\Omega)^*$ the VI in (1) can equivalently be expressed as

$$\begin{aligned} a(y, v) &= \int_\Gamma u\, v\, dx - \langle \xi, v \rangle \quad \forall\, v \in H^1(\Omega) \\ y \leq \psi, &\quad \xi \geq 0, \quad \langle \xi, y - \psi \rangle = 0. \end{aligned}$$

If one omits the slackness condition $\langle \xi, y - \psi \rangle = 0$, then an auxiliary optimal control problem arises, whose feasible set is convex. The counterexample is now constructed such that the objective is also convex (so that the auxiliary problem is a convex program) and the strong stationarity conditions imply the Karush-Kuhn-Tucker (KKT) conditions for this auxiliary problem. As it is convex, the KKT-conditions are sufficient, which leads to a contradiction, since the considered local optimum can be shown to be not optimal for the auxiliary problem. As stated above, only second-order sufficient conditions involving strong stationarity conditions are known up to now. To be more precise, these conditions include sign conditions on the multipliers which are even more restrictive than the ones contained in strong stationarity. Using a technique introduced in [1], analogous sufficient conditions can be established for (1). There is thus a large gap between necessary and sufficient conditions in case of boundary control of the obstacle problem, which gives rise to future research.

References

[1] C. Meyer and T. Betz, *Second-order sufficient optimality conditions for optimal control of static elastoplasticity with hardening*, submitted to ESAIM Control Optim. Calc. Var. (2013).

[2] M. Hintermüller and I. Kopacka, *Mathematical programs with complementarity constraints in function space: C- and strong stationarity and a path-following algorithm*, SIAM J. Optimization **20** (2009), 868–902.

[3] K. Kunisch and D. Wachsmuth, *Sufficient optimality conditions and semi-smooth Newton methods for optimal control of stationary variational inequalities*, ESAIM Control Optim. Calc. Var. **18** (2011), 520–547.

[4] C. Meyer and O. Thoma, *A Priori Finite Element Error Analysis for Optimal Control of the Obstacle Problem*, SIAM J. Numer. Anal. **51** (2013), 605–628.

[5] F. Mignot, *Contrôle dans les inéquations variationelles elliptiques*, J. Functional Analysis **22** (1976), 130–185.

[6] F. Mignot and J.-P. Puel, *Optimal control in some variational inequalities*, SIAM J. Control Optim. **22** (1984), 466–476.

[7] A. Schiela, D. Wachsmuth, *Convergence Analysis of Smoothing Methods for Optimal Control of Stationary Variational Inequalities*, ESAIM: Mathematical Modelling and Numerical Analysis **47** (2013), 771–787.

Forced mean curvature motions: 1. Homogenization, 2. Spirals

R. Monneau

We present here two independent recent results about forced mean curvature motions: a result about homogenization/non homogenization (see the joint work with L.A. Caffarelli [1]) and results on the dynamics of spirals (see the joint works with N. Forcadel and C. Imbert [2, 3]). We refer the reader to the cited works for a review of the literature on those two topics.

Homogenization questions

We consider the geometric evolution of hypersurfaces in $\mathbb{R}^N$, whose the normal

velocity is given by

$$V = \kappa + c(x)$$

where κ is the mean curvature of the hypersurface and c is a $\mathbb{Z}^N$-periodic function which is Lipschitz. Then for $\varepsilon > 0$, we rescale the problem with the new normal velocity:

$$V^\varepsilon = \varepsilon\kappa + c(\frac{x}{\varepsilon})$$

We will show, as ε goes to zero, in some sense that V^ε converges to an effective geometric law

$$V^0 = \bar{c}(n)$$

where n is the normal to the homogenized hypersurface.

We work with the level set formulation of the problem, the hypersurface being then a level set of a function u. Then $u(t,x)$ solves the following PDE

(1)
$$\begin{cases} u_t^\varepsilon = \varepsilon \text{ trace} \left\{ D^2 u^\varepsilon \cdot \left(I - \dfrac{Du^\varepsilon}{|Du^\varepsilon|} \otimes \dfrac{Du^\varepsilon}{|Du^\varepsilon|} \right) \right\} + c(x)|Du^\varepsilon| & \text{on } (0,+\infty) \times \mathbb{R}^N, \\ u^\varepsilon(0,x) = u_0(x) & \text{for all } x \in \mathbb{R}^N \end{cases}$$

For this equation we have

Theorem 1. (Homogenization of mean curvature motion in dimension 2, [1])
Under the previous assumptions for $N = 2$, $c > 0$ and the initial data u_0 globally Lipschitz continuous, the unique viscosity solution u^ε of (1) converges locally uniformly to the unique viscosity solution u^0 of

$$\begin{cases} u_t^\varepsilon = \bar{c}\left(\dfrac{Du^0}{|Du^0|} \right) |Du^0| & \text{on} \quad (0,+\infty) \times \mathbb{R}^N, \\ u^0(0,x) = u_0(x) & \text{for all} \quad x \in \mathbb{R}^N \end{cases}$$

for some continous function $\bar{c}$.

Here, for a unit vector n, the function $\bar{c}(n)$ is determined by the existence of a periodic bounded function v (called corrector) of the following cell equation

$$\bar{c}(n) = F(D^2 v, n + Dv, x) \quad \text{on} \quad \mathbb{R}^N \tag{2}$$

By contrast we also show a counter-example in dimensions $N \geq 3$:

Theorem 2. (Counter-example to homogenization in dimension $N \geq 3$, [1])
For $N \geq 3$, there exists a unit vector n and a C^∞ and $\mathbb{Z}^N$-periodic function $c > 0$ such that, for all real values of $\bar{c}(n)$, there is no bounded solutions v of (2).

We can even prove that the thickness of an initial flat level set increases linearly in time for long time, which prevents the possibility of strong homogenization result in such a case.

Spiral dynamics

Motivated by the modeling of crystal growth and the description of Frank-Read sources of dislocations in cystals, we are interested in the geometric motion in the plane $\mathbb{R}^2$ of a spiral attached to the origin, whose the normal velocity is given by

$$V = 1 + \kappa$$

where κ is the curvature of the spiral. The (time dependent) spiral is parametrized in polar coordinates (r, θ) as

$$\theta = -u(t, r)$$

and it can be checked that u solves the following PDE

(3)
$$\begin{cases} ru_t = \sqrt{1 + (ru_r)^2} + u_r \left(\dfrac{2 + (ru_r)^2}{1 + (ru_r)^2} \right) + \dfrac{ru_{rr}}{1 + (ru_r)^2} & \text{on } (0, +\infty) \times (0, +\infty), \\ u(0, r) = u_0(r) & \text{for all } r \in (0, +\infty) \end{cases}$$

As we see, this equation is degenerated at $r = 0$, and for this reason we do not impose any condition at $r = 0$. We also introduce the curvature of the spiral

$$\kappa_u = u_r \left(\frac{2 + (ru_r)^2}{(1 + (ru_r)^2)^{\frac{3}{2}}} \right) + \frac{ru_{rr}}{(1 + (ru_r)^2)^{\frac{3}{2}}}$$

Then we have the following result:

Theorem 3. (Existence and uniqueness, [2]**)**
Assume that $u_0 \in W^{2,\infty}_{loc}(0, +\infty)$ is globally Lipschitz continuous and satisfies

$$(u_0)_r \in W^{1,\infty}(0, +\infty) \quad or \quad \kappa_{u_0} \in L^\infty(0, +\infty)$$

and that there exists a radius $r_0 > 0$ such that

$$|1 + \kappa_{u_0}| \leq Cr \quad for \quad 0 \leq r \leq r_0$$

Then there exists a unique viscosity solution of (3) which is globally Lipschitz in space and time.

We can also identify a self-similar solution $\lambda t + \varphi(r)$. Under certain assumptions on the initial data, we can show, as the time goes to infinity, that solutions $u(t, r)$ of (3) behave like the self-similar profile (up to addition of constants that may depend on the chosen subsequences in time, see [3] for more details).

References

[1] L.A. Caffarelli, R. Monneau, *Counter-example in 3D and homogenization of geometric motions in 2D*, preprint HAL: hal-00720954 (version 1) (2012).

[2] N. Forcadel, C. Imbert, R. Monneau, *Uniqueness and existence of spirals moving by forced mean curvature motion*, Interfaces and Free Boundaries **14** (2012), 365–400.

[3] N. Forcadel, C. Imbert, R. Monneau, work in progress.

On general existence results for one-dimensional singular diffusion equations with spatially inhomogeneous driving force

Atsushi Nakayasu
(joint work with Mi-Ho Giga, Yoshikazu Giga)

We study an anisotropic mean curvature flow with singular interfacial energy and spatially inhomogeneous driving force for a curve in a plane given by the graph of a periodic function $u = u(t, x)$. This problem is formulated as a one-dimensional quasilinear diffusion equation of the form

$$u_t = a(u_x)[(W'(u_x))_x + \sigma(t, x)] \quad \text{in } (0,\ infty) \times \mathbb{T}$$

with a nonnegative continuous function a, a convex function W and the driving force term σ. We are concerned with the case when $W = W(p)$ may not be differentiable at some slopes p so that singularity appears in the equation.

Since the diffusion effect is very strong, the equation becomes nonlocal. Indeed, it turns out that the quantity of $\Lambda_W^\sigma(u) := (W'(u_x))_x + \sigma$ is characterized by a corresponding obstacle problem. Moreover, $\Lambda_W^\sigma(u)$ is well-defined for so-called faceted functions u since the obstacle problem admits a unique minimizer. A notion of a solution to the singular diffusion equation is defined by a viscosity sense testing the smooth faceted functions instead of smooth functions to an unknown function.

We point out that when the driving force σ is spatially homogeneous, the theory for the singular diffusion equation is easy to develop since the obstacle problem becomes trivial and the quantity of $\Lambda_W^\sigma(u)$ is constant on each facet. In fact, a unique existence of a viscosity solution for initial value problems was established by Giga and Giga [1]. However, when σ depends on the space variable, their method does not work well since $\Lambda_W^\sigma(u)$ may not be constant. In particular, there is no general existence results for initial value problems although a comparison theorem has been shown by Giga, Giga and Rybka in their recent work [2].

In this talk we show a global in time existence of a solution in the viscosity sense to the singular diffusion equation with a continuous periodic initial datum. The main tool to prove the existence theorem is Perron's method and so we also show a Perron type existence result stating that if there exists a subsolution and a supersolution then the supremum function of subsolutions between the given sub- and supersolution is a solution. When one tries to prove the Perron type existence, it is necessary to modify a smooth faceted test function keeping its property. The main idea to solve this problem is to find a small effective region which determines the quantity of the nonlocal curvature. We construct a modification as in the previous work [1] using the effective region instead of the faceted region. Then the argument works for our setting with the spatially inhomogeneous driving force term σ.

Our results can be applied to one-dimensional total variation flow as well as the singular anisotropic mean curvature flow for graphs. We also note that fully nonlinear singular diffusion equations of the form

$$u_t + F(t, u_x, \Lambda_W^\sigma(u)) = 0 \quad \text{in } (0,\ infty) \times \mathbb{T}$$

can be handled by our theory.

References

[1] M.-H. Giga and Y. Giga, *Evolving graphs by singular weighted curvature*, Arch. Rational Mech. Anal. **141** (1998), no. 2, 117–198.

[2] M.-H. Giga, Y. Giga, and P. Rybka, *A comparison principle for singular diffusion equations with spatially inhomogeneous driving force for graphs*, preprint.

Stability of bunched spirals and inactive pair in evolution of spirals with an eikonal-curvature flow

Takeshi Ohtsuka

(joint work with Yen-Hsi Richard Tsai and Yoshikazu Giga)

We consider several evolving spirals in the plane with an eikonal-curvature flow equation of the form

$$V = C - \kappa, \tag{1}$$

where V and κ is the normal velocity and the curvature of the spirals, and C is a constant. The authors [4, 5] introduced a level set formulation for the spirals with a single auxiliary function and a sheet structure function. Let Ω be a bounded domain. Assume that spirals, which is denoted by Γ_t for $t \in [0, \infty)$, are associated with several fixed centers $a_1, \dots, a_N \in \Omega$. However we remove closure of discs $B_{\rho_j}(a_j) = \{x \in \mathbb{R}^2;\ |x - a_j| < \rho_j\}$ from Ω for technical reason, and thus we consider $\Gamma_t \subset \overline{W}$. In the level set formulation by [4] or [5] we set

$$\Gamma_t = \{x \in \overline{W};\ u(t,x) - \theta(x) \equiv 0 \mod 2\pi\mathbb{Z}\} \tag{2}$$

with an auxiliary function u and a sheet structure function $\theta(x) = \sum_{j=1}^{N} m_j \arg(x - a_j)$. Note that θ is a multiple valued function to describe spirals completely. The coefficient $m_j \in \mathbb{Z} \setminus \{0\}$ denotes a signed number of spirals associated with a_j; if $m_j > 0$ (resp. $m_j < 0$) then $|m_j|$ spirals are associated with a_j with anti-clockwise (resp. clockwise) rotational orientation provided that $V > 0$.

Although θ is a multiple valued function, we can regard (2) as the usual level set of a smooth function $u - \theta$ locally, we obtain

$$\mathbf{n} = -\frac{\nabla(u-\theta)}{|\nabla(u-\theta)|}, \quad V = \frac{u_t}{|\nabla(u-\theta)|}, \quad \kappa = -\mathrm{div}\frac{\nabla(u-\theta)}{|\nabla(u-\theta)|}$$

by analogy of the usual level set method (see [1] for details). Then, we now consider (1) with a right angle condition between Γ_t and ∂W and obtain the level set equation of the form

$$u_t - |\nabla(u-\theta)| \left\{ \mathrm{div}\frac{\nabla(u-\theta)}{|\nabla(u-\theta)|} + C \right\} = 0 \quad \text{in } (0,T) \times W, \tag{3}$$

$$\langle \vec{\nu}, \nabla(u-\theta) \rangle = 0 \quad \text{on } (0,T) \times \partial W, \tag{4}$$

where $\vec{\nu}$ is an outer unit normal vector field of ∂W, and $\langle \cdot, \cdot \rangle$ denotes a usual inner product of $\mathbb{R}^2$. The comparison principle, existence and uniqueness of a

solution for a continuous initial datum in viscosity sense are obtained in [4], and the uniqueness of level sets is obtained by [2], respectively.

The goal of this talk is to prove the following two results with our level set formulation.

(I) Assume that $N = 1$, $a_1 = 0$, $W = B_R(0) \setminus \overline{B_\rho(0)}$, $m > 1$ and thus $\theta(x) = m \arg x$. If a bunch of m spirals Γ_t is in a thin domain at $t = 0$, then there exists a family of thin domains including Γ_t for $t > 0$.

(II) Assume that $N = 2$, $m_1 = -m_2 = 1$ ($\theta(x) = \arg(x - a_1) - \arg(x - a_2)$), $W = \Omega \setminus (\overline{B_\rho(a_1)} \cup \overline{B_\rho(a_2)})$, i.e., $\rho_1 = \rho_2 = \rho$, and $|a_1 - a_2| < 2/C$. Prove that no growth occurs in this case.

A negative result for the problem (I) is obtained by [3] with a reaction diffusion equation denoting evolution of spirals with (1) and the right angle condition. Note that our equation (3)–(4) is derived from the equation in [3] by formal asymptotic expansion. However, we obtain the stability result for (3)–(4).

To state our main results exactly we now introduce a covering space $\mathfrak{X}$ of $\overline{W}$ of the form

$$\mathfrak{X} = \{(x, \xi) \in \overline{W} \times \mathbb{R}^N;\ \xi = (\xi_1, \dots, \xi_N),\ (\cos \xi_j, \sin \xi_j) = \frac{x - a_j}{|x - a_j|}\}.$$

Then, $\tilde{u}(t, x, \xi) := u(t, x) - \sum_{j=1}^N m_j \xi_j$ on $[0, T] \times \mathfrak{X}$ plays the role of $u - \theta$. Moreover, $\mathfrak{X}$ is divided into three subsets $\widetilde{\Gamma}_t$, $\widetilde{I}_t$, and $\widetilde{O}_t$ with $\tilde{u}$ of the form

$$\begin{aligned} &\widetilde{\Gamma}_t = \{(x, \xi) \in \mathfrak{X};\ \tilde{u}(t, x, \xi) = 0\}, \\ &\widetilde{I}_t = \{(x, \xi) \in \mathfrak{X};\ \tilde{u}(t, x, \xi) > 0\}, \quad \widetilde{O}_t = \{(x, \xi) \in \mathfrak{X};\ \tilde{u}(t, x, \xi) < 0\}, \end{aligned} \tag{5}$$

which are regarded as Γ_t, "interior" and "exterior" of Γ_t, respectively.

We are now in the position to state our main result for the problem (I).

Theorem 1. *Let $N = 1$, $a_1 = 0$, $W = B_R(0) \setminus \overline{B_\rho(0)}$, and $m > 1$. Let u be a viscosity solution to (3)–(4) in $(0, T) \times \overline{W}$. Assume that there exists $\zeta_0 \in C([\rho, R])$ and $\alpha > 0$ satisfying*

$$\{(x, \xi) \in \mathfrak{X};\ \tilde{u}(0, x, \xi) = 2\pi j\} \subset \{(x, \xi) \in \mathfrak{X};\ |\xi - (\zeta_0(|x|) + 2\pi k_j)| \le \alpha\}$$

with a constant $k_j \in \mathbb{Z}$ for $j = 0, 1, \dots, m - 1$. Then, there exists $\zeta \in C([0, \infty) \times [\rho, R])$ such that $w(t, x) = \zeta(t, |x|)$ is a viscosity solution to (3)–(4) with $N = 1$, $a_1 = 0$ and $m = 1$, and

$$\{(x, \xi) \in \mathfrak{X};\ \tilde{u}(t, x, \xi) = 2\pi j\} \subset \{(x, \xi) \in \mathfrak{X};\ |\xi - (\zeta(t, |x|) + 2\pi k_j)| \le \alpha\}$$

for $j = 0, 1, \dots, m - 1$ and $t > 0$.

For the problem (II), we may assume that $a_1 = (-\alpha, 0)$, $a_2 = (\alpha, 0)$ with $\alpha \in (0, 1/C)$ without loss of generality. We now consider

$$q_1(\sigma) = p_1(\sigma) + \frac{1}{C}(\sin \sigma, -\cos \sigma), \quad q_2(\sigma) = p_2(\sigma) + \frac{1}{C}(-\sin(\pi - \sigma), -\cos(\pi - \sigma))$$

with $p_1(\sigma) = a_1 + \rho(\cos\sigma, \sin\sigma)$ and $p_2(\sigma) = a_2 + \rho(\cos(\pi-\sigma), \sin(\pi-\sigma))$. Then, there exists σ_1, σ_2 satisfying $0 < \sigma_1 < \sigma_2 < \pi$ and

$$b_1 = (0, -\beta) = q_1(\sigma_1) = q_2(\sigma_1), \quad b_2 = (0, \beta) = q_1(\sigma_2) = q_2(\sigma_2)$$

for some $\beta > 0$. Then, the curve

$$R_i = \left\{ b_i + \frac{1}{C}\left(\cos\left(\frac{\pi}{2}+\sigma\right), \sin\left(\frac{\pi}{2}+\sigma\right)\right);\ \sigma \in [-\sigma_i, \sigma_i] \right\}$$

satisfies $R_i \perp \partial W$ for $i = 1, 2$. Since R_i is a part of the circle whose radius is $1/C$, then R_i should be a stationary solution to (1) with the right angle condition. However, if we consider (3)–(4) with $\theta \equiv 0$, i.e., the evolution of closed curve with (1), then there are no continuous stationary solutions describing $\{x \in \mathbb{R}^2;\ |x| = 1/C\}$. Since our equation may have no continuous stationary solution describing R_i by analogy of the above, we construct discontinuous viscosity solutions describing R_i.

Theorem 2. *Let $N = 2$ and $m_1 = -m_2 = 1$ and thus $\theta = \arg(x-a_1) - \arg(x-a_2)$, $a_1 = (-\alpha, 0)$, $a_2 = (\alpha, 0)$ with $\alpha \in (0, 1/C)$. Assume that $R_i \subset \overline{W}$. Then $v = \theta_{R_i}$, which is a branch of θ whose discontinuities are only on R_i, is a viscosity solution to* (3)–(4).

Consequently we obtain the no evolution result from the above.

Corollary 3. *Under the same hypothesis in Theorem 2, let $u \in C([0,\infty) \times \overline{W})$ be a viscosity solution to* (3)–(4). *Then, there exists $k \in \mathbb{Z}$ such that*

$$\{(x,\xi) \in \mathfrak{X};\ \tilde{u}(t,x,\xi) > 0\} \subset \{(x,\xi) \in \mathfrak{X};\ v(x) + 2\pi k - (\xi_1 - \xi_2) > 0\}.$$

The crucial properties on (3)–(4) to prove the main results is the comparison of interior and exterior sets obtained in [2].

The crucial difference between ours and [3] for the first problem (1) is that our equation is degenerate parabolic, in particular, there is no diffusion in the direction of $\mathbf{n}$. This implies that each spiral still evolves by (1) without interactions with each other. Then, we obtain Theorem 1 with a construction of a solution $w(t,x) = \zeta(t,|x|)$ and the comparison of interior or exterior between Γ_t, $\mathcal{C}_t = \{x \in \overline{W};\ \zeta(t,|x|) - \arg x \equiv 0 \mod 2\pi\mathbb{Z}\}$ and a rotation of $\mathcal{C}_t$. For the second problem (II) the curve R_i is described with a discontinuous stationary solution to (3)–(4), then R_i plays role of bound for all solutions.

References

[1] Y. Giga, *Surface evolution equations: A level set approach*, volume 99 of Monographs in Mathematics, Birkhäuser Verlag, Basel, 2006.

[2] S. Goto, M. Nakagawa, and T. Ohtsuka, Uniqueness and existence of generalized motion for spiral crystal growth, Indiana University Mathematics Journal, **57**(2008), 2571–2599.

[3] T. Ogiwara, and K.-I. Nakamura, Spiral traveling wave solutions of nonlinear diffusion equations related to a model of spiral crystal growth, Publ. Res. Inst. Math. Sci., **39**(2003), 767–783.

[4] T. Ohtsuka, A level set method for spiral crystal growth, Advances in Mathematical Sciences and Applications, **13**(2003), 225–248.
[5] T. Ohtsuka, Y.-H. R. Tsai, and Y. Giga, A level set approach reflecting sheet structure with single auxiliary function for evolving spirals on crystal surfaces, Hokkaido University Preprint Series in Mathematics, #1025(2012), 1–36.

Constrained Shape Optimization for Polymer Distributors

René Pinnau
(joint work with Chrisitian Leithäuser)

Synthetic fibers and nonwovens have become increasingly important in recent years and find applications in a broad variety of products: The range goes from hygienic products, like diapers, over various filter materials towards high-tech applications like battery separators. The production process for nonwoven materials is as follows: In a first step molten polymer with high viscosity is pressed from an extruder through a distributor geometry onto the spinneret plate. This is a plate containing small capillaries which are used for spinning the polymer into fibers. Turbulent air flow is applied for drawing and swirling the fibers. Finally, many fibers are deposited on a moving belt to form a nonwoven material. There are many variations of this process, for example, the deposition step can be left out to produce yarn or short-fibers.

This talk is motivated by the following problem: The polymer is routed through tubes into the geometry which distributes it onto the spinneret plate. However, this is often a time-critical step because the polymer can degenerate or cool down if its occupation time is too long, which results in a poor fiber quality. It can lead to fiber breakage or even blockage of capillaries or parts of the distributor. Especially, in regions close to the walls, polymer can stagnate or solidify. Research and practical applications at Fraunhofer ITWM have shown that this can be greatly improved by designing geometries which avoid regions with low wall shear stress: The wall shear stress measures the velocity gradient at the wall. At the wall itself the flow velocity is zero and so the wall shear stress indicates how fast the velocity rises with increasing distance to the wall. A low wall shear stress means that there is a large boundary layer with low velocity, where polymer degeneration can take place. Increasing the wall shear stress results in a reduction of this layer and an improvement of the fiber quality. This leads us to the following mathematical problem, which was thoroughly investigated in [4]:

> Find a geometry for a polymer flow distributor with an improved wall shear stress distribution.

The solution of this problem leads to several interesting questions concerning shape dependent operators, which are discussed in the following:

- Are specific wall shear stress distributions reachable by a change of the geometry?
- Is it possible to attain a desired wall shear stress distribution in a uniform way?

The question of reachability was studied in [3], where it was possible to characterize the image space of the potential flow shape operator. Note, that this problem is inherently nonlinear due to the dependence on the shape of the domain. The reachability is in particular depending on the number of stagnation points along the observed part of the wall.

Focussing instead on the concept of approximate controllability, where the image of linearized shape operator needs to be dense, it was possible to prove the approximate controllability for the potential flow shape operator, the Stokes flow shape operator and the heat equation shape operator (for details see [4]).

The second question leads to an optimal shape design problem with respect to the L^∞–norm. This can be formulated as an optimal control problem with state constraints. The crucial part, however, is to deal with the shape-dependence. The shape-dependent problem can be finally transformed by conformal maps into a standard state constrained optimal control problem. This leads after discretization to a large NLP, which can be solved by modern NLP solvers [1, 2].

Further, the threedimensional industrial problem was solved by a steepest descent algorithm based on gradient information derived from shape calculus [4].

References

[1] Ch. Leithäuser, R. Feßler, R. Pinnau, *Shape Optimization for Stokes Flows using Conformal Metrics*, PAMM, Volume 10, Issue 1, pages 581–582, 2010

[2] Ch. Leithäuser, R. Feßler, R. Pinnau, *An Approach to Shape Optimization with State Constraints*, PAMM, Volume 12, Issue 1, pages 685–686, 2012

[3] Ch. Leithäuser and R. Feßler, *Characterizing the image space of a shape-dependent operator for a potential flow problem*, Applied Mathematics Letters, 2012

[4] Ch. Leithäuser *On the Theory and Practice of Shape-Dependent Operators*, PhD Thesis, TU Kaiserslautern, 2013

Unfitted finite element methods for surface partial differential equations

Thomas Ranner

(joint work with Klaus P. Deckelnick, Charles M. Elliott)

Surface partial differential equations have grown in popularity within the last twenty years with applications in fluid mechanics, biology and material sciences becoming increasingly common. These equations are posed on curved domains, which often have complex evolving morphology, and combine surface and bulk effects, hence computational techniques are required.

To simplify the presentation, we will consider a surface elliptic problem:

$$-\Delta_\Gamma u + u = f \quad \text{on } \Gamma. \tag{1}$$

It is well known [1] that (1) equation has a unique solution satisfying the regularity estimate:

$$\|u\|_{H^2(\Gamma)} \leq c\|f\|_{L^2(\Gamma)}.$$

Alternative approaches given in the literature include using the surface finite element method [4], which has been successfully extended to evolving surfaces [5] and coupled bulk-surface problems [6], an implicit surface method [2] and the closest point method [8]. The methodology presented here has similarities with the methods of [3, 7].

Unfitted finite element methods: Let $\Gamma = \{x \in \mathbb{R}^{n+1} : d(x) = 0\}$ be an n-dimensional hypersurface in $\mathbb{R}^{n+1}$ and d a signed distance function defined in a polyhedral narrow band U about the surface.

We write $\mathcal{T}_h$ for a regular triangulation of U consisting of closed simplices, with h the maximum element diameter of elements in $\mathcal{T}_h$. Let X_h be the space of piecewise linear bulk finite element functions on U and $I_h \colon C(\bar{U}) \to X_h$ denote the usual Lagrangian interpolation operator. We have for $T \in \mathcal{T}_h$, $f \in W^{2,p}$ $(1 \leq p \leq \infty)$:

$$\|f - I_h f\|_{L^p(T)} + h\|\nabla(f - I_h f)\|_{L^p(T)} \leq ch^2 \|f\|_{W^{2,p}(T)}. \tag{2}$$

We define our computational domains Γ_h and D_h as follows:

$$\Gamma_h := \{x \in \mathbb{R}^{n+1} : I_h d(x) = 0\}, \qquad D_h := \{x \in \mathbb{R}^{n+1} : |I_h d(x)| < h\}.$$

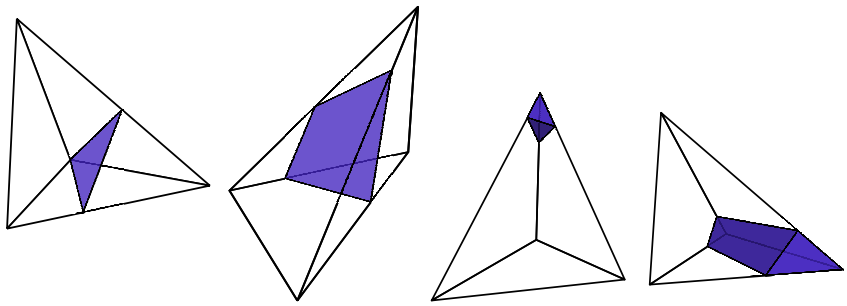

FIGURE 1. Examples of intersections of $\Gamma_h \cap T$ (left two images) and $D_h \cap T$ (right two images).

Method one – sharp interface method: We define $\widetilde{\mathcal{T}}_h^I := \{T \in \mathcal{T}_h : \mathrm{meas}_n(T \cap \Gamma_h) > 0\}$. The intersection of Γ_h with one element of $\widetilde{\mathcal{T}}_h^I$ is either a triangle or quadrilateral. It is possible that $T \cap \Gamma_h$ is the face of two adjoining elements. In this case, we discount one of the two elements from $\widetilde{\mathcal{T}}_h^I$ and call the remaining elements $\mathcal{T}_h^I$. We define $U_h^I := \bigcup\{T : T \in \mathcal{T}_h^I\}$ and the finite element space V_h as the space of piecewise linear functions on U_h^I. The finite element space has the following interpolation result:

$$\|z^e - I_h z^e\|_{L^2(\Gamma_h)} + h\|\nabla(z^e - I_h z^e)\|_{L^2(\Gamma_h)} \leq ch^2 \|z\|_{H^2(\Gamma)}. \tag{3}$$

Here z^e is an extension of $z \colon \Gamma \to \mathbb{R}$ to U constant in the normal direction.

The finite element problem is: find $u_h \in V_h$ such that

$$\int_{\Gamma_h} \nabla u_h \cdot \nabla \phi_h + u_h \phi_h \,\mathrm{d}\sigma_h = \int_{\Gamma_h} f^e \phi_h \,\mathrm{d}\sigma_h \quad \text{for all } \phi_h \in V_h. \tag{4}$$

It can be shown that (4) is well posed and using a variant of the Stang lemma and the interpolation results (2, 3), we have the following error bound between u the solution of (1) and u_h the solution of the sharp interface method (4).

$$\|u^e - u_h\|_{L^2(\Gamma_h)} + h\|\nabla(u^e - u_h)\|_{L^2(\Gamma_h)} \leq ch^2\|u\|_{H^2(\Gamma)}. \tag{5}$$

Method two – narrow band method: We define $\mathcal{T}_h^B := \{T \in \mathcal{T}_h : \text{meas}_{n+1}(T \cap D_h) > 0\}$ and $U_h^B := \{T : T \in \mathcal{T}_h^B\}$. We define the finite element space V_h as the space of piecewise linear functions on U_h^B. This space has the following approximation property

$$\frac{1}{\sqrt{h}}\|z^e - I_h z^e\|_{L^2(D_h)} + \sqrt{h}\|\nabla(z^e - I_h z^e)\|_{L^2(D_h)} \leq ch^2\|z\|_{H^2(\Gamma)}. \tag{6}$$

The second finite element scheme is: find $u_h \in V_h$ such that

$$\frac{1}{2h}\int_{D_h} \nabla u_h \cdot \nabla \phi_h + u_h\phi_h \,\mathrm{d}x = \frac{1}{2h}\int_{D_h} f^e\phi_h \,\mathrm{d}x. \tag{7}$$

This equation is clearly well posed and applying similar techniques as above we have the following bound between between u the solution of (1) and u_h the solution of the narrow band method (7):

$$\left(\frac{1}{2h}\int_{D_h} |\nabla(u^e - u_h)|^2 + |u^e - u_h|^2 \,\mathrm{d}x\right)^{\frac{1}{2}} \leq ch\|f\|_{L^2(\Gamma)}. \tag{8}$$

This result is optimal for the H^1 norm, but not the L^2 norm.

Numerical results: As a computational example, we consider Γ to be a torus with inner radius $r = 0.6$ and outer radius $R = 1$. We take the right hand side so that the exact solution is $u(\varphi, \theta) = \cos(3\varphi)\sin(3\theta + \varphi)$. The results for the sharp interface method are on the left and narrow band method on the right hand side. Both methods demonstrate quadratic convergence in the $L^2(\Gamma_h)$ norm. Similar results are available for $\|\nabla(u^e - u_h)\|_{L^2(\Gamma_h)}$ which also gives control over the normal component of the error away from the surface.

h	$\|u^e - u_h\|_{L^2(\Gamma_h)}$	eoc
$2^{-1}\sqrt{3}$	6.03053	—
$2^{-2}\sqrt{3}$	1.67739	1.846067
$2^{-3}\sqrt{3}$	$7.10825 \cdot 10^{-1}$	1.238652
$2^{-4}\sqrt{3}$	$1.90004 \cdot 10^{-1}$	1.903465
$2^{-5}\sqrt{3}$	$4.73865 \cdot 10^{-2}$	2.003482
$2^{-6}\sqrt{3}$	$1.19721 \cdot 10^{-2}$	1.984800
$2^{-7}\sqrt{3}$	$3.01376 \cdot 10^{-3}$	1.990040

h	$\|u^e - u_h\|_{L^2(\Gamma_h)}$	eoc
$2^{-1}\sqrt{3}$	2.49823	—
$2^{-2}\sqrt{3}$	1.62953	0.616450
$2^{-3}\sqrt{3}$	$7.13768 \cdot 10^{-1}$	1.190929
$2^{-4}\sqrt{3}$	$2.35902 \cdot 10^{-1}$	1.597268
$2^{-5}\sqrt{3}$	$7.26544 \cdot 10^{-2}$	1.699066
$2^{-6}\sqrt{3}$	$1.99335 \cdot 10^{-2}$	1.865855
$2^{-7}\sqrt{3}$	$5.14142 \cdot 10^{-3}$	1.954956

References

[1] T. Aubin. *Nonlinear analysis on manifolds, Monge-Ampère equations.* Springer-Verlag, New York, 1982.

[2] M. Bertalmio, G. Sapiro, and S. Osher. Variational problems and PDEs on implicit surfaces. *Proceedings IEEE Workshop on Variational and Level Set Methods in Computer Vision* (2001), 186–193.

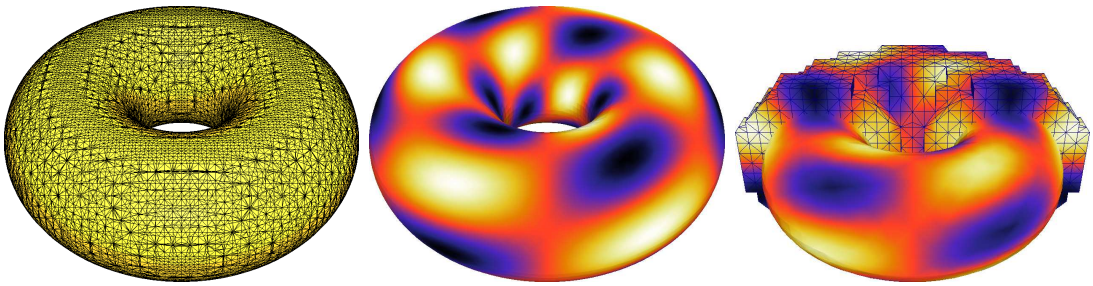

FIGURE 2. Plots of the solutions of both methods. Left is shown the induced mesh on Γ_h, central is shown the solution on Γ_h for the sharp interface method and right is shown the computational domain and the solution on Γ_h for the narrow band method.

[3] K. Deckelnick, G. Dziuk, C.M. Elliott, and C.-J. Heine. *An h-narrow band finite-element method for elliptic equations on implicit surfaces*. IMA Journal of Numerical Analysis **30** (2009), 351–376.
[4] G. Dziuk. Finite Elements for the Beltrami operator on arbitrary surfaces. In Stefan Hildebrandt and Rolf Leis, editors, *Partial Differential Equations and Calculus of Variations*, volume 1357 of *Lecture Notes in Mathematics* (1988), 142–155.
[5] G. Dziuk and C.M. Elliott. *Finite elements on evolving surfaces*. IMA Journal of Numerical Analysis **27** (2007), 262–292.
[6] C.M. Elliott and T. Ranner *Finite element analysis for a coupled bulk-surface partial differential equation*. IMA Journal of Numerical Analysis **33** (2013), 377–302.
[7] M.A. Olshanskii, A. Reusken, and J. Grande. *A finite element method for elliptic equations on surfaces*. SIAM Journal on Numerical Analysis **47** (2009), 3339–3358.
[8] S.J. Ruuth and B. Merriman. *A simple embedding method for solving partial differential equations on surfaces*. Journal of Computational Physics **227** (2008), 1943–1961.

An Eulerian space-time finite element method for PDEs on evolving surfaces

ARNOLD REUSKEN
(joint work with Maxim Olshanskii)

1. INTRODUCTION

Partial differential equations (PDEs) posed on evolving surfaces arise in many applications. One example is the diffusion equation that models the concentration distribution of surface active agents attached to an interface between two phases of immiscible fluids, cf. [1].

Recently, several approaches for solving PDEs on evolving surfaces numerically have been introduced. The finite element method of Dziuk and Elliott [2] is based on the *Lagrangian* description of a surface evolution. If one considers the *Eulerian* description of a surface evolution, e.g., based on the level set method, then the surface is usually defined implicitly. In this case, regular surface triangulations and material trajectories of points on the surface are not easily available. Hence, Eulerian numerical techniques for the discretization of PDEs on surfaces have been

studied in the literature. Numerical approaches were introduced that are based on extensions of PDEs off a two-dimensional surface to a three-dimensional neighbourhood of the surface. Then one can apply a standard finite element or finite difference disretization to treat the extended equation in $\mathbb{R}^3$. The extension, however, leads to degenerate parabolic PDEs and requires the solution of equations in a higher dimensional domain. For a detailed discussion of this extension approach we refer to, e.g., [3].

A different Eulerian technique for the numerical solution of an elliptic PDE posed on a hypersurface in $\mathbb{R}^3$ was introduced in [4, 5]. The main idea of this method is to use finite element spaces that are induced by the volume triangulations of a bulk domain in order to discretize a partial differential equation on the embedded surface. This method does not use an extension of the surface partial differential equation. It is instead based on a restriction (trace) of the outer finite element spaces to the discrete surface. This leads to discrete problems for which the number of degrees of freedom corresponds to the two-dimensional nature of the surface problem, similar to the Lagrangian approach. At the same time, the method is essentially Eulerian as a surface is not tracked by a surface mesh and may be defined implicitly as the zero level of a level set function. For the discretization of the PDE on the surface this zero level then has to be reconstructed. The approach was further developed in [6, 7], where adaptive and streamline diffusion variants of this surface finite element were introduced and analysed. These papers [4, 5, 6, 7], however, treated elliptic and parabolic equations on *stationary* surfaces.

In this note we outline a method that generalizes the approach from [4] to diffusion equations on *evolving* surfaces. An evolving surface defines a three-dimensional *space-time manifold* in the space-time continuum $\mathbb{R}^4$. The surface finite element method that we introduce is based on the *traces* on this space-time manifold of outer *space-time* finite element functions, which are piecewise polynomials with respect to a volume mesh, consisting of cylinders (tetrahedra times time interval). For this finite element technique it is natural to start with a variational formulation of the diffusion problem on the space-time manifold. To our knowledge such a formulation has not been studied in the literature, yet. Therefore, we first introduce such a space-time variational formulation. We then explain the space-time discretization method.

2. Variational formulation

Consider a surface $\Gamma(t)$ passively advected by a smooth velocity field $\mathbf{w} = \mathbf{w}(\mathbf{x}, t)$, i.e. the normal velocity of $\Gamma(t)$ is given by $\mathbf{w} \cdot \mathbf{n}$, with $\mathbf{n}$ the unit normal on $\Gamma(t)$. We assume that for all $t \in [0, T]$, $\Gamma(t)$ is a smooth hypersurface that is closed ($\partial\Gamma = \emptyset$), connected, oriented, and contained in a fixed domain $\Omega \subset \mathbb{R}^3$. The conservation of a scalar quantity u with a diffusive flux on $\Gamma(t)$ leads to the surface PDE:

$$\dot{u} + (\mathrm{div}_\Gamma \mathbf{w})u - \varepsilon \Delta_\Gamma u = 0 \qquad \text{on } \Gamma(t),\ t \in (0, T], \tag{1}$$

with initial condition $u(x,0) = u_0(x)$ for $x \in \Gamma(0)$. Here $\dot{u} = \frac{\partial u}{\partial t} + \mathbf{w} \cdot \nabla u$ denotes the advective material derivative, div_Γ is the surface divergence and Δ_Γ is the Laplace-Beltrami operator, $\varepsilon > 0$ is the constant diffusion coefficient.

Consider the space-time manifold

$$\Gamma_* = \bigcup_{t \in (0,T)} \Gamma(t) \times \{t\}, \quad \Gamma_* \subset \mathbb{R}^4,$$

and let $H^1(\Gamma_*)$ be the usual Sobolev space on Γ_*. We introduce the space

$$H = \{\, v \in L^2(\Gamma_*) \mid \|\nabla_\Gamma v\|_{L^2(\Gamma_*)} < \infty \,\}, \tag{2}$$

$$(u,v)_H = (u,v)_{L^2(\Gamma_*)} + (\nabla_\Gamma u, \nabla_\Gamma v)_{L^2(\Gamma_*)}, \tag{3}$$

and consider the material derivative as a linear functional on H. Recall the Leibniz formula

$$\int_{\Gamma(t)} \dot{v} + v \,\mathrm{div}_\Gamma \mathbf{w}\, ds = \frac{d}{dt} \int_{\Gamma(t)} v \, ds, \quad v \in C^1(\Gamma_*), \tag{4}$$

which implies the integration by parts identity:

$$\begin{aligned} &\int_0^T \int_{\Gamma(T)} \dot{u}v + \dot{v}u + uv \,\mathrm{div}_\Gamma \mathbf{w}\, ds\, dt \\ &= \int_{\Gamma(T)} u(s,T)v(s,T)\, ds - \int_{\Gamma(0)} u(s,0)v(s,0)\, ds \quad \text{for all } u, v \in C^1(\Gamma_*). \end{aligned} \tag{5}$$

for all $u, v \in C^1(\Gamma_*)$. Based on (5) we define the material derivative for $u \in H$ as the functional $\dot{u}$:

$$\langle \dot{u}, \phi \rangle = -\int_0^T \int_{\Gamma(t)} u\dot{\phi} + u\phi \,\mathrm{div}_\Gamma \mathbf{w}\, ds\, dt \quad \text{for all } \phi \in C_0^1(\Gamma_*). \tag{6}$$

Using

$$\|\dot{u}\|_{H'} = \sup_{\phi \in C_0^1(\Gamma_*)} \frac{\langle \dot{u}, \phi \rangle}{\|\phi\|_H}$$

we define the space

$$W = \{\, v \in H \mid \dot{v} \in H' \,\}, \quad \text{with } \|v\|_W^2 := \|v\|_H^2 + \|\dot{v}\|_{H'}^2.$$

Using smoothness assumptions on the space-time manifold, useful *density and trace properties* of the spaces H and W can be derived. In the analysis of well-posedness we transform the original problem (1) such that we have a zero initial condition. Furthermore, instead of the surface diffusion problem we consider the following slightly more general surface PDE:

$$\begin{aligned} \dot{u} + \alpha\, u - \varepsilon \Delta_\Gamma u &= f \qquad \text{on } \Gamma(t),\ t \in (0,T], \\ u &= 0 \qquad \text{on } \Gamma(0), \end{aligned} \tag{7}$$

with $\alpha \in L^\infty(\Gamma_*)$ and a generic right-hand side $f \in L^2(\Gamma_*)$. We define the inner product and symmetric bilinear form

$$(u,v)_0 = \int_0^T \int_{\Gamma(t)} uv \, ds \, dt, \quad a(u,v) = \varepsilon(\nabla_\Gamma u, \nabla_\Gamma v)_0 + (\alpha u, v)_0, \quad u, v \in H.$$

The following problem can be shown to be *well-posed*: Given $f \in H'$, find $u \in \overset{\circ}{W} := \{ v \in W \mid v(\cdot,0) = 0 \quad \text{on } \Gamma_0 \}$. such that

$$\langle \dot{u}, v \rangle + a(u,v) = \langle f, v \rangle \quad \text{for all } v \in H. \tag{8}$$

3. Space-time finite element discretization

We outline our Eulerian discretization method for the surfactant transport problem (1). The space-time domain is denoted by $Q = \Omega \times (0,T] \subset \mathbb{R}^{d+1}$. A partitioning of the time interval is given by $0 = t_0 < t_1 < \ldots < t_N = T$, with a uniform time step $\Delta t = T/N$. Corresponding to each time interval $I_n := (t_{n-1}, t_n]$ we assume a given shape regular simplicial triangulation $\mathcal{T}_n$ of the spatial domain Ω. In general this triangulation is *not fitted* to the interface $\Gamma(t)$. Let V_n be the finite element space of continuous piecewise linear functions on $\mathcal{T}_n$. The spatial mesh size parameter corresponding to V_n is denoted by h_n. A corresponding space-time finite element space on the time slab $Q^n := \Omega \times I_n$ is given by

$$W_n := \{ w : Q^n \to \mathbb{R} \mid w(x,t) = \phi_0(x) + t\phi_1(x), \ \phi_0, \phi_1 \in V_n \}. \tag{9}$$

The symbol Γ_*^n denotes the space-time interface in Q^n, i.e., $\Gamma_*^n := \cup_{t \in I_n} \Gamma(t)$, and $\Gamma_* := \cup_{1 \le n \le N} \Gamma_*^n$. The *volume* space-time spaces W_n, $1 \le n \le N$, induce corresponding *trace* spaces:

$$W_n^\Gamma := \{ v : \Gamma_*^n \to \mathbb{R} \mid v = w_{|\Gamma_*^n}, \ w \in W_n \}, \ 1 \le n \le N, \tag{10}$$

$$W^{\Gamma_*} := \{ v : \Gamma_* \to \mathbb{R} \mid v_{|\Gamma_*^n} \in W_n^\Gamma, \ 1 \le n \le N \}. \tag{11}$$

We need the standard DG jump terms across the end points of the time intervals:

$$v^n(x) := v(x,t_n), \quad [v]^n(x) := v_+^n(x) - v^n(x), \quad 0 \le n \le N-1, \quad \text{with } v^0(x) := 0.$$

On the cross sections $\Gamma(t_n) \times \{t_n\}$, $0 \le n \le N$, of Γ_* the L^2 scalar product is denoted by $(\psi,\phi)_{t_n} := \int_{\Gamma(t_n)} \psi\phi \, ds$. We now introduce a bilinear form $B(\cdot,\cdot)$ on $W^{\Gamma_*} \times W^{\Gamma_*}$. The bilinear form $a^n(\cdot,\cdot)$, $1 \le n \le N$, is given by

$$a^n(u,v) = \int_{t_{n-1}}^{t_n} \int_{\Gamma(t)} \dot{u}v + uv \, \mathrm{div}_\Gamma \mathbf{w} + \nabla_\Gamma u \cdot \nabla_\Gamma v \, ds \, dt.$$

The bilinear form $d^n(\cdot,\cdot)$, $1 \le n \le N$, is given by

$$d^n(u,v) = ([u]^{n-1}, v_+^{n-1})_{t_{n-1}}.$$

Corresponding global bilinear forms are obtained by summing over the time slabs:

$$a(u,v) = \sum_{n=1}^N a^n(u,v), \ d(u,v) = \sum_{n=1}^N d^n(u,v).$$

We also need a right hand-side functional given by

$$f(v) = (u_0, v_+^0)_{t_0}.$$

These bilinear forms and the functional f are well-defined on the space-time trace space W^{Γ_*}. The space-time discretization is defined as follows. Determine $U \in W^{\Gamma_*}$ such that

$$\begin{aligned} &B(U,V) = f(V) \quad \text{for all } V \in W^{\Gamma_*}, \\ &B(U,V) := a(U,V) + d(U,V). \end{aligned} \tag{12}$$

Note that this formulation allows to solve the space-time problem time slab by time slab.

References

[1] S. Gross, A. Reusken, *Numerical Methods for Two-phase Incompressible Flows*, Springer, Berlin (2011).

[2] G. Dziuk, C. Elliott, *Finite elements on evolving surfaces*, IMA J. Numer. Anal. **27** (2007), 262–292.

[3] K. Deckelnick, G. Dziuk, C. Elliott, C.-J. Heine, *An h-narrow band finite element method for elliptic equations on implicit surfaces*, IMA J. Numer. Anal. **30** (2010), 351-376.

[4] M.A. Olshanskii, A. Reusken, J. Grande, *A finite element method for elliptic equations on surfaces*, SIAM J. Numer. Anal. **47** (2009), 3339-3358.

[5] M.A. Olshanskii, A. Reusken, *A finite element method for surface PDEs: matrix properties*, Numer. Math. **114** (2009), 491–520.

[6] A. Demlow, M.A. Olshanskii, *An adaptive surface finite element method based on volume meshes*, SIAM J. Numer. Anal. **50** (2012), 1624–1647.

[7] M.A. Olshanskii, A. Reusken, X. Xu, *A stabilized finite element method for advection-diffusion equations on surfaces*, To appear in IMA J. Numer. Anal. (2013).

Existence and long-time dynamics of a nonlocal Cahn-Hilliard-Navier-Stokes system with nonconstant mobility

Elisabetta Rocca

(joint work with Sergio Frigeri and Maurizio Grasselli)

In cooperation with Sergio Frigeri (University of Milan) and Maurizio Grasselli (Politecnico of Milan) we have recently considered in [11] the so-called *nonlocal model H*: a Cahn-Hilliard-Navier-Stokes system characterized by a nonlocal Cahn-Hilliard equation for the order parameter φ with a non-constant (possibly degenerate) mobility m and a singular (e.g., logarithmic) potential F'

$$\varphi_t + u \cdot \nabla \varphi = \operatorname{div}(m(\varphi)\nabla \mu), \quad \mu = a\varphi - J * \varphi + F'(\varphi) \tag{1}$$

$$u_t - \nu \Delta u + (u \cdot \nabla)u + \nabla \pi = \mu \nabla \varphi + h, \quad \operatorname{div}(u) = 0 \tag{2}$$

$$\frac{\partial \mu}{\partial n} = 0, \quad u = 0 \quad \text{on } \partial\Omega \times (0,T) \tag{3}$$

$$u(0) = u_0, \quad \varphi(0) = \varphi_0 \quad \text{in } \Omega, \tag{4}$$

where $J * \varphi(x) := \int_\Omega J(x-y)\varphi(y)\,dy$. Model H is a diffuse interface model for incompressible isothermal two-phase flows which consists of the Navier-Stokes equations for the (averaged) velocity u nonlinearly coupled with a convective Cahn-Hilliard equation for the (relative) concentration difference φ (cf., for instance, [1, 18, 19, 20]).

A more realistic version of the Cahn-Hilliard equation is characterized by a (spatially) nonlocal free energy. The physical relevance of nonlocal interactions was already pointed out in the pioneering paper [23]. Though isothermal and nonisothermal models containing nonlocal terms have only recently been studied from the analytical viewpoint (cf., e.g., [3, 6, 12, 16, 17] and their references). The difference between local and nonlocal models consists in the choice of the interaction potential. The nonlocal contribution to the free energy has typically the form $\int_\Omega J(x,y)\,|\varphi(x)-\varphi(y)|^2\,dy$ with a given symmetric kernel J defined on $\Omega \times \Omega$; its local Ginzburg-Landau counterpart has the form $(\sigma/2)|\nabla\varphi(x)|^2$ with a positive parameter σ. The latter can be obtained as a formal limit as $m \to \infty$ from the nonlocal one with the choice $J(x,y) = m^{d+2}J(|m(x-y)|^2)$, where J is a nonnegative function with support in $[0,1]$. As a consequence, the local Cahn-Hilliard equation can be viewed as an approximation of the nonlocal one.

Nonlocal interactions have been taken into account in a series of recent papers (see [5, 8, 9, 10]) where a modification of the model H with matched densities has been considered and analyzed .

Nonlocal system (1)-(2) is more challenging with respect to the local model H, even in dimension two. One of the reasons is that φ has a poorer regularity and this influences the treatment of the Navier-Stokes system through the so-called Korteweg force $\mu\nabla\varphi$ (see, for instance, [5, Remark 8]). Due to this difficulty, only the constant mobility case has been considered so far (though viscosity depending on φ has been handled). On the other hand, in the rigorous derivation of the nonlocal Cahn-Hilliard equation done in [16] the mobility depends on φ and degenerates at the pure phases (for the local Cahn-Hilliard equation see [7] and references therein).

In this contribution we want to generalize some of the existing results on the so-called nonlocal Cahn-Hilliard-Navier-Stokes system to the case of nonconstant mobility. As we shall see, such an extension requires extra efforts which are not merely technical.

In the seminal paper [7] the authors established the existence of a weak solution to the local Cahn-Hilliard equation with degenerate mobility and singular potentials endowed with no-flux boundary conditions. This result was then extended to the standard Cahn-Hilliard-Navier-Stokes system in [4]. The nonlocal Cahn-Hilliard equation with degenerate mobility and logarithmic potential was rigorously justified and analyzed in [16]. In particular, in the case of periodic boundary conditions, an existence and uniqueness result was proven in [17]. Then a more general case was considered in [12] . More recently, the convergence to single equilibria was studied in [21, 22].

Here we generalize the strategy devised in [7] to the nonlocal case by first taking a non-degenerate mobility m and a regular potential F with polynomial growth. We prove the existence of a global weak solution which satisfies an energy inequality (equality if $d = 2$). This result extends [8] and allows us to construct a rigorous approximation of the case where m is degenerate and F is singular (e.g. logarithmic). Therefore we can pass to the limit and obtain a similar result for the latter case. In addition, since the energy identity holds in two dimensions, we can construct a semiflow which possesses a global attractor by using Ball's method (see [2]). By means of the same approach we also show that the convective nonlocal Cahn-Hilliard equation with degenerate mobility and singular potential has a unique solution and it posseses a global attractor (even if $d = 3$). Note that this result entails, in particular, that the nonlocal Cahn-Hilliard equation which has been obtained as hydrodynamic limit in [16] possesses a global attractor. We point out that uniqueness of solutions is still an open issue in the local case.

Let us notice here that the main difficulty encountered while dealing with the degenerate mobility case is that the gradient of the chemical potential μ in (1) can no longer be controlled in any L^p space. Hence, in order to get an existence result a suitable notion of weak solution need to be introduced. More precisely, in this new formulation the gradient of μ does not appear anymore. It worth observing that, in the present case, our main theorem does not require the (conserved) mean value of the order parameter φ to be strictly in between -1 and 1, but $|\int_\Omega \varphi_0| \leq |\Omega|$ suffices. Thus the model allows pure phase solutions for all $t \geq 0$. This was not possible in the case of constant or *strongly degenerate* mobility.

References

[1] D.M. Anderson, G.B. McFadden, A.A. Wheeler, *Diffuse-interface methods in fluid mechanics*, Annu. Rev. Fluid Mech. **30**, Annual Reviews, Palo Alto, CA, 1998, 139-165.

[2] J.M. Ball, *Continuity properties and global attractors of generalized semiflows and the Navier-Stokes equation*, J. Nonlinear Sci. **7** (1997), 475-502 (Erratum, J. Nonlinear Sci. **8** (1998), 233).

[3] P.W. Bates, J. Han, *The Neumann boundary problem for a nonlocal Cahn-Hilliard equation*, J. Differential Equations **212** (2005), 235-277.

[4] F. Boyer, *Mathematical study of multi-phase flow under shear through order parameter formulation*, Asymptot. Anal. **20** (1999), 175-212.

[5] P. Colli, S. Frigeri, M. Grasselli, *Global existence of weak solutions to a nonlocal Cahn-Hilliard-Navier-Stokes system*, J. Math. Anal. Appl. **386** (2012), 428-444.

[6] P. Colli, P. Krejčí, E. Rocca, J. Sprekels, *Nonlinear evolution inclusions arising from phase change models*, Czechoslovak Math. J. **57** (2007), 1067-1098.

[7] C.M. Elliott, H. Garcke, *On the Cahn-Hilliard equation with degenerate mobility*, SIAM J. Math. Anal. **27** (1996), 404-423.

[8] S. Frigeri, M. Grasselli, *Global and trajectories attractors for a nonlocal Cahn-Hilliard-Navier-Stokes system*, J. Dynam. Differential Equations **24** (2012), 827-856.

[9] S. Frigeri, M. Grasselli, *Nonlocal Cahn-Hilliard-Navier-Stokes systems with singular potentials*, Dyn. Partial Differ. Equ. **9** (2012), 273-304.

[10] S. Frigeri, M. Grasselli, P. Krejčí, *Strong solutions for two-dimensional nonlocal Cahn-Hilliard-Navier-Stokes systems,* arXiv: 1301.2346.

[11] S. Frigeri, M. Grasselli, E. Rocca, *Nonlocal Cahn-Hilliard-Navier-Stokes systems with non-constant mobility*, preprint arXiv:1303.6446 (2013).

[12] H. Gajewski, K. Zacharias, *On a nonlocal phase separation model*, J. Math. Anal. Appl. **286** (2003), 11-31.
[13] C.G. Gal, M. Grasselli, *Asymptotic behavior of a Cahn-Hilliard-Navier-Stokes system in 2D*, Ann. Inst. H. Poincaré Anal. Non Linéaire **27** (2010), 401-436.
[14] C.G. Gal, M. Grasselli, *Trajectory attractors for binary fluid mixtures in 3D*, Chinese Ann. Math. Ser. B **31** (2010), 655-678.
[15] C.G. Gal, M. Grasselli, *Instability of two-phase flows: a lower bound on the dimension of the global attractor of the Cahn-Hilliard-Navier-Stokes system,* Phys. D **240** (2011), 629-635.
[16] G. Giacomin, J.L. Lebowitz, *Phase segregation dynamics in particle systems with long range interactions. I. Macroscopic limits*, J. Statist. Phys., **87** (1997), no. 1-2, 37–61.
[17] G. Giacomin, J.L. Lebowitz, *Phase segregation dynamics in particle systems with long range interactions. II. Interface motion*, SIAM J. Appl. Math., **58** (1998), no. 6, 1707–1729.
[18] M.E. Gurtin, D. Polignone, J. Viñals, *Two-phase binary fluids and immiscible fluids described by an order parameter*, Math. Models Meth. Appl. Sci. **6** (1996), 8-15.
[19] P.C. Hohenberg, B.I. Halperin, *Theory of dynamical critical phenomena*, Rev. Mod. Phys. **49** (1977), 435-479.
[20] D. Jasnow, J. Viñals, *Coarse-grained description of thermo-capillary flow*, Phys. Fluids **8** (1996), 660-669.
[21] S.-O. Londen, H. Petzeltová, *Convergence of solutions of a non-local phase-field system*, Discrete Contin. Dyn. Syst. Ser. S **4** (2011), 653-670.
[22] S.-O. Londen, H. Petzeltová, *Regularity and separation from potential barriers for a non-local phase-field system*, J. Math. Anal. Appl. **379** (2011), 724-735.
[23] J.S. Rowlinson, Translation of J.D.van der Waals, *The thermodynamic theory of capillarity under the hypothesis of a continuous variation of density*, J. Statist. Phys., **20** (1979), 197-244.

Minimization of bending energies under constraints

Matthias Röger

(joint work with Stefan Müller and with Patrick Dondl, Luca Mugnai)

In this talk we investigate certain constrained minimization problems for the Willmore energy, in particular under a confinement condition defined by an outer container. In the first part of this talk we report on joint work with Stefan Müller (HCM Bonn), where we analyze the constrained minimization for embeddings of the sphere into the unit ball. In the second part, which is joint work with Patrick Dondl (Durham) and Luca Mugnai (MPI Leipzig), we consider confined simply connected surfaces and propose a phase-field approximation.

Part 1: Confined sphere-type surfaces. Let $a > 0$ be given and denote by B the unit ball in $\mathbb{R}^3$. We denote by $\mathcal{M}_a$ the class of smoothly embedded surfaces $\Sigma \subset B$ of sphere type with $ar(\Sigma) = a$ and consider the constrained minimization problem for the Willmore energy,

$$\mathrm{w}(a) := \inf_{\Sigma \in \mathcal{M}_a} \mathcal{W}(\Sigma), \quad \mathcal{W}(\Sigma) := \frac{1}{4} \int_\Sigma |\vec{H}|^2 \, d\mathcal{H}^2. \tag{1}$$

We are interested in the dependence of $\mathrm{w}(a)$ on the surface area a. The infimum $\mathrm{w}(a)$ may not be attained, as limit points of minimal sequences need not to be embedded. Even if one is able to obtain an Euler–Lagrange equation in a suitable class of surfaces, the constraints will induce a complex set of Lagrange multipliers.

We instead use general geometric identities to derive lower bounds and explicit constructions of minimizing sequences for upper bounds. Our first result is a general lower bound.

Theorem 1. *For any $\Sigma \in \mathcal{M}_a$ as above we have*

$$\mathcal{W}(\Sigma) \geq a. \tag{2}$$

In particular, $w(a) \geq a$ holds for all $a > 0$.

This estimate is derived from the first variation formula

$$\int_\Sigma \mathrm{div}_{T_x\Sigma}\eta(x)\, d\mathcal{H}^2(x) = -\int_\Sigma \vec{H}(x)\cdot x\, d\mathcal{H}^2(x) \quad \text{for } \eta \in C^1(\mathbb{R}^3,\mathbb{R}^3)$$

applied to the vector field $\eta(x) := x$ and using the confinement condition.

By an extension of the previous argument we also show that equality in (2) is only possible if $a = 4\pi k$, $k \in \mathbb{N}$. Then the lower bound is sharp.

Theorem 2. *Let $a = 4k\pi$ for $k \in \mathbb{N}$. Then $w(a) = a$.*

The main idea for $k = 2$ is to take two concentric spheres, one with radius one and the other with radius close to one. For both spheres we remove a cap close to the north-pole, deform the upper halves, and connect them by a catenoid-like structure.

The previous results show that optimal structures always approach for $a \approx 4k\pi$ the unit sphere. The behavior when a just exceeds the area of a sphere is therefore particularly illustrative. We find a sharp increase in Willmore energy at 4π, with a square-root type relation between Willmore deficit and the area deficit.

Proposition 3. *For all $\delta > 0$ there exists a constant $C > 0$ such that*

$$w(a) - 4\pi k \leq C\cdot\sqrt{a-4\pi} \tag{3}$$

for all $4\pi k \leq a < 4\pi k + \delta$, $k \in \mathbb{N}$.

This bound is achieved by modifying the unit sphere and growing a 'bump', directed inwards and supported close to $(0,0,1)$. By two parameters $0 < s, t \ll 1$ we control the support of the bump and its extension, respectively. Optimizing in the relation between this parameters and letting $s, t \to 0$ we obtain (3).

The main contribution of this work is a corresponding improved lower bound.

Theorem 4. *There exists $c > 0$ such that for all $\Sigma \in \mathcal{M}_a$, $a \geq 4\pi$*

$$w(a) - 4\pi \geq c\sqrt{a-4\pi}. \tag{4}$$

The main ingredients of the proof are first a Minkowsky–Steiner type formula,

$$ar(\Sigma) - 4\pi = -\int_\Sigma \Big(1 - (x\cdot\nu(x))^2 + \frac{1}{2}|x - (x\cdot\nu(x))\nu(x)|^2\Big)K(x)\, d\mathcal{H}^2(x) \tag{5}$$

for any $\Sigma \in \mathcal{M}_a$. This formula shows in particular that $K \geq 0$ on Σ implies $ar(\Sigma) \leq 4\pi$ and that there is no C^2-approximation of the unit sphere in $\bigcup_{a>4\pi}\mathcal{M}_a$.

The second key ingredient are rigidity estimates for nearly umbilical surfaces derived by De Lellis and Müller [2, 3]. In fact, by the Gauss–Bonnet Theorem we obtain for any $\Sigma \in \mathcal{M}_a$

$$\mathcal{W}(\Sigma) - \mathcal{W}(S^2) \;=\; \frac{1}{4}\int_\Sigma H^2\, d\mathcal{H}^2 - 4\pi \;=\; \frac{1}{2}\int_\Sigma (\kappa_1-\kappa_2)^2\, d\mathcal{H}^2, \tag{6}$$

where κ_1, κ_2 are the principal curvatures of Σ. By (6) the Willmore deficit controls in an L^2 sense how far away Σ is from being umbilical. In this situation Müller and De Lellis [2, 3] prove that Σ can be conformally parametrized over the sphere such that this parametrization is $W^{2,2}$ close to the identity. For details we refer to a forthcoming paper [5].

Part 2: Confined simply connected surfaces. Here we propose a phase-field approximation of the following sharp interface variational problem. Let $n = 2, 3$ and $\Omega \subset \mathbb{R}^n$ be a given open bounded set. Denote by $\mathcal{S}_a$ the set of all $E \subset\subset \Omega$ open, s.th. ∂E is smooth and connected, with $ar(\partial E) = a$. Minimize the Willmore energy of ∂E in the class $\mathcal{S}_a$. We propose the following diffuse analogue,

$$\begin{aligned}
\mathcal{E}_\varepsilon(u) \;&:= \mathcal{W}_\varepsilon(u) + \varepsilon^{-\frac{3}{2}}\left(\mathcal{A}_\varepsilon(u) - a\right)^2 + \varepsilon^{-\frac{1}{4}}\mathcal{C}_\varepsilon(u),\\
\mathcal{A}_\varepsilon(u) \;&:= \int_\Omega \left(\frac{\varepsilon}{2}|\nabla u|^2 + \frac{1}{\varepsilon}W(u)\right) dx,\\
\mathcal{W}_\varepsilon(u) \;&:= \int_\Omega \frac{1}{\varepsilon}\left(\varepsilon\Delta u - \frac{1}{\varepsilon}W'(u)\right)^2 dx,\\
&\mathcal{C}_\varepsilon \quad \text{penalizes non-connectedness,}
\end{aligned}$$

where we minimize $\mathcal{E}_\varepsilon(u)$ subject to clamped boundary conditions. This replaces the area constraint by a soft constraint and the usual Modica–Mortola diffuse surface area energy. For the Willmore energy we use the well-known De Giorgi approximation. The new contribution is the functional $\mathcal{C}_\varepsilon$ that detects multiple components and that is given by the following 'inner' variational problem,

$$\begin{aligned}
\mathcal{C}_\varepsilon(u) \;&:= \left(c_{\varepsilon,u}(1) - \inf_\phi c_{\varepsilon,u}(\phi)\right)^2 \qquad \text{for } \phi \in BV(\Omega;\{\pm 1\}),\\
c_{\varepsilon,u}(\phi) \;&:= \left|\int_\Omega \varepsilon^{-1} G(u)\,\phi\, dx\right| + \int_\Omega \varepsilon^{-\frac{3}{2}} G_\lambda(u)\, d|\nabla\phi|.
\end{aligned}$$

Here G is cut-off function that is one on $[-1+2\delta, 1+2\delta]$ and zero outside $(-1+\delta, 1-\delta)$, and G_λ is a suitably rescaled version of G. We justify the approximation property of $\mathcal{E}_\varepsilon$ by an upper- and lower-bound statement.

Theorem 5. *(1) For $E \in \mathcal{S}_a$ and $u = 2\mathcal{X}_E - 1$ there exists $(u_\varepsilon)_{\varepsilon>0}$ such that*

$$u_\varepsilon \;\to\; u \quad \text{in } L^1(\Omega) \quad \text{and} \quad \lim_{\varepsilon\to 0}\mathcal{E}_\varepsilon(u_\varepsilon) \;=\; \mathcal{W}(\partial E).$$

(2) Consider a sequence $(u_\varepsilon)_{\varepsilon>0}$. Associate diffuse surface area measures μ_ε, $d\mu_\varepsilon := \left(\frac{\varepsilon}{2}|\nabla u_\varepsilon|^2 + \frac{1}{\varepsilon}W(u_\varepsilon)\right) dx$ and assume

$$\mathcal{E}_\varepsilon(u_\varepsilon) \;<\; \Lambda, \qquad u_\varepsilon \;\to\; u, \qquad \mu_\varepsilon \;\to\; \mu.$$

Then $u = 2\mathcal{X}_E - 1$, $\mu(\mathbb{R}^n) = a$, $\mu \leq |\nabla u|$, μ *is an integral varifold with* $\vec{H} \in L^2(\mu)$,

$$\frac{1}{4}\int_\Omega |\vec{H}|^2 \, d\mu \;\leq\; \liminf_{\varepsilon\to 0} \mathcal{E}_\varepsilon(u_\varepsilon)$$

and μ *represents a connected structure in the following sense: There are no two open sets* $\Omega_1, \Omega_2 \subset \mathbb{R}^n$ *with disjoint closure such that*

$$\mu(\Omega_i) \;>\; 0\,(i = 1, 2) \quad \text{and} \quad \mu\big(\mathbb{R}^n \setminus (\Omega_1 \cup \Omega_2)\big) \;=\; 0.$$

The proof of the upper bound employs the standard construction by a rescaled optimal profile and signed distance function, see for example [1]. In addition we have to show here that the connectedness term $\mathcal{C}_\varepsilon$ yields no contribution in the limit. The proof of the lower bound relies on an application and extension of results from [6]. The difficult part is to show that $\mathcal{C}_\varepsilon$ in fact induces the connectedness of the limit structure. For details we refer to a forthcoming paper [4].

References

[1] G. Bellettini and L. Mugnai. On the approximation of the elastica functional in radial symmetry. *Calc. Var. Partial Differential Equations*, 24(1):1–20, 2005.

[2] Camillo De Lellis and Stefan Müller. Optimal rigidity estimates for nearly umbilical surfaces. *J. Differential Geom.*, 69(1):75–110, 2005.

[3] Camillo De Lellis and Stefan Müller. A C^0 estimate for nearly umbilical surfaces. *Calc. Var. Partial Differential Equations*, 26(3):283–296, 2006.

[4] Patrick W. Dondl, Luca Mugnai, and Matthias Röger. A phase field model for the optimization of the Willmore energy in the class of connected surfaces. In preparation, 2013.

[5] Stefan Müller and Matthias Röger. Confined structures of least bending energy. In preparation, 2013.

[6] Matthias Röger and Reiner Schätzle. On a modified conjecture of De Giorgi. *Math. Z.*, 254(4):675–714, 2006.

Voronoi Implicit Interfaces: Method and Applications

Robert I. Saye, James A. Sethian

A variety of problems, both theoretical and highly practical, involve the interaction of multiply-connected regions moving together. These include liquid foams (e.g. polyurethane and colloidal mixtures) and solid foams, such as wood and bone. In such problems, multiple domains share common walls which meet at multiple junctions. Boundaries move under forces which depend on both local and global geometric properties, such as surface tension and volume constraints, as well long-range physical forces, including incompressible flow, membrane permeability, and elastic forces.

A familiar example comes from soap bubbles, in which gaseous pockets are separated by thin film lamellae, whose position and shape are controlled by surface tension and force balances. Over time, the fluid in the thin membrane drains, until at some point the membrane ruptures, causing macroscale disequilibrium. Large-scale rearrangement then occurs, in which the gases move and the remaining

membranes stretch and respond, until a new equilibrium is reached. Drainage then continues until rupture occurs again.

Another example comes from grain metal coarsening, in which surface energy, often associated with temperature changes, drives a system to larger structures. This is a common process in the formation of metallic substances, and understanding the time-dependent motion is important in determining the ultimate shape. One simple mathematical idealization of the phenomenon is characterized by a set of regions locally driven by curvature.

Producing good mathematical models and numerical algorithms that capture the motion of these interfaces is challenging, especially at junctions where multiple interfaces meet, and when topological connections change. Methods have been proposed, including front tracking, volume of fluid, variational, and level set methods. It has remained a challenge to robustly and accurately handle the wide range of possible motions of an evolving, highly complex, multiply-connected interface separating a large number of phases under time-resolved physics.

Recently, we introduced a set of computational techniques, known as "Voronoi Implicit Interface Methods" [4, 5], to track such multiphase-multiphysics problems. Rather than track the interfaces separating the regions, or the individual regions themselves, the method characterizes the entire system by a single scalar function defined in all of space, and updates this function by solving a time-dependent initial value problem.

In more detail, consider a collection of non-overlapping phases, with the "interface" defined as the set of points where these phases touch together. In two dimensions, this interface may consist of single curves touched by only two phases, as well as triple points, where three regions meet; higher order junctions are also possible. In three dimensions, more elaborate interfaces are possible.

We may characterize this entire system through an implicit representation as follows. For each point x in the plane, define $\phi(x)$ as the distance to the closest interface. Additionally, define $\chi(x)$ as an integer-valued function which indicates the phase. Then, the interface itself is given as the zero level set $\{\phi(x) = 0\}$ of this unsigned distance function. Thus, for example, if $\phi(x) = 5$ and $\chi(x) = 4$, then we know that the point x is located in phase 4, and the closest interface point is located a distance 5 away.

We can advance this interface through a two-step procedure. Imagine the interface moves with a speed F in its normal direction. Then

- Advance ϕ through k time steps using the standard level set methodology introduced by Osher and Sethian in [3]. That is, use upwind operators to produce ϕ^{n+1} from ϕ^n by solving a discrete finite difference approximation to

$$\phi_t + F|\nabla\phi| = 0$$

- Use the ϵ level sets of this time-advanced solution to reconstruct a new unsigned distance function. This is done by first computing the Voronoi interface from the ϵ level sets: this corresponds to the set of all points

equidistant from at least two of the ϵ level sets from different phases. This Voronoi interface is then used to rebuild the unsigned distance function.

This is the most straightforward implementation of the method. More efficient and sophisticated techniques include the use of narrow banding [1] to limit computational labor to a small region near the interface, a fast Eikonal solver [2] to find the new unsigned distance from the ϵ level sets without explicitly constructing the front, and careful data structures which allow any non-negative value for ϵ, including $\epsilon = 0^+$. For details, see [4, 5].

As application, Figure 1, taken from [5], illustrates the results for a two-dimensional simulation of a variable density fluid flow, computed on a 256^2 grid with slip boundary conditions, using $\epsilon = 0^+$. As discussed in [5], the heavier phase, initially having nine separate components of circular shape, is colored orange. The other phases, of which there are initially approximately 35, are colored shades of blue and green. Figure 1 shows snapshots of the simulation at different times of note, showing plots of phase evolution, streamlines and stream function, and pressure fields. We note several features of our results. Most of the components of the heavy phase (shown in orange) sink to the bottom. In particular, the component initially attached to the top, first falls down, leaving behind it a trailing tail. It then detaches from the top boundary, forming a jet that quickly retracts (as seen at $t = 1.32$). On the other hand, the two smallest components of the heavy phase do not sink, and remain embedded in the foam at time $t = 1.81$. Here, the local forces of surface tension, particularly at the triple points, dominate the force of gravity and prevent them from falling. This is similar to an air bubble at the surface of water: depending on its diameter, the bubble can range from being almost fully submersed and spherical in shape to entirely on the surface with a hemispherical shape.

References

[1] Adalsteinsson, D., and Sethian, J.A., *A Fast Level Set Method for Propagating Interfaces*, J. Comp. Phys., 118(2), pp. 269–277, 1995.

[2] Chopp, D.L. *Some Improvements of the Fast Marching Method*, SIAM Journal Scientific Computing, 23(1), pp. 230–244, 2001.

[3] Osher, S., and Sethian, J.A., *Fronts Propagating with Curvature-Dependent Speed: Algorithms based on Hamilton-Jacobi Formulations*, J. Comp. Phys., 79(1), pp. 12–49, (1988).

[4] Saye, R. and Sethian, J.A., *The Voronoi Implicit Interface Method for Computing Multiphase Physics*, Proceedings of the National Academy of Sciences, 108(49), pp. 19498–19503, (2011)

[5] Saye, R. and Sethian, J.A., *Analysis and applications of the Voronoi Implicit Interface Method*, J. Comp. Phys., 231(18), pp. 6051–6085, 2012.

[6] Sethian, J.A., *Level Set Methods and Fast Marching Methods*, Cambridge Univ. Press, 1999.

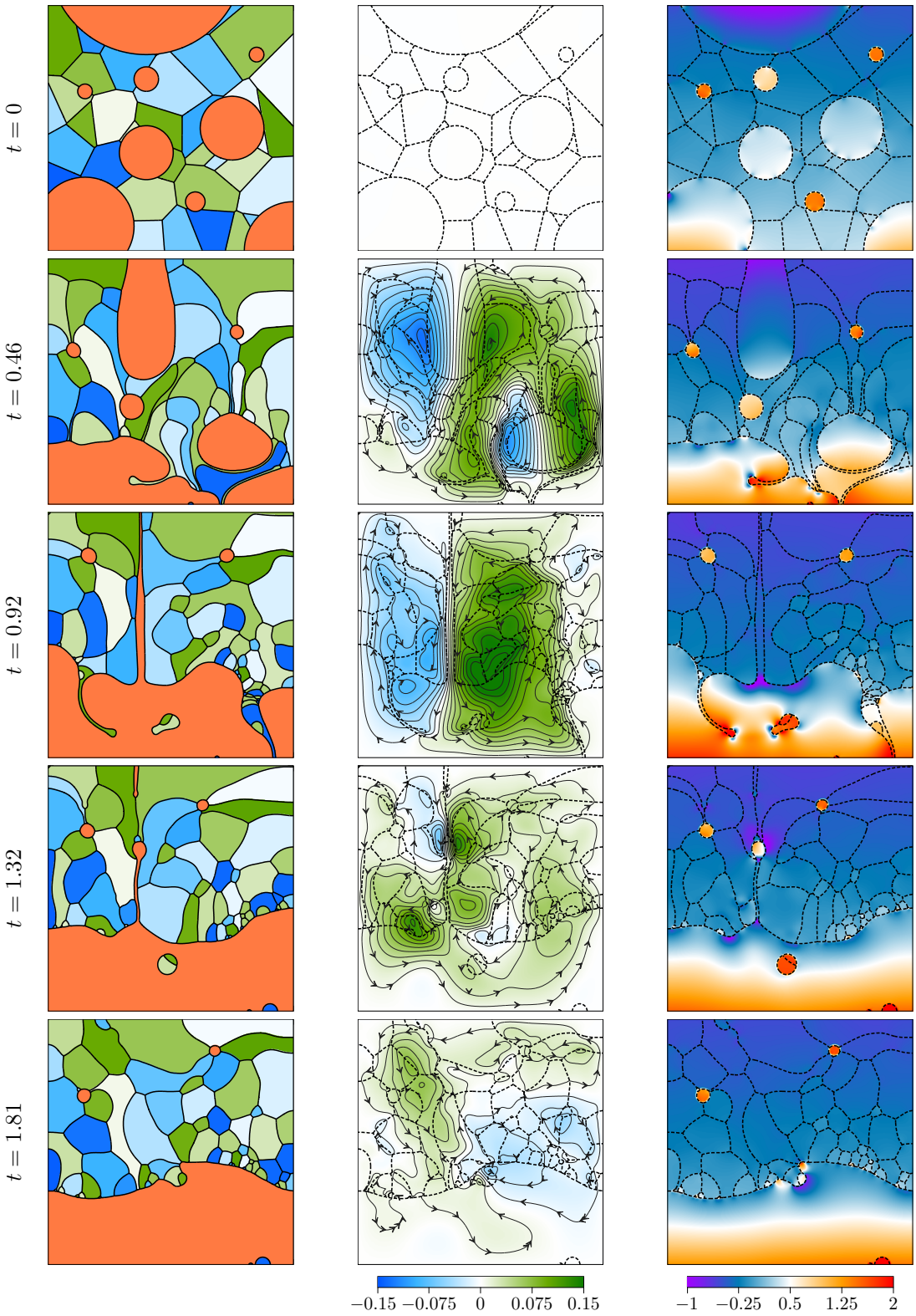

FIGURE 1. Results of a fluid flow simulation with gravity, in which the orange colored phase is more viscous and more dense than the other phases.

Phase-field modelling of two-phase flow with soluble surfactant

Björn Stinner
(joint work with Harald Garcke and Kei Fong Lam)

Surface active agents (surfactants) reduce the surface tension of fluid interfaces and, via surface tension gradients, can lead to tangential forces resulting in Marangoni effects. Biological systems take advantage of their impact, but they are also of relevance in technical applications such as the stabilisation of emulsions. While often much experience and knowledge is available on how surfactants influence the rheology of multi-phase fluids, the goal is to understand how exactly the presence of a surfactant influences coalescence and segregation of droplets. In order to facilitate such investigations our goal has been to describe two-phase flow with surfactants, possibly soluble in the fluids, by a diffuse interface model based on the phase field methodology such that

- a sharp interface model is obtained as the interfacial thickness converges to zero where the relation is established using matched asymptotic expansions,
- thermodynamic consistency is guaranteed, thus leading to natural energy estimates as a prerequisite for a rigorous analysis,
- data from the related sharp interface model, i.e., parameters but also relations such as the dependence of surface tension on the surfactant density (equation of state), can easily be transferred.

We first consider a sharp interface model that we aim to approximate. The exchange of surfactant between the bulk phases and the fluid interfaces is governed by processes of adsorption and desorption. Following [2] we need to distinguish two cases. In many systems it may be considered as taking place instantaneously resulting in an equilibrium condition for surface surfactant density on the interface and the bulk surfactant density in the sublayer close to the interface. This condition is expressed by an *isotherm*. However, there are systems where the adsorption takes place on a time scale comparable to that of the bulk transport, in which case we talk about dynamic adsorption, and the upshot will be a condition involving the mass fluxes from the adjacent bulk.

We take an energetic approach and postulate

$$\int_{\Omega^{(1)}(t)} [\tfrac{\overline{\rho}^{(1)}}{2}|\boldsymbol{v}|^2 + G_1(c^{(1)})] + \int_{\Omega^{(2)}(t)} [\tfrac{\overline{\rho}^{(2)}}{2}|\boldsymbol{v}|^2 + G_2(c^{(2)})] + \int_{\Gamma(t)} \gamma(c^\Gamma).$$

where $\overline{\rho}^{(i)}$ are the mass densities, $\boldsymbol{v}$ is the velocity, the $G_i(c^{(i)})$ are bulk free energy densities depending on the bulk surfactant densities $c^{(i)}$, $i = 1, 2$, and $\gamma(c^\Gamma)$ is a surface free energy density depending on the surface surfactant density c^Γ. Starting with usual balance equations for mass, momentum, and energy, requiring nonnegative energy dissipation, and making some constitutive assumptions we arrive at the following sharp interface model:

In the bulk domains $\Omega^{(i)}(t)$, $i = 1, 2$:

$$\begin{aligned} \nabla \cdot \boldsymbol{v} &= 0 \\ \partial_t(\overline{\rho}^{(i)}\boldsymbol{v}) + \nabla \cdot (\overline{\rho}^{(i)}\boldsymbol{v} \otimes \boldsymbol{v}) &= \nabla \cdot \Big(-p\boldsymbol{I} + 2\eta^{(i)} D(\boldsymbol{v})\Big) \\ \partial_t^\bullet c^{(i)} &= \nabla \cdot (M_c^{(i)} \nabla G_i'(c^{(i)})). \end{aligned}$$

Here $\eta^{(i)}$ is the viscosity of fluid i, $D(\boldsymbol{v}) = \frac{1}{2}(\nabla \boldsymbol{v} + (\nabla \boldsymbol{v})^\perp)$ is the rate of deformation tensor, p is the pressure, $\boldsymbol{I}$ is the identity tensor, $\partial_t^\bullet(\cdot) = \partial_t(\cdot) + \boldsymbol{v} \cdot \nabla(\cdot)$ is the material derivative, $M_c^{(i)}$ is the mobility of surfactants in fluid i.
On the interface $\Gamma(t)$:

$$\begin{aligned} [\boldsymbol{v}]_1^2 &= 0, \quad \boldsymbol{v} \cdot \boldsymbol{\nu} = u_\Gamma \\ \Big[p\boldsymbol{I} - 2\eta^{(i)} D(\boldsymbol{v})\Big]_1^2 \boldsymbol{\nu} &= \sigma(c^\Gamma)\kappa\boldsymbol{\nu} + \nabla_\Gamma \sigma(c^\Gamma), \\ \partial_t^\bullet c^\Gamma + c^\Gamma \nabla_\Gamma \cdot \boldsymbol{v} &= \nabla_\Gamma \cdot (M_\Gamma \nabla_\Gamma \gamma'(c^\Gamma)) + [M_c^{(i)} \nabla G_i'(c^{(i)})]_1^2 \cdot \boldsymbol{\nu} \\ \alpha^{(i)}(-1)^i M_c^{(i)} \nabla G_i'(c^{(i)}) \cdot \boldsymbol{\nu} &= -(\gamma'(c^\Gamma) - G_i'(c^{(i)})). \end{aligned}$$

Here u_Γ is the normal velocity, $\boldsymbol{\nu}$ is the unit normal on Γ pointing into $\Omega^{(2)}$, $\sigma(c^\Gamma) = \gamma(c^\Gamma) - c^\Gamma \gamma'(c^\Gamma)$ is the surfactant density dependent surface tension, κ is the mean curvature of Γ, ∇_Γ is the surface gradient operator, $M_\Gamma(c^\Gamma)$ is the mobility of the interfacial surfactants, and $\alpha^{(i)} \geq 0$ is a kinetic factor that relates to the speed of adsorption. Instantaneous adsorption corresponds to the case $\alpha^{(i)} = 0$ and dynamic adsorption to $\alpha^{(i)} > 0$. Exemplary, for $G(c) = Bc(\log(Kc) - 1)$ and $\gamma(c^\Gamma) = \sigma_0 + B\left(c^\Gamma \log \frac{c^\Gamma}{c_M^\Gamma - c^\Gamma} + c_M^\Gamma \log(1 - \frac{c^\Gamma}{c_M^\Gamma})\right)$ we obtain from $G'(c) = \gamma(c^\Gamma)$ the Langmuir isotherm $Kc = \frac{c^\Gamma}{c_M^\Gamma - c^\Gamma}$, and the surface tension is $\sigma(c^\Gamma) = \sigma_0 + Bc_M^\Gamma \log\left(1 - \frac{c^\Gamma}{c_M^\Gamma}\right)$.

Previous phase field models approximating the above system are based on an energy but then lack flexibility with respect to implementing different isotherms and equations of state [5, 4, 6] or lack thermodynamic consistency [3]. Our approach is based on [1]. An order parameter φ is introduced to distinguish the two phases. Writing the surfactant equations in a distributional form and smoothing these distributions in terms of φ yields

$$\begin{aligned} \partial_t(\xi_i c^{(i)}) + \nabla \cdot (\xi_i c^{(i)} \boldsymbol{v} - \xi_i M(c^{(i)}) \nabla G_i'(c^{(i)})) &= \delta j_i, \quad i = 1, 2, \\ \partial_t(\delta c^\Gamma) + \nabla \cdot (\delta c^\Gamma \boldsymbol{v} - \delta M_\Gamma(c^\Gamma) \nabla \gamma'(c^\Gamma)) &= -\delta(j_1 + j_2), \end{aligned}$$

with $j_i = \frac{1}{\alpha^{(i)}}(\gamma'(c^\Gamma) - G_i'(c^{(i)}))$ and $\delta(\varphi, \nabla\varphi) = \frac{\varepsilon}{2}|\nabla\varphi|^2 + \frac{1}{\varepsilon}W(\varphi)$ and $\xi_2(\varphi) = 1 - \xi_1(\varphi) = \frac{1}{2}(1 + \frac{1}{2}\varphi(3 - \varphi^2))$. Coupling with the fluid flow such that the free energy with the density

$$e = \rho\frac{|\boldsymbol{v}|^2}{2} + K\delta(\varphi, \nabla\varphi)\gamma(c^\Gamma) + \xi_1(\varphi)G_1(c^{(1)}) + \xi_2(\varphi)G_2(c^{(2)}).$$

is dissipated and making suitable constitutive assumptions yields the following Navier-Stokes-Cahn-Hilliard system:

$$\begin{aligned}
\nabla \cdot \boldsymbol{v} &= 0, \\
\partial_t(\rho \boldsymbol{v}) + \nabla \cdot (\rho \boldsymbol{v} \otimes \boldsymbol{v}) &= \nabla \cdot \Big(-p\boldsymbol{I} + 2\eta(\varphi) D(\boldsymbol{v}) + \boldsymbol{v} \otimes \tfrac{\overline{\rho}^{(2)} - \overline{\rho}^{(1)}}{2} m(\varphi) \nabla \mu \Big) \\
&\quad + \nabla \cdot \big(K\sigma(c^\Gamma)(\delta(\varphi, \nabla\varphi)\boldsymbol{I} - \varepsilon \nabla\varphi \otimes \nabla\varphi) \big), \\
\partial_t \varphi + \nabla \cdot (\varphi \boldsymbol{v}) &= \nabla \cdot (m(\varphi) \nabla \mu), \\
\mu + \nabla \cdot (K\varepsilon\sigma(c^\Gamma)\nabla\varphi) &= \frac{K}{\varepsilon}\sigma(c^\Gamma) W'(\varphi) + \sum_{i=1,2} \xi_i'(\varphi)(G_i(c^{(i)}) - G_i'(c^{(i)})c^{(i)}).
\end{aligned}$$

The above model covers the case of dynamic adsorption $\alpha^{(i)} > 0$. We observed in numerical experiments that when reducing this kinetic adsorption parameter the system gets closer to local equilibrium at the interface. Using the chemical potential q as unknown field rather than the surfactant densities is possible if the free energy densities G_i and γ are convex. Then also the case of instantaneous adsorption can be dealt with.

We stress again that both models are thermodynamically consistent. Moreover, an asymptotic analysis can be carried out relating the phase field models to the above sharp interface model in the limit as $\varepsilon \to 0$.

References

[1] H. Abels, H. Garcke, and G. Grün, *Thermodynamically consistent, frame indifferent diffuse interface models for incompressible two-phase flows with different densities*, Mathematical Models and Methods in Applied Sciences **22** (2011), 1150013, 40pp.

[2] H. Diamant and D. Andelman, *Kinetics of surfactant adsorption at fluid–fluid interfaces*, Journal of Physical Chemistry **100** (1996), 13732–13742.

[3] K.E. Teigen, P. Song, J. Lowengrub, and A. Voigt, *A diffuse-interface method for two-phase flows with soluble surfactants*, Journal of Computational Physics **230** (2011), 375–393.

[4] T. Teramoto and F. Yonezawa, *Droplet growth dynamics in a water/oil/surfactant system*, Journal of Colloid and Interface Science **235** (2001), 329–333.

[5] O. Theissen and G. Gompper, *Lattice-Boltzmann study of spontaneous emulsification*, The European Physical Journal B-Condensed Matter and Complex Systems **11** (1999), 91–100.

[6] R.G.M. van der Sman and S. van der Graaf, *Diffuse interface model of surfactant adsorption onto flat and droplet interfaces*, Rheology Acta **46** (2006), 3–11.

Backward difference time discretisation of parabolic partial differential equations on evolving surfaces

Chandrasekhar Venkataraman
(joint work with Christian Lubich, Dhia Mansour)

We consider the linear parabolic differential equation on a moving surface

$$\dot{u} + u\nabla_{\Gamma(t)} \cdot \mathbf{v} - \Delta_{\Gamma(t)} u = f \quad \text{ on } \Gamma(t), t \in (0, T].$$

Discretisation in space by the evolving surface finite element method (ESFEM) [1] leads to a system of ordinary differential equations for the coefficient vector $\mathbf{U}(t)$ of the semidiscrete (space) solution, of the form

$$\frac{\mathrm{d}}{\mathrm{d}\, t} \left(\mathbf{M}(t)\mathbf{U}(t)\right) + \mathbf{A}(t)\mathbf{U}(t) = \mathbf{F},$$

here $\mathbf{M}$, $\mathbf{A}$ are the evolving mass and stiffness matrices respectively. For the numerical integration of the system of ODEs, we consider the k-step backward difference formula (BDF) method with step size $\tau > 0$ given by

$$\frac{1}{\tau} \sum_{j=0}^{k} \delta_j \mathbf{M}(t_{n-j})\mathbf{U}_{n-j} + \mathbf{A}(t_n)\mathbf{U}_n = \mathbf{F}(t_n), \quad n \geq k,$$

with given starting values $\mathbf{u}_0, \ldots, \mathbf{u}_{k-1}$. The coefficients of the method are determined by

$$\delta(\zeta) = \sum_{j=0}^{k} \delta_j \zeta^k = \sum_{\ell=1}^{k} \frac{1}{\ell} (1-\zeta)^\ell.$$

For the stability analysis of the fully discrete scheme we make use of the following results

Lemma. (Dahlquist [3]). *Let $\delta(\zeta)$ and $\mu(\zeta)$ be polynomials of degree at most k (at least one of them of exact degree k) that have no common divisor. Let $\langle \cdot, \cdot \rangle$ be an inner product on $\mathbb{R}^N$ with associated norm $|\cdot|$. If*

$$\mathrm{Re}\, \frac{\delta(\zeta)}{\mu(\zeta)} > 0 \quad \textit{for } |\zeta| < 1,$$

then there exists a symmetric positive definite matrix $\mathbf{G} = (g_{ij}) \in \mathbb{R}^{k \times k}$ and real $\gamma_0, \ldots, \gamma_k$ such that for all $\mathbf{v}_0, \ldots, \mathbf{v}_k \in \mathbb{R}^N$

$$\Big\langle \sum_{i=0}^{k} \delta_i \mathbf{v}_{k-i}, \sum_{j=0}^{k} \mu_j \mathbf{v}_{k-j} \Big\rangle = \sum_{i,j=1}^{k} g_{ij} \langle \mathbf{v}_i, \mathbf{v}_j \rangle - \sum_{i,j=1}^{k} g_{ij} \langle \mathbf{v}_{i-1}, \mathbf{v}_{j-1} \rangle + \Big| \sum_{i=0}^{k} \gamma_i \mathbf{v}_i \Big|^2.$$

In combination with the preceding result for $\mu(\zeta) = 1 - \eta\zeta$, the following property of BDF methods up to order 5 plays a key role in our stability analysis.

Lemma. (Nevanlinna & Odeh [4]). *If $k \leq 5$, then there exists $0 \leq \eta < 1$ such that for $\delta(\zeta) = \sum_{\ell=1}^{k} \frac{1}{\ell}(1-\zeta)^\ell$,*

$$\operatorname{Re} \frac{\delta(\zeta)}{1-\eta\zeta} > 0 \quad \text{for } |\zeta| < 1.$$

The smallest possible value of η is found to be $\eta = 0, 0, 0.0836, 0.2878, 0.8160$ for $k = 1, \ldots, 5$, respectively.

In order to formulate our stability result we introduce the following time-dependent norm

$$\|\mathbf{w}\|_t^2 := \mathbf{w}^T \mathbf{M}(t)\mathbf{w}, \qquad \mathbf{w} \in \mathbb{R}^N,$$

and seminorm

$$|\mathbf{w}|_t^2 := \mathbf{w}^T \mathbf{A}(t)\mathbf{w}, \qquad \mathbf{w} \in \mathbb{R}^N.$$

We consider the error between the fully discrete and semidiscrete (space) solutions $\mathbf{e}_n = \mathbf{U}_n - \mathbf{U}(t_n)$. The error satisfies the fully discrete scheme up to a defect $\mathbf{d}_n$, which is merely the error of backward differentiation (and is thus $\mathcal{O}(\tau^k)$ in suitable norms). Applying the above results and using the fact that the mass and stiffness matrices associated with the ESFEM are positive definite and semidefinite respectively and some basic estimates shown in [5], we obtain the following stability result for the error

Lemma. (Stability [2]). *For the k-step BDF method with $k \leq 5$, there exists a $\tau_0 > 0$, such that for $\tau \leq \tau_0$ and $t_n \leq T$, the errors $\mathbf{e}_n$ between the fully discrete and semidiscrete solutions are bounded by*

$$\|\mathbf{e}_n\|_{t_n} 2 + \tau \sum_{j=k}^{n} |\mathbf{e}_j|_{t_j} 2 \leq C\, \tau \sum_{j=k}^{n} \|\mathbf{d}_j\|_{*,t_j} 2 + C \max_{0 \leq i \leq k-1} \|\mathbf{e}_i\|_{t_i} 2$$

where $\|\mathbf{w}\|_{*,t} 2 = \mathbf{w}^T(\mathbf{A}(t)+\mathbf{M}(t))^{-1}\mathbf{w}$ and τ_0 and C are independent of the spatial grid size h.

The proof is based on energy arguments where following Nevanlinna & Odeh [4] we test with $\mathbf{e}_n - \eta \mathbf{e}_{n-1}$.

The stability result above is then used to obtain an error bound for the full discretisation where we compare the fully discrete solution with a projection of the solution to the continuous equation into the surface finite element space. We focus on the case that the projection is the linear Lagrange interpolant (although one could consider a suitable Ritz projection). Applying the results of Dziuk & Elliott [1] we show the following error bound for the full discretisation

theorem. (Error bound [2]) *Consider the space discretisation of the parabolic equation by the ESFEM and time discretisation by the BDF method of order $k \leq 5$. Assuming sufficient regularity on the geometry, the solution u of the parabolic equation and the discretised surfaces $\Gamma_h(t)$ (see [2] for details), there exist $h_0 > 0$ and $\tau_0 > 0$ such that for $h \leq h_0$ and $\tau \leq \tau_0$ the following holds for the errors*

$$e_h^n = u_h^n - (I_h u)(t_n)$$

between the fully discrete numerical solution u_h^n and the piecewise linear Lagrange interpolant $(I_h u)(t_n)$ of the exact solution on the discrete surface $\Gamma_h(t_n)$ for $t_n = n\tau \le T$: whenever the errors e_h^i of the starting values are bounded by $c\tau^k + ch$ in the $L2(\Gamma_h(t_i))$ norm for $i = 0, \dots, k-1$, then the errors are bounded by

$$\max_{k\le j\le n} \|e_h^j\|_{L_2(\Gamma_h(t_j))} + \Big(\tau \sum_{j=k}^{n} \|\nabla_{\Gamma_h(t_j)} e_h^j\|^2_{L_2(\Gamma_h(t_j))}\Big)^{1/2} \le C\tau^k + Ch,$$

where C is independent of h and τ.

References

[1] G. Dziuk and C.M. Elliott, *Finite elements on evolving surfaces,* IMA J. Numer. Anal. **27** (2007), 262-292.

[2] Ch. Lubich, D. Mansour, and C. Venkataraman, *Backward difference time discretization of parabolic differential equations on evolving surfaces,* IMA J. Numer. Anal. *In press.*

[3] G. Dahlquist, *G-stability is equivalent to A-stability,* BIT **18** (1978), 384-401.

[4] O. Nevanlinna and F. Odeh, *Multiplier techniques for linear multistep methods,* Numer. Funct. Anal. Optim. **3** (1981), 377-423.

[5] G. Dziuk, Ch. Lubich and D. Mansour, *Runge–Kutta time discretization of parabolic differential equations on evolving surfaces,* IMA J. Numer. Anal. (2011), doi:10.1093/imanum/drr017.

Optimal fine-scale structure in elastic shape optimization

Benedikt Wirth

(joint work with Robert Kohn)

We consider the optimization of the topology and geometry of an elastic structure $\mathcal{O} \subset \mathbb{R}^2$ subjected to fixed loads $F : \Gamma \to \mathbb{R}^2$, where Γ is a fixed prescribed part of the boundary $\partial\mathcal{O}$. The objective functional measures the elastic compliance, the material volume, as well as the perimeter of the design. For certain parameter regimes, optimal geometries will exhibit very fine-scale structure, which we analyze in simple geometries by proving an energy scaling law.

In detail, we aim to minimize a weighted sum

$$\mathrm{J}^{\alpha,\beta,\varepsilon,\mu,F,\ell}[\mathcal{O}] = \alpha\mathrm{Comp}(\mathcal{O}) + \beta\mathrm{Vol}(\mathcal{O}) + \varepsilon\mathrm{Per}(\mathcal{O})$$

of structure compliance $\mathrm{Comp}(\mathcal{O})$, material volume $\mathrm{Vol}(\mathcal{O}) = \mathcal{L}^2(\mathcal{O})$, and structure perimeter $\mathrm{Per}(\mathcal{O}) = \mathcal{H}^1(\partial\mathcal{O})$. The compliance is defined in the usual way as the surface load potential

$$\mathrm{Comp}(\mathcal{O}) = \tfrac{1}{2}\int_\Gamma F \cdot u \,\mathrm{d}a$$

for the equilibrium displacement $u : \mathcal{O} \to \mathbb{R}^2$, which is the minimizer of the free energy

$$\mathrm{E}[u] = \int_{\mathcal{O}} \mu|\epsilon(u)|^2 \,\mathrm{d}x - \int_\Gamma F \cdot u \,\mathrm{d}a \quad \text{with } \epsilon(u) = \frac{1}{2}(\nabla u + \nabla u^T)$$

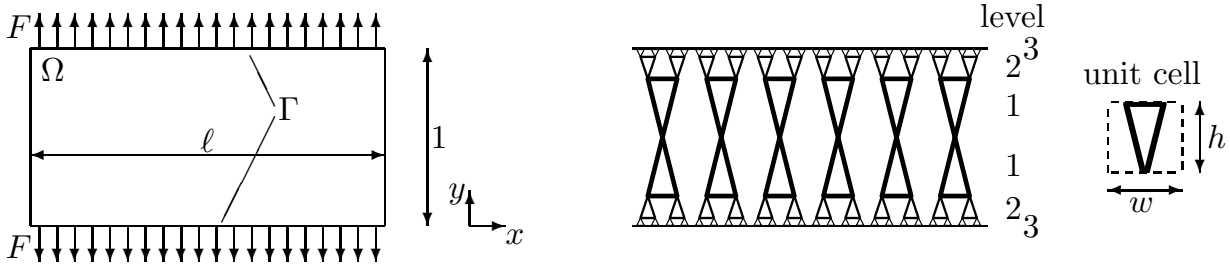

FIGURE 1. Left: Load geometry considered in Theorem 1 with a uniform normal tension F at the top and bottom. The optimal design $\mathcal{O}$ is sought inside Ω. Right: Sketch of optimal construction (here with three branching levels) and a single unit cell.

(for simplicity, we here consider an isotropic material with shear modulus μ and zero Poisson's ratio). The superscript ℓ of J comprises the geometric parameters of the problem. Using the scale invariance

$$\mathrm{J}^{\alpha,\beta,\varepsilon,\mu,F,\ell}[\mathcal{O}] = \beta \mathrm{J}^{1,1,\frac{\varepsilon}{\beta},\frac{1}{4},F\sqrt{\frac{\alpha}{4\mu\beta}},\ell}[\mathcal{O}]$$

it is obviously sufficient to consider the case $\alpha = \beta = 1$, $\mu = \frac{1}{4}$ which we assume from now on. For the load geometry given in Figure 1 one can prove the following result.

Theorem 1 (Optimal energy scaling for uniaxial normal load)**.** *In the regime* $\max(|F|, \varepsilon) < 1$, $\varepsilon < \min(\ell^3|F|, |F|^4)$*, there exist* $c, C > 0$ *with*

$$c\varepsilon^{\frac{2}{3}}\ell|F|^{\frac{1}{3}} \leq \min_{\mathcal{O}\subset\Omega} \mathrm{J}^{\varepsilon,F,\ell}[\mathcal{O}] - \mathrm{J}_0^{*,F,\ell} \leq C\varepsilon^{\frac{2}{3}}\ell|F|^{\frac{1}{3}}$$

for $\mathrm{J}_0^{*,F,\ell} = 2\ell|F|$.

The upper bound in this theorem is proved by constructing a particular design $\mathcal{O}$ and estimating its energy. By the lower bound, up to a constant factor there is no design with smaller energy so that the construction from the proof provides an intuition of how optimal geometries look like. The design features a fine-scale branching structure which results from the balance between structure compliance, volume, and perimeter: Penalization of the volume prevents the use of much material, while the distributed surface load requires stiff support all along Γ to reduce the compliance. The perimeter penalization then induces a structure coarsening further away from Γ.

The proof of Theorem 1 is sketched below. It proceeds in three basic steps which in a similar form are also employed in many related problems of analysing physical patterns via energy scaling laws (e. g. [1, 2]). In our particular case it makes use of the classical dual reformulation of the compliance via a stress field σ,

$$\mathrm{Comp}(\mathcal{O}) = \min_{\sigma\in\Sigma_{\mathrm{ad}}^{\mathcal{O}}} \int_{\mathcal{O}} |\sigma|^2 \,\mathrm{d}x\,,$$

where (writing n for the unit normal to $\partial\mathcal{O}$) the set of admissible stresses is given by

$$\Sigma_{\mathrm{ad}}^{\mathcal{O}} = \{\sigma : \mathcal{O} \to \mathbb{R}^{2\times 2}_{\mathrm{sym}} \;:\; \mathrm{div}\sigma = 0 \text{ in } \mathcal{O},\ \sigma n = F \text{ on } \Gamma,\ \sigma n = 0 \text{ on } \partial\mathcal{O}\setminus\Gamma\}\,.$$

Step 1: The relaxed problem. Here one identifies $\mathrm{J}_0^{*,F,\ell}$ with the infimum of the objective functional for $\varepsilon = 0$. Via the identification $\mathcal{O} = \{x \in \Omega \,:\, \sigma(x) \neq 0\}$, this infimum can be expressed as

$$\mathrm{J}_0^{*,F,\ell} = \inf_{\sigma \in \Sigma_{\mathrm{ad}}^{\Omega}} \int_\Omega |\sigma|^2 + 1_{\sigma \neq 0} \,\mathrm{d}x\,,$$

where $1_{\sigma\neq 0}$ is the characteristic function of $\{x \in \Omega \,:\, \sigma(x) \neq 0\}$. The relaxation of this problem is well-known [3] and leads to

$$\mathrm{J}_0^{*,F,\ell} = \min_{\sigma \in \Sigma_{\mathrm{ad}}^{\Omega}} \int_\Omega g(\sigma)\,\mathrm{d}x \quad \text{with } g(\sigma) = \begin{cases} 2(|\sigma_1| + |\sigma_2| - |\sigma_1\sigma_2|) & \text{if } |\sigma_1| + |\sigma_2| \leq 1, \\ 1 + \sigma_1^2 + \sigma_2^2 & \text{else,} \end{cases}$$

where σ_1, σ_2 denote the eigenvalues of σ. The minimum value $\mathrm{J}_0^{*,F,\ell} = 2\ell|F|$ is achieved by $\sigma = \left(\begin{smallmatrix} 0 & 0 \\ 0 & |F| \end{smallmatrix}\right)$.

Step 2: Lower bound. Abbreviating $\hat{\mathrm{J}} = \min_{\mathcal{O}} \mathrm{J}^{\varepsilon,F,\ell}[\mathcal{O}]$ and $\Delta\mathrm{J} = \hat{\mathrm{J}} - \mathrm{J}_0^{*,F,\ell}$, it is clear that for a generic cross-section $\hat{y} \sim \frac{1}{2}$ we have at most $\sim \frac{\Delta \mathrm{J}}{\varepsilon}$ interfaces and at most a material volume fraction of $\sim \frac{\hat{\mathrm{J}}}{\ell}$. Let the material gaps on $y = \hat{y}$ be denoted by $\tilde{\Gamma} = ([x_1^l, x_1^r] \cup \ldots \cup [x_N^l, x_N^r]) \times \{\hat{y}\}$. Upon introducing a Lagrange multiplier $u : \Omega \to \mathbb{R}^2$ for the constraint $\mathrm{div}\sigma = 0$ and integrating by parts, we obtain

$$\hat{\mathrm{J}} \geq \min_{\substack{\sigma \in \Sigma_{\mathrm{ad}}^{\Omega} \\ \sigma n = 0 \text{ on } \tilde{\Gamma}}} \int_\Omega g(\sigma)\,\mathrm{d}x = \min_{\sigma:\Omega\to\mathbb{R}^{2\times 2}_{\mathrm{sym}}} \max_{u:\Omega\to\mathbb{R}^2} \int_{\Omega\setminus\tilde{\Gamma}} g(\sigma) - \epsilon(u) : \sigma \,\mathrm{d}x + \int_\Gamma u \cdot F \,\mathrm{d}a\,.$$

Swapping min and max and denoting the Legendre–Fenchel dual to g by g^*, we arrive at

$$\hat{\mathrm{J}} \geq \max_{u:\Omega\to\mathbb{R}^2} -\int_{\Omega\setminus\tilde{\Gamma}} g^*(\epsilon(u))\,\mathrm{d}x + \int_\Gamma u \cdot F\,\mathrm{d}a \geq \max_{\substack{u:\Omega\to\mathbb{R}^2 \\ |\epsilon(u)|^2 \leq 4 \text{ on } \Omega\setminus\tilde{\Gamma}}} \int_\Gamma u \cdot F\,\mathrm{d}a\,.$$

Here, g^* is most easily computed by noting $\tilde{g} \geq g \geq \tilde{g}^{**}$ for $\tilde{g}(\sigma) = 1_{\sigma\neq 0} + |\sigma|^2$ and its convex envelope $\tilde{g}^{**}(\sigma) = \max(2|\sigma|, 1 + |\sigma|^2)$ so that from $\tilde{g}^* \leq g^* \leq (\tilde{g}^{**})^*$ and $\tilde{g}^* = (\tilde{g}^{**})^*$ we obtain $g^* = (\tilde{g}^{**})^*$. Using the ansatz $u = \left(\begin{smallmatrix} 0 \\ 2\gamma y \end{smallmatrix}\right) + 2f(x)\left(\begin{smallmatrix} 0 \\ \mathrm{sign}(y-\hat{y}) \end{smallmatrix}\right)$ and optimizing for $f(x)$ (among all piecewise linear functions) and $\gamma \in \mathbb{R}$ one arrives at

$$\Delta\mathrm{J} \geq 2|F|\ell\left(\sqrt{1 + \tfrac{\mathcal{H}^1(\tilde{\Gamma})^4}{2N^2\ell^2}} - 1\right).$$

Using the bound on the volume fraction (which implies $\mathcal{H}^1(\tilde{\Gamma}) \sim \ell$) and on the number $2N$ of interfaces, this can be shown to imply $\Delta\mathrm{J} \gtrsim |F|\ell\frac{\mathcal{H}^1(\tilde{\Gamma})^4}{N^2\ell^2} \sim |F|\frac{\ell^3\varepsilon^2}{\Delta\mathrm{J}^2}$, which immediately yields the desired lower bound.

Step 3: Upper bound. It suffices to provide a construction with the correct energy scaling. A sketch of the construction is shown in Figure 1. It consists of several branching levels which successively refine from the coarsest level at the center (level 1) towards Γ. Each level is composed of an array of unit cells, each of which contains a truss-like structure at its center. We take the unit cell width on level 1 to be $w_1 \sim \sqrt[3]{\varepsilon/|F|}$ and the width on level i to be $w_i = w_1/2^{i-1}$;

furthermore, the unit cell height on level i shall be $h_i = \sqrt{|F|w_i^3/\varepsilon}$. The thickness of the trusses in each unit cell is now chosen such that the (uniaxial) stress inside has magnitude 1. Finally, the branching is stopped as soon as $h_i \leq w_i$, and a thin material layer of thickness $\sim w_i$ is inserted as a boundary layer. A careful estimate of the energy for this construction reveals that it is compatible with the desired upper bound.

Note that the same argument works with slight adaptations for slightly varied load geometries such as tilted loads. The proof of the lower bound can also be extended to some non-uniaxial load geometries such as a shear load all around a rectangular domain.

References

[1] R. Kohn and S. Müller, *Relaxation and regularization of nonconvex variational problems*, Rendiconti del Seminario Matematico e Fisico di Milano **62** (1992), 89–113.

[2] R. Choksi, R. V. Kohn, and F. Otto, *Energy minimization and flux domain structure in the intermediate state of a type-I superconductor*, Journal of Nonlinear Science **14** (2004), 119–171.

[3] R. Kohn and G. Strang, *Optimal design and relaxation of variational problems II*, Communications on Pure and Applied Mathematics **39** (1986), 139–182.

Inverse problems of determining subboundaries: uniqueness and stability

Masahiro Yamamoto

We discuss an inverse problem of determining shapes of subboundaries where the solution of partial differential equation satisfies some homogeneous boundary condition. Our main purpose is to prove conditional stability for the inverse problem.

Let $\Omega_0 \subset \mathbf{R}^n$, $n = 2, 3$ be a bounded domain with smooth boundary $\partial\Omega_0$, and let

$$(Au)(x) := -\sum_{i,j=1}^{n} \partial_i(a_{ij}(x)\partial_j u) + c(x)u, \quad x \in \Omega_0,$$

where $a_{ij} = a_{ji} \in C^1(\overline{\Omega_0})$, $c \in L^\infty(\Omega)$, $1 \leq i, j \leq n$. We assume that $0 \leq c$ in Ω_0. Let $D \subset \Omega_0$ be a domain such that ∂D is of C^2-class, $0 \in D$, $\overline{D} \subset \Omega_0$. We set

$$\Omega = \Omega_0 \setminus \overline{D}.$$

Let $\Gamma \subset \partial\Omega_0$ be an arbitrarily chosen subboundary and let $u = u(D)$ satify

$$Au = 0 \quad \text{in } \Omega,$$

$$u|_{\partial D} = 0.$$

Inverse Problem: Determine the shape of ∂D by $u, \partial_A u$ on Γ.

Here we set $\partial_A u = \sum_{i,j=1}^{n} a_{ij}(\partial_j u)\nu_i$ where $\nu = (\nu_1, ..., \nu_n)$ denotes the unit outward normal vector to $\partial\Omega_0$.

We propose an arugument mainly based on Carleman esitmate in order to prove conditional stability. Our main result asserts a single logarithmic stability estimate under some a priori assumptions on curvatures, etc. of unknown subboundaries.

We formulate the stability problem. Let $D_1, D_2 \subset \Omega_0$ be domains such that $0 \in D_j$, $\overline{D_j} \subset \Omega_0$ and ∂D_j is of C^2-class. Let $\Omega_j = \Omega_0 \setminus \overline{D_j}$, $j = 1, 2$. Moreover let ∂D_j be parametrized by $\psi \in S^{n-1} := \{x \in \mathbf{R}^n;\ |x| = 1\}$. Let $u_j = u(D_j)$ satisfy

$$Au_j = 0 \quad \text{in } \Omega_j, \tag{1}$$

$$u_j|_{\partial D_j} = 0 \tag{2}$$

$$u_j|_\Gamma = g_j, \quad \partial_A u_j|_\Gamma = h_j. \tag{3}$$

We assume:

Condition A

$$|\partial D_j| \le M, \quad \|u_j\|_{C^1(\overline{\Omega_j})} + \|u_j\|_{H^{m_0}(\Omega_j)} \le M, \quad j = 1, 2$$
$$\operatorname{dist}(\partial D_j, \partial\Omega_0) \ge \delta_0 > 0$$

with fixed $\delta_0 > 0$ and

Condition B

$$\inf_\Gamma |g_j| \ge \delta_0, \quad j = 1, 2. \tag{4}$$

Here $\delta_0 > 0$ and $M > 0$ are arbitrarily fixed and $m_0 = \max\left\{4, \left[\frac{n}{2}\right] + 2\right\}$.

We are ready to state the main result.

Theorem

Under Conditions A and B, there exists a constant $\theta \in (0, 1)$ such that

$$d(\partial D_1, \partial D_2) = O\left(\left(\frac{1}{\log \frac{1}{\|u_1 - u_2\|_{H^3(\Gamma)} + \|\partial_A(u_1 - u_2)\|_{H^2(\Gamma)}}}\right)^\theta\right)$$

for small $\|u_1 - u_2\|_{H^3(\Gamma)} + \|\partial_A(u_1 - u_2)\|_{H^2(\Gamma)}$. Here d $(\partial D_1, \partial D_2)$ is the Hausdorff distance.

Our argument is applied to other types of equations such as Lamé system, the Navier-Stokes equations to yield the single logarithmic conditional stability.

The proof is based on interior and boundary estimates for a Cauchy problem where Dirichlet and Neumann data are given on some lateral subboundary.

Reporter: Michael Hinze

Participants

Prof. Dr. Helmut Abels
Fakultät für Mathematik
Universität Regensburg
Universitätsstr. 31
93053 Regensburg
GERMANY

Prof. Dr. Hans Wilhelm Alt
Zentrum Mathematik
TU München
Arcisstr. 21
80333 München
GERMANY

Prof. Dr. Sören Bartels
Abteilung für Angewandte Mathematik
Universität Freiburg
Hermann-Herder-Str. 10
79104 Freiburg
GERMANY

Prof. Dr. Giovanni Bellettini
Dipartimento di Matematica
Universita di Roma Tor Vergata
Via della Ricerca Scientif. 1
00133 Roma
ITALY

Prof. Dr. Luise Blank
Fakultät für Mathematik
Universität Regensburg
Universitätsstr. 31
93053 Regensburg
GERMANY

Charles Brett
Mathematics Institute
University of Warwick
Coventry CV4 7AL
UNITED KINGDOM

Prof. Dr. Dorin Bucur
Laboratoire de Mathématiques
Université de Savoie
73376 Le Bourget du Lac Cedex
FRANCE

Prof. Dr. Antonin Chambolle
Centre de Mathématiques Appliquées
École Polytechnique
91128 Palaiseau Cedex
FRANCE

Prof. Dr. Klaus Deckelnick
Institut für Analysis u. Numerik
Otto-von-Guericke-Universität
Magdeburg
Universitätsplatz 2
39106 Magdeburg
GERMANY

Prof. Dr. Charles M. Elliott
Mathematics Institute
University of Warwick
Gibbet Hill Road
Coventry CV4 7AL
UNITED KINGDOM

Prof. Dr. Xiaobing H. Feng
Department of Mathematics
University of Tennessee
218 Ayres Hall
Knoxville, TN 37996-1300
UNITED STATES

Julian Fischer
Department Mathematik
Universität Erlangen-Nürnberg
Cauerstr. 11
91058 Erlangen
GERMANY

Dr. Nicolas Forcadel
CEREMADE
Université Paris Dauphine
Place du Marechal de Lattre de Tassigny
75775 Paris Cedex 16
FRANCE

Hans Fritz
Abteilung f. Angewandte Mathematik
Universität Freiburg
Eckerstr. 1
79104 Freiburg
GERMANY

Prof. Dr. Harald Garcke
Fakultät für Mathematik
Universität Regensburg
93040 Regensburg
GERMANY

Prof. Dr. Mi-Ho Giga
Graduate School of Mathematical Sciences
University of Tokyo
3-8-1 Komaba, Meguro-ku
Tokyo 153-8914
JAPAN

Prof. Dr. Yoshikazu Giga
Graduate School of Mathematical Sciences
The University of Tokyo
3-8-1 Komaba, Meguro-ku
Tokyo 153-8914
JAPAN

Dr. Carsten Gräser
Fachbereich Mathematik & Informatik
Freie Universität Berlin
Arnimallee 6
14195 Berlin
GERMANY

Nao Hamamuki
Graduate School of Mathematical Sciences
University of Tokyo
3-8-1 Komaba, Meguro-ku
Tokyo 153-8914
JAPAN

Prof. Dr. Michael Hintermüller
Fachbereich Mathematik
Humboldt-Universität Berlin
Unter den Linden 6
10117 Berlin
GERMANY

Prof. Dr. Michael Hinze
Fachbereich Mathematik
Universität Hamburg
Bundesstr. 55
20146 Hamburg
GERMANY

Prof. Dr. Dr.h.c. Karl-Heinz Hoffmann
Zentrum Mathematik - M6
Technische Universität München
Boltzmannstr. 3
85747 Garching
GERMANY

Christian Kahle
Department Mathematik
Universität Hamburg
Bundesstr. 55
20146 Hamburg
GERMANY

Prof. Dr. Nobuyuki Kenmochi
School of Education (Mathematics)
Bukkyo University
96, Kitahananobo-cho,
Murasakino, Kita-ku
Kyoto 603-8301
JAPAN

Prof. Dr. John R. King
School of Mathematical Sciences
The University of Nottingham
University Park
Nottingham NG7 2RD
UNITED KINGDOM

Prof. Dr. Ralf Kornhuber
Institut für Mathematik
Freie Universität Berlin
Arnimallee 6
14195 Berlin
GERMANY

Kei Fong Lam
Mathematics Institute
University of Warwick
Coventry CV4 7AL
UNITED KINGDOM

Prof. Dr. Günter Leugering
Department Mathematik
FAU Erlangen-Nürnberg
Cauerstraße 11
91058 Erlangen
GERMANY

Prof. Dr. Stephan Luckhaus
Mathematisches Institut
Universität Leipzig
Johannisgasse 26
04103 Leipzig
GERMANY

Dr. Holger Marschall
Center of Smart Interfaces,
Mathematical Modeling and Analysis
Technische Universität Darmstadt
Petersenstraße 17
64287 Darmstadt
GERMANY

Prof. Dr. Christian Meyer
Fakultät für Mathematik
Technische Universität Dortmund
Vogelpothsweg 87
44227 Dortmund
GERMANY

Prof. Dr. Regis Monneau
CERMICS - ENPC
Cite Descartes, Champs-sur-Marne
6 et 8 avenue Blaise Pascal
77455 Marne-la-Vallee Cedex 2
FRANCE

Atsushi Nakayasu
Grad. School of Mathematical Sciences
University of Tokyo
3-8-1 Komaba, Meguro-ku
Tokyo 153-8914
JAPAN

Prof. Dr. Ricardo H. Nochetto
Department of Mathematics
University of Maryland
College Park, MD 20742-4015
UNITED STATES

Prof. Dr. Takeshi Ohtsuka
Department of Mathematics
Gunma University
Aramaki-machi 4-2
Maebashi 371-8510
JAPAN

Prof. Dr. René Pinnau
Fachbereich Mathematik
T.U. Kaiserslautern
Erwin-Schrödinger-Straße
67653 Kaiserslautern
GERMANY

Tom Ranner
Mathematics Institute
University of Warwick
Gibbet Hill Road
Coventry CV4 7AL
UNITED KINGDOM

Prof. Dr. Arnold Reusken
Institut für Geometrie und
Praktische Mathematik
RWTH Aachen
Templergraben 55
52061 Aachen
GERMANY

Prof. Dr. Elisabetta Rocca
Dipartimento di Matematica
Universita di Milano
Via C. Saldini, 50
20133 Milano
ITALY

Prof. Dr. Matthias Röger
Fachbereich Mathematik
Technische Universität Dortmund
Vogelpothsweg 87
44227 Dortmund
GERMANY

Prof. Dr. James A. Sethian
Department of Mathematics
University of California
Berkeley CA 94720-3840
UNITED STATES

Prof. Dr. Gieri Simonett
Department of Mathematics
Vanderbilt University
1326 Stevenson Center
Nashville, TN 37240
UNITED STATES

Prof. Dr. Jürgen Sprekels
Weierstraß-Institut für
Angewandte Analysis und Stochastik
Mohrenstr. 39
10117 Berlin
GERMANY

Dr. Björn Stinner
Mathematics Institute
University of Warwick
Gibbet Hill Road
Coventry CV4 7AL
UNITED KINGDOM

Dr. Vanessa Styles
Department of Mathematics
University of Sussex
Falmer
Brighton BN1 9QH
UNITED KINGDOM

Prof. Dr. Yen-Hsi Richard Tsai
Department of Mathematics
The University of Texas at Austin
1 University Station C1200
Austin, TX 78712-1082
UNITED STATES

Dr. Chandrashekar Venkataraman
Department of Mathematics
University of Sussex
Falmer
Brighton BN1 9QH
UNITED KINGDOM

Dr. Benedikt Wirth
Courant Institute of
Mathematical Sciences
New York University
251, Mercer Street
New York, NY 10012
UNITED STATES

Dr. Gabriele Witterstein
Zentrum Mathematik
TU München
80290 München
GERMANY

Prof. Dr. Masahiro Yamamoto
Department of Mathematical Sciences
University of Tokyo
3-8-1 Komaba, Meguro-ku
Tokyo 153-8914
JAPAN